



UNIVERSITAT DE
BARCELONA

Role of CD44 in clear cell renal cell carcinoma invasiveness after antiangiogenic treatment

María Aparicio García

ADVERTIMENT. La consulta d'aquesta tesi queda condicionada a l'acceptació de les següents condicions d'ús: La difusió d'aquesta tesi per mitjà del servei TDX (www.tdx.cat) i a través del Dipòsit Digital de la UB (diposit.ub.edu) ha estat autoritzada pels titulars dels drets de propietat intel·lectual únicament per a usos privats emmarcats en activitats d'investigació i docència. No s'autoritza la seva reproducció amb finalitats de lucre ni la seva difusió i posada a disposició des d'un lloc aliè al servei TDX ni al Dipòsit Digital de la UB. No s'autoritza la presentació del seu contingut en una finestra o marc aliè a TDX o al Dipòsit Digital de la UB (framing). Aquesta reserva de drets afecta tant al resum de presentació de la tesi com als seus continguts. En la utilització o cita de parts de la tesi és obligat indicar el nom de la persona autora.

ADVERTENCIA. La consulta de esta tesis queda condicionada a la aceptación de las siguientes condiciones de uso: La difusión de esta tesis por medio del servicio TDR (www.tdx.cat) y a través del Repositorio Digital de la UB (diposit.ub.edu) ha sido autorizada por los titulares de los derechos de propiedad intelectual únicamente para usos privados enmarcados en actividades de investigación y docencia. No se autoriza su reproducción con finalidades de lucro ni su difusión y puesta a disposición desde un sitio ajeno al servicio TDR o al Repositorio Digital de la UB. No se autoriza la presentación de su contenido en una ventana o marco ajeno a TDR o al Repositorio Digital de la UB (framing). Esta reserva de derechos afecta tanto al resumen de presentación de la tesis como a sus contenidos. En la utilización o cita de partes de la tesis es obligado indicar el nombre de la persona autora.

WARNING. On having consulted this thesis you're accepting the following use conditions: Spreading this thesis by the TDX (www.tdx.cat) service and by the UB Digital Repository (diposit.ub.edu) has been authorized by the titular of the intellectual property rights only for private uses placed in investigation and teaching activities. Reproduction with lucrative aims is not authorized nor its spreading and availability from a site foreign to the TDX service or to the UB Digital Repository. Introducing its content in a window or frame foreign to the TDX service or to the UB Digital Repository is not authorized (framing). Those rights affect to the presentation summary of the thesis as well as to its contents. In the using or citation of parts of the thesis it's obliged to indicate the name of the author.



UNIVERSITAT DE
BARCELONA

UNIVERSITAT DE BARCELONA
FACULTAT DE MEDICINA
PROGRAMA DE DOCTORAT EN BIOMEDICINA

**ROLE OF CD44 IN CLEAR CELL RENAL CELL CARCINOMA
INVASIVENESS AFTER ANTIANGIOGENIC TREATMENT**

MARIA APARICIO GARCIA
2020



UNIVERSITAT DE BARCELONA

FACULTAT DE MEDICINA

PROGRAMA DE DOCTORAT EN BIOMEDICINA

ROLE OF CD44 IN CLEAR CELL RENAL CELL CARCINOMA INVASIVENESS AFTER ANTIANGIOGENIC TREATMENT

MARIA APARICIO GARCIA

2020

Memòria presentada per Maria Aparicio Garcia per optar al grau de Doctor/a per la
Universitat de Barcelona

Dr. Oriol Casanovas Casanovas

Director

Dr. Francesc Viñals Canals

Tutor

Maria Aparicio Garcia

Autora

AGRAÏMENTS

Fa tres anys passejava tranquil·la pels carrers de Sants gaudint de la festa major del barri. Avui, entre mascaretes i gel desinfectant intento mantenir la “distància de seguretat” amb la gent. I és que tres anys han estat suficients perquè la vida, tal i com la coneixíem, donés una volta de 180º, així com també tres anys han estat suficients per realitzar una tesi, que en breus em tocarà defensar. Durant aquest temps he pogut conèixer persones meravelloses que m’han permès créixer i arribar fins on sóc ara, i és per això que es mereixen el meu més sincer agraïment. Els que em coneixeu, sabeu que les dedicatòries i mostres d’afecte no són el meu fort, però en temps de pandèmia i distanciament social poques opcions em queden per agrair-vos haver estat al meu costat durant aquest temps.

Primer de tot, agrair-li a l’**Oriol** per donar-me l’oportunitat de realitzar la tesi en els seus laboratoris. Sense la teva ajuda i els teus consells, aquest projecte no hauria avançat ni evolucionat tal i com ho ha fet. També agrair a la resta de caps de recerca del **ProCure** pels consells i el bon ambient que sempre intenteu generar tant dins com fora del laboratori.

Per altra banda, agrair als membre d’angio pel suport que sempre m’han donat. En primer lloc al **Jordi**, per adoptar-me en el seu projecte i fer-me sentir que també era meu. Tot i les nostres discrepàncies en la manera de treballar, m’has introduït al món de la ciència i la investigació i m’has ensenyat que sempre s’ha de buscar el perquè de les coses. Espero que el llarg camí que et queda en la ciència vagi d’allò més bé. A la **Mariona**, la persona més ocupada del món mundial que conec, companya de viatges amb moto a casa i que sempre ha estat al meu costat quan l’he necessitat. Tot i no haver coincidit molt temps al laboratori, em quedo amb grans moments i riures viscuts al teu costat. A **Iratxe**, la vasca más catalana e indepe que he conocido. Eres una persona con las ideas muy claras y que nunca se rinde hasta conseguir sus metas y eso, créeme, es de admirar. Te deseo mucha suerte en tu aventura en San Francisco y si vuelves por aquí estaré encantada de brindar con un chupito de Jagger en la Flama. A **Júlia**, por ser la paz

y serenidad que alguien necesita en su vida. Por todas las conversaciones y consejos, por dejar que me sincere a tu lado sabiendo que no me vas a juzgar nunca. Tu marcha a Brasil fue inesperada y no hubo mucho tiempo para despedidas, pero sé que estarás bien y superarás todos los obstáculos que se te pongan por delante. A la **Roser**, la menorquina crossfitera del grup i companya de taula a becaris. Per ser la persona més hiperactiva del lab i animar-nos els dies només entrant per la porta. Gràcies per compartir ciència, riures i bailoteos al meu costat. T'anirà bé allà on vagis i en allò que desitgis acabar sent. A **Iván**, la última incorporación en el angio team. Las ideas que propones y tus consejos valen oro. Vas a hacer una gran tesis y llegarás muy lejos, estoy 100% segura de ello. Gracias de verdad por aguantar todas mis paranoias, cuidarme las células y escuchar las notas de voz de 4 minutos. A **Gabi**, por ser la primera persona que me acogió en el grupo y enseñarme a confiar en mí y luchar por lo que quiero. Gracias por tener siempre un consejo preparado para cualquier ocasión y dedicarme un minuto sin tenerlo. Te desearía suerte en el proyecto de Angiotheragnostics, pero no la necesitas. Irá genial, lo sé. A la **Mar**, la veterinària indispensable en el nostre grup. Saps que sense tu cap dels nostres projectes haguessin arribat on ho han fet, formes part de tots i cada un d'ells. Per no deixar-te vèncer mai i ensenyar-me a perseverar. Els maleïts cultius primaris acabaran sortint! A **Alba**, por estar siempre dispuesta a ayudarte en todo y escucharte cuando más lo necesitas. Gracias por hacernos el trabajo más fácil en el lab procurando que nunca nos falte de nada. A **Nick**, el viajero italiano más calmado y sereno que ha habido en el grupo. Gracias por nuestras charlas y cervezas en plaça Osca.

També vull agrair a tots els "becaris" que han compartit totes les coses bones i també les dolentes d'aquests tres anys amb mi. A la **Jana**, per ser la persona més boja, hiperactiva, estressada i tranquil·la a la vegada. Gràcies per les festes plenes de xapes mútues, els riures per tot allò que dius i fas. De veritat, hi ha coses que només et poden passar a tu. Espero que tinguis molta sort a Suïssa, aquí t'esperarem amb una birreta a la mà. A **Carmen**, la persona més amable y con más buena intención del mundo. No tienes maldad alguna, siempre dispuesta a echar una mano con lo que sea sin pedir nada a cambio. Gracias por estar a mi lado en momentos difíciles y por atarme con las llaves

para que no me fuera a casa las noches de Flama. Después de todo lo que has soportado no me quedan dudas de que te irá genial en Inglaterra, te lo mereces. Al **Martí**, per ser el millor profe de citometria, company de hyal, immunos i westerns que podria demanar. Gràcies per els xistes malos que a mi em fan riure i per les conduccions nocturnes de cotxe entre gintònics. A la **Nerea**, la persona més intensa i amb més caràcter del lab. Sempre disposada a trobar solucions a tots els problemes que es plantegen. Gràcies per escoltar-me i estar al meu costat sempre que ho he necessitat. M'has fet tocar de peus a terra quan era el moment i també m'has fet còmplice de les teves bogeries nocturnes. Per compartir aquest final de tesi que ens porta pel camí de l'amargura, però que ja és aquí! A la **Sònia**, pel teu caràcter, les teves idees clares i la teva sinceritat. Compartir l'hora del te i xerrar amb tu, sempre ha estat dels millors moments del dia. Gràcies per compartir pensaments amb mi, tant bons com dolents. I gràcies també per compartir manifestacions i caminades fins a l'aeroport sense saber com tornar. A **Álvaro**, porque no siempre se tienen que compartir pensamientos para poder llevarte bien con alguien. Y es que, quitando temas políticos y discusiones varias, también se puede hablar, compartir cervezas, barbacoas y romper palés contigo. Gracias por resolverme las dudas que he podido tener durante este tiempo y también por las risas que nos hemos echado. A **Adrián**, el viejoven del laboratorio que no deja de sorprenderme con su mezcla de frases de abuela y de millennial. Eres la persona más inocente y asustadiza que conozco, pero también estas lleno de bondad. No lo pierdas nunca. Gracias por ofrecerte siempre a ayudar en todo, tenderme una mano en momentos difíciles y por alegrarme las tardes en cultivos cantando como si no hubiera mañana. A la **Gemma**, la persona del laboratori més calmada i estressada a la vegada. I per ser la que menys entén les coses... Gràcies per les converses a la sala de becaris mentre esperava que passessin les hores del Wound Healing i animar-me en moments baixos. A la **Laura**, l'esbojarrada i despreocupada, la persona que crec que mai he vist estressar-se. Creu-me, tens un do, no el perdis. Gràcies per transmetre'm pau i per saber parlar de temes profunds i de temes sense sentit. A **Kiko**, el canario más fiestero. Por las cenas, los vinos y las cervezas compartidas. Aunque digas que no, sé que me vas a echar muchísimo de menos, y yo a ti también. Pero nos seguiremos encontrando en plaça Osca, de mí no te vas a deshacer tan rápido... Nos

queda pendiente un carnaval en las Canarias. A la **Núria**, la persona més dolça i bondadosa. Ets un sac de saviesa i meticulositat, que juntament amb les ganes de combatre el món et faran arribar lluny. Gràcies per oferir-me sempre un cop de mà, dins i fora del laboratori, i per escoltar les meves xapes quan les coses es compliquen. A la **Sandra**, l'última incorporació de predocs. No perdis l'energia i innocència que et caracteritzen. Sort i ànims en aquest camí que iniciés en la ciència. A la **Sílvia**, per tenir sempre un somriure a la cara i compartir amb mi aquesta afició pels mixinus. Al **Xin**, company d'agulletes i persona fit de les que a mi m'agrada, fer esport per poder menjar guarrades. A la **Maria**, incorporació recent al laboratori. Tímida i riallera, que sempre sap transmetre bon humor i serenitat.

A part dels predocs, al laboratori hi ha més gent que també forma part de la gran família que és LRT1 i a la que també vull agrair els moments compartits durant aquest temps. Als postdocs: **Agnès, Paqui, Eli, Rana, Samu i Rafa**, sempre esteu disposats a donar consells i buscar solucions. Ha estat un plaer compartir aquests anys de recerca amb vosaltres. També a la **Nadia, María, Mónica i Anabel**, per la vostra ajuda i els bons moments. Per acabar a la **Laura** i la **Natàlia**, per mantenir l'ordre al laboratori encara que a vegades sigui un caos.

Tot i que aquests tres últims anys han estat força marcats pel doctorat, sempre he tingut gent al costat que ha estat disposada a fer-me desconnectar. Gràcies Montse per buscar sempre un racó per mi en la teva ocupada vida, per no deixar-me caure i animar-me en els dies de bajón. Tot i que ens veiem poc, quan ho fem sembla que res hagi canviat. Arreglar el món i les nostres vides amb una birra a la mà és un dels meus hobbies preferits. Crec que no podria haver tingut una millor companya de pis i d'aventures, juntament amb la Mar i la Gemma hem viscut grans moments. A les "nenes" Míriam, Clàudia, Cristina i Raquel, les de sempre, perquè per molt que ens veiem poc i cada una hagi fet el seu camí, sé que si us necessito hi sereu. Sou amor i us trobo a faltar.

También tengo que agradecer al Crossfit por no dejarme perder el norte durante la tesis y ser mi vía de escape. Pero sobretodo, le tengo que agradecer que pusiera a gente genial

en mi vida. A Dani, también conocido por coach D, por hacerme creer que puedo hacer cosas increíbles y animarnos la cuarentena con sus entrenos. Y por último a las toias, Eva, Juanca y Manel, por el dolor, sudor y sufrimiento compartido en el box. Por la definición y las noches de Domino's y Mc Flurrys. Por ese viajecito a Menorca que acabó en cuarentena y porque me alegráis los días. Espero que nos sigamos aguantando mucho tiempo más. Y sobre todo gracias a ti, Manel, por estar a mi lado aportándome todo el optimismo que muchas veces yo no sé encontrar, por buscar soluciones cuando estoy ofuscada y hacerme reír cuando lo necesito. Aunque sabes que Freud es mío y quieras robármelo... si quieres lo podemos compartir, y es que a tu lado me siento en casa.

I ara sí, ja per acabar, només em falta agrair a la meva família tot el suport que sempre m'han donat. Sé que no és fàcil bregar amb mi i el meu caràcter, que a vegades tinc més ocells que plans al cap, però sempre heu estat al meu costat, recolzant-me i animant-me a seguir endavant, fins i tot quan no sabíeu ni què era un doctorat. Sóc una afortunada per tenir-vos, no em falteu mai.

Ah! No em puc oblidar de vosaltres, Freud i Bruc, el gat més gos que podia tenir i el gos més mimós que existeix. Perquè la vostra companyia no la canviaria per res del món!

I això és tot, tanco una etapa que ha estat repleta d'alts i baixos, però necessaris cada un d'ells per arribar on sóc. Gràcies a tots per formar-ne part, no podria haver tingut millors companys d'aventura.

TABLE OF CONTENTS

TABLE OF CONTENTS	1
LIST OF ABBREVIATIONS.....	6
LIST OF FIGURES	13
LIST OF TABLES	16
SUMMARY.....	17
RESUM	21
INTRODUCTION	25
1. Cancer.....	27
1.1 Renal Cell carcinoma	28
1.2 Classification of renal cell carcinoma	29
1.2.1 Clear cell Renal Cell Carcinoma (ccRCC).....	30
1.3 Histological classification of RCC	31
1.4 Clinical classification of RCC	32
1.5 RCC treatment.....	34
2. Angiogenesis.....	34
2.1 Antiangiogenic therapies.....	37
2.2 Other therapies.....	40
2.2.1 Immunotherapy	40
2.2.2 Targeted therapies.....	40
2.2.3 Combined therapies.....	40
2.3 Resistance to antiangiogenic therapies	42
2.3.1 Intrinsic resistance	43
2.3.2 Acquired resistance.....	44
2.4 Strategies to overcome antiangiogenic resistance	45
3. Tumor malignization: increase aggressiveness after antiangiogenic therapy.....	46
3.1 Metastatic process.....	47
3.2 Role of extracellular matrix in tumor malignization	50
4. Previous results	51

4.1 Tumor malignization after antiangiogenic therapies	51
4.1.1 Efficacy of the antiangiogenic treatment	53
4.1.2 Increase invasiveness after antiangiogenic treatment.....	54
4.2 Pro-invasive candidates after antiangiogenic treatment	55
4.2.1 Implication of CD44 in tumor invasion	57
4.2.2 CD44.....	59
HYPOTHESIS AND OBJECTIVES	63
MATERIALS AND METHODS	67
1. In vitro.....	69
1.1 Cell culture.....	69
1.1.1 Cell lines	69
1.1.2 Primary cell lines.....	69
1.1.3 Cell line maintenance	70
1.1.4 Mycoplasma Test.....	71
1.1.5 Cell counting.....	71
1.1.6 Cell freezing and cryopreservation.....	71
1.1.7 Cell line treatment.....	72
1.2 Molecular analysis.....	73
1.2.1 RNA detection	73
1.2.1.1 RNA extraction from cells.....	73
1.2.1.2 Getting cDNA from RNA	74
1.2.1.3 Real-Time quantitative PCR	74
1.2.2 Protein detection.....	75
1.2.2.1 Preparation of protein lysates from cell culture.....	75
1.2.2.2 Quantification of protein extracts	75
1.2.2.3 Protein analysis by Western Blotting.....	76
1.2.2.4 Protein detection by Immunocytofluorescence	77
1.2.2.5 Protein detection by Flow Cytometry	79
1.2.3 Inducible downregulation system	80
1.2.3.1 Doxycycline inducible shRNA system	80
1.2.3.2 Plasmid amplification	80
1.2.3.3 Large scale DNA preparations.....	80

1.2.3.4	Lentiviral production	81
1.2.3.5	Lentiviral infections	81
1.3	<i>In vitro</i> assays	82
1.3.1	Migration assays	82
1.3.1.1	Wound Healing assay.....	82
1.3.1.2	Transwell migration assay.....	82
1.3.2	Invasion assays.....	83
2.	In vivo	83
2.1	<i>Animals and conditions</i>	83
2.2	<i>Patient-derived orthoxenograft mouse model from RCC human biopsy</i>	84
2.3	<i>Cell lines mouse models</i>	84
2.3.1	Kidney tumors.....	84
2.4	<i>Tumor and organ collection</i>	85
2.5	<i>Paraffin inclusion</i>	85
2.6	<i>Determination of tumor burden</i>	85
2.7	<i>Animal treatment</i>	85
2.8	<i>Evaluation of tumor local invasiveness</i>	86
2.9	<i>Molecular analysis</i>	86
2.9.1	Protein detection	86
2.9.1.1	Protein extraction of tumor samples and quantification.	86
2.9.1.2	Protein analysis by Western Blotting	87
2.9.1.3	Immunohistochemistry in paraffin-embedded sections	87
2.9.1.4	Immunofluorescence in paraffin-embedded sections	89
2.9.1.5	Hematoxylin-Eosin staining in paraffin sections	90
3.	Clinical validation: in silico analyses	90
3.1	<i>TCGA analyses</i>	90
3.2	<i>Data from Sunitinib-treated patients</i>	90
4.	Statistical analysis	91
5.	Figure design	91
RESULTS	93
1.	CD44 as a pro-invasive candidate	95

1.1	Expression of CD44 in different cell lines and primary cells and tumors	95
1.2	CD44 downregulation	96
1.2.1	Validation of shRNAs functioning	97
1.3	Functional validation of CD44 downregulation in vitro	101
1.3.1	Effects of CD44 knockdown on cell migration	101
1.3.2	Effects of CD44 knockdown on cell invasion.....	108
1.4	Downregulation of CD44 in vivo	111
1.4.1	Tumor characterization: vessel density and cell proliferation.....	116
1.4.2	Effects of CD44 downregulation on tumor invasion	119
2.	Migration and invasion mechanisms downstream CD44	122
2.1	Migration effect of inhibiting the candidate pathways downstream CD44	123
2.2	Double inhibition of candidate pathways and CD44	126
2.2.1	Ruxolitinib	127
2.2.2	Bosutinib	130
3.	Induction of CD44 expression and activation	135
3.1	Hyaluronic Acid.....	135
3.1.1	Presence of HA in our cell models.....	136
3.1.2	Presence of HA in our tumor models	137
3.1.3	Effects of Hyaluronidase on cell migration	139
3.1.4	Migration consequences of blocking CD44 through HA binding site	142
3.1.5	Changes in CD44 activity using different fragments of HA.....	143
3.2	Others co-modulators of CD44	145
3.2.1	CD82.....	146
3.2.2	CCL5	147
3.2.3	Serglycin (SRGN)	147
3.2.3.1	Serglycin expression in cells	149
3.2.3.2	Serglycin expression in tumors	151
3.2.3.3	Determination of Serglycin localization	152
4.	Importance of CD44 expression in patients	154
	DISCUSSION	159
1.	Antiangiogenic treatment and tumor malignization	161

2. Studying the role of CD44 protein: shRNA system.....	163
3. Role of CD44 in tumor migration and invasion	166
4. CD44 downstream signaling	170
5. CD44 upstream signaling	175
6. Relevance of CD44 and Serglycin in the clinics	180
CONCLUSIONS	185
REFERENCES	189

LIST OF ABBREVIATIONS

%	Percentage
∞	Infinity
Δ	Delta
Ω	Ohm
°C	Centigrade degrees
μg	Microgram
μl	Microliter
μm	Micrometer
μM	Micromolar
AAALAC	Association for Assessment and Accreditation of Laboratory Animal Care
ACK	Ammonium-chloride-potassium
AJCC	American Joint Committee on Cancer
AKT	Protein Kinase B
APS	Ammonium persulfate
BCA	Bicinchoninic acid
BM	Basement membrane
BSA	Bovine serum albumin
CAF	Cancer associated fibroblast
ccRCC	Clear cell renal cell carcinoma
cDNA	Complementary DNA
CEIC	Centre Ètic d'Investigació Clínica
cm	Centimeter
CMV	Cytomegalovirus
CO₂	Carbon dioxide
Cpm	Counts per million

CSIC	Consell Superior d'Investigacions Científiques
Ct	Threshold cycle
CTC	Circulating tumor cells
CTLA	Cytotoxic T-Lymphocyte Antigen
Ctrl	Control
DAB	3,3'-Diaminobenzidine
DAPI	4',6-Diamidino-2-phenylindole dihydrochloride
dH₂O	Distilled water
ddH₂O	Bi-distilled water
ddNTP	2',3' dideoxynucleotides
DMEM	Dulbecco's Modified Eagle's Medium
DMSO	Dimethyl sulfoxide
DNA	Deoxyribonucleic acid
DOX	Doxycycline
DPX	Distyrene, plasticiser and xylene
DTT	Dithiothreitol
ECGF	Endothelial Cell Growth Factor
ECGFR	Endothelial Cell Growth Factor Receptor
ECM	Extracellular matrix
EDTA	Ethylenediaminetetraacetic acid
EGF	Epidermal growth factor
EMA	European Medicine Agency
EMT	Epithelial-mesenchymal transition
ERK	Extracellular-signal-regulated kinase
ERM	Ezrin-radixin-moesin
FACs	Flow Cytometry Staining Buffer

FAK	Focal Adhesion Kinase
FBS	Fetal bovine serum
FC	Fold change
FDA	Food and Drug Administration
FGF	Fibroblast Growth Factor
FGFR	Fibroblast Growth Factor Receptor
FGS	Fuhrman Grading System
GAG	Glycosaminoglycan
G	Gauge
g	Gram
GEO	Gene Expression Omnibus
GSEA	Gene set enrichment analysis
h	Hour
HA	Hyaluronic Acid
HABP	Hyaluronan binding protein
HE	Hematoxylin and eosin
H₂O₂	Hydrogen peroxide
HCl	Chloridric acid
HEPES	4-(2-hydroxyethyl)-1-piperazineethanesulfonic acid
HIF	Hypoxia-Inducible Factor
Hyal	Hyaluronidase
HMWHA	High Molecular Weigh Hyaluronic Acid
HRP	Horseradish peroxidase
ICO	Institut Català d'Oncologia
IDIBELL	Institut d'Investigació Biomèdica de Bellvitge
IGF	Insuline-like Growth Factor
IgG	Immunoglobulin G

IL	Interleukin
INF	Interferon
ISUP	International Society of Urology and Pathology
JAK	Janus Kinase
KDa	Kilodalton
Kg	Kilogram
KH₂PO₄	Potassium phosphate monobasic
KIRC	Kidney renal clear cell carcinoma
L	Liter
LB	Loading buffer
LMWHA	Low Molecular Weigh Hyaluronic Acid
MET	Mesenchymal-epithelial transition
mg	Milligram
min	Minute
ml	Milliliter
mm	Millimeter
mm²	Square millimeter
mm³	Cubic millimeter
mM	Millimolar
MMP	Matrix metalloprotease
mRCC	Metastatic renal cell carcinoma
mRNA	Messenger ribonucleic acid
MSC	Mesenchymal Stem Cell
NaCl	Sodium chloride
NaF	Sodium fluoride
Na₂HPO₄	Monosodium phosphate

NCI	National Cancer Institute
NEAA	Non-essential amino acids
O/N	Over night
OCT	Optimum cutting temperature compound
ORR	Objective Response Rate
OS	Overall Survival
OT	Orthotopic
PAGE	Polyacrylamide gel electrophoresis
PBS	Phosphate buffered saline
PCNA	Proliferating cell nuclear antigen
PCR	Polymerase chain reaction
PD	Programmed Cell Death Protein
PDGF	Platelet-derived growth factor
PDGFR	Platelet-derived growth factor receptor
PDL	Programmed Cell Death Ligand
PDX	Patient-derived xenograft
PDOX	Patient-derived orthoxenograft
PEI	Polyethylenimine
PES	Polyethersulfone
PFA	Paraformaldehyde
PFS	Progression-Free Survival
PLGF	Placental Growth Factor
proCure	Programa Contra la Resistència Terapèutica del Càncer
RCC	Renal Cell Carcinoma
RECIST	Response Evaluation Criteria In Solid Tumors
RFP	Red fluorescent protein

RIPA	Radioimmunoprecipitation assay buffer
RNA	Ribonucleic acid
RNAseq	Ribonucleic acid sequencing
rpm	Revolutions per minute
RPMI	Roswell Park Memorial Institute
RT	Room temperature
RT-qPCR	Real-time quantitative PCR
s	Second
SD	Standard deviation
SDS	Sodium dodecyl sulfate
shRNA	Short hairpin RNA
SPF	Specific pathogen free
Src	SRC Proto-Oncogene, Non-Receptor Tyrosine Kinase
SRGN	Serglycin
Stat	Signal transducer and activator of transcription
TAE	Tris-acetate-EDTA
TAM	Tumor-associated macrophage
TBS	Tris-buffered saline
TCGA	The Cancer Genome Atlas
TEMED	Tetramethylethylenediamine
TF	Transcription Factor
TGFβ	Transforming Growth Factor beta
TLDA	Taqman Low Density Array
TNM	Tumor-node-metastasis
U	Units
UV	Ultraviolet

V	Volt
VEGF	Vascular Endothelial Growth Factor
VEGFR	Vascular Endothelial Growth Factor Receptor
VHL	Von Hippel-Lindeau
WHO	World Health Organization
WT	Wild type

Amino acids

F Phe, phenylalanine	S Ser, serine	Y Tyr, tyrosine	K Lys, lysine	W Trp, tryptophan
L Leu, leucine	P Pro, proline	H His, histidine	D Asp, aspartic acid	R Arg, arginine
I Ile, isoleucine	T Thr, threonine	Q Gln, glutamine	E Glu, glutamic acid	G Gly, glycine
M Met, methionine	A Ala, alanine	N Asn, asparagine	C Cys, cysteine	V Val, valine

Nucleotides

A adenine	T thymine	G guanine	C cytosine	U uracil
------------------	------------------	------------------	-------------------	-----------------

LIST OF FIGURES

Figure 1. clear cell Renal Cell Carcinoma (ccRCC)	30
Figure 2. Representation of the angiogenic switch	35
Figure 3. Treatment evolution of metastatic renal cell carcinoma over time	41
Figure 4. Representation of the intrinsic resistance	43
Figure 5. Representation of the acquired resistance.....	44
Figure 6. Representation of the metastasis cascade	47
Figure 7. Effect of antiangiogenic therapy on tumor progression, invasiveness and metastatization in 786O- orthoxenograft tumor model	52
Figure 8. Effects of antiangiogenic drugs in REN-PDOX tumor models	53
Figure 9. Effect of antiangiogenic therapies on the local invasion of Ren-PDOX	55
Figure 10. Whole-genome RNA sequencing	56
Figure 11. Immunohistochemistry evaluation of CD44 expression	58
Figure 12. Correlation of CD44 expression with invasion	58
Figure 13. Representation of CD44 and its isoforms	60
Figure 14. Inducible Dharmacon™ pTRIPZ™ Lentiviral shRNA plasmid	80
Figure 15. Western Blot of CD44	95
Figure 16. Western Blot screening of different cell lines and their respective tumors	96
Figure 17. Doxycycline induction of shRNAs system in 786O- cells	97
Figure 18. Western Blot of CD44 expression in different cells	98
Figure 19. RNA levels of human CD44 in different cells	99
Figure 20. Flow Cytometry analysis of CD44 expression	100
Figure 21. CD44 knockdown didn't affect the migration capacity of SN12C cells	102
Figure 22. CD44 knockdown didn't affect the migration capacity of SN12C cells	103
Figure 23. CD44 knockdown produced a reduction of the Ren13 cell migration	104
Figure 24. CD44 knockdown produced a reduction of the migration in Ren13 cells	105
Figure 25. CD44 knockdown produced a slight reduction, but not statistically significant, of the migration in 786O- cells	106
Figure 26. CD44 knockdown produced a slight reduction of the 786O- cell migration	107
Figure 27. CD44 knockdown didn't produce any changes in the invasion capacity of SN12C cells	108
Figure 28. CD44 knockdown produced a decrease in the invasion capacity of Ren13 cells ...	109

Figure 29. Invasion transwell assay developed in 786O- cells	110
Figure 30. Expression of CD44 protein and its downregulation in tumors generated from SN12C shCD44-1 cells	112
Figure 31. Expression of CD44 protein and its downregulation in tumors generated from 786O- shCD44-2 cells	115
Figure 32. Characterization of SN12C tumors through immunoassays	117
Figure 33. Characterization of 786O- tumors through Immunohistochemistry	118
Figure 34. Determination of the invasion in tumors generated from SN12C shCD44-1 cells ...	120
Figure 35. Determination of the invasion in tumors generated from 786O- shCD44-2 cells ...	121
Figure 36. Migration effects of Perifosine in Ren13 WT cells	124
Figure 37. Migration effects of Ruxolitinib in Ren13 WT cells	125
Figure 38. Migration effects of Bosutinib in Ren13 WT cells	126
Figure 39. Migration effects of Ruxolitinib and doxycycline in Ren13 cells	128
Figure 40. Ruxolitinib inhibited the JAK/Stat signaling pathway	129
Figure 41. Migration effects of Bosutinib and doxycycline in Ren13 cells	131
Figure 42. Invasion transwell assay to determine the effect of Bosutinib in Ren13 cells	132
Figure 43. Bosunitinb inhibited the Src signaling pathway.....	133
Figure 44. CD44 silencing didn't affect the Src signaling pathway	134
Figure 45. Representation of Hyaluronic Acid	135
Figure 46. Representation of the interaction between CD44 and Hyaluronic Acid.....	136
Figure 47. Ren13 cell cultured in normal conditions expressed Hyaluronic Acid	137
Figure 48. Hyaluronic Acid was expressed in SN12C tumors.....	138
Figure 49. Hyaluronic Acid was expressed in 786O- tumors	139
Figure 50. Hyaluronidase didn't affect the migration capacity of cells.....	140
Figure 51. Hyaluronidase in combination with doxycycline didn't affect the migration capacity of cells.....	141
Figure 52. The CD44 blocking antibody IM-7 didn't affect the migration capacity of cells	142
Figure 53. Hyaluronan fragment didn't produce changes in the migration capacity of cells ...	143
Figure 54. Hyaluronic Acid fragments didn't produce changes in the protein expression	144
Figure 55. Diagram of the process followed to find some other candidates able to bind or interact with CD44.....	145
Figure 56. Correlation between CD44 and the candidate genes	146
Figure 57. CD44-SRGN interaction and signaling	148

Figure 58. Expression of Serglycin in different cell models	149
Figure 59. Expression of Serglycin in different cell models where CD44 is downregulated	149
Figure 60. RNA levels of human SRGN in different cells	150
Figure 61. Serglycin was expressed in tissue tumor samples	151
Figure 62. Serglycin expression in induced and non-induced Ren13 shCD44-1 cells	152
Figure 63. Serglycin expression in induced and non-induced 786O- shCD44-2 cells	153
Figure 64. Survival probability of kidney renal clear cell carcinoma patients over time depending on the CD44 expression	154
Figure 65. Expression of CD44 in untreated and Sunitinib-treated patients	155
Figure 66. Survival probability of kidney renal clear cell carcinoma patients over time depending on the Serglycin expression	156
Figure 67. Expression of Serglycin in untreated and Sunitinib-treated patients	156
Figure 68. Expression of Serglycin depending on ALDH1A3	157

LIST OF TABLES

Table 1. WHO Classification of RCC	30
Table 2. Nuclear grade classification of Renal Cell Carcinoma	32
Table 3. Stages of Renal Cell Carcinoma (RCC)	33
Table 4. List of the most common antiangiogenic drugs used in the clinic	39
Table 5. List of cell lines derived from human tissue used	69
Table 6. List of primary cell lines derived from PDOX	69
Table 7. Mediums used for cell culture	70
Table 8. Oligonucleotides used for the detection of mycoplasma contamination	71
Table 9. Inhibitors used for <i>in vitro</i> assays.....	72
Table 10. Hyaluronic Acid oligosaccharides used for <i>in vitro</i> assays.....	73
Table 11. Specific probes used in TaMan® analyses	74
Table 12. Primary antibodies used for Western Blot	77
Table 13. Primary antibodies used for protein detection by Immunocytofluorescence	78
Table 14. Secondary antibodies used for protein detection by Immunocytofluorescence	78
Table 15. Primary antibodies used for protein detection by Immunohistochemistry.....	88

SUMMARY

The arrival of antiangiogenic therapies represented a huge advance in the treatment of different tumors, such as renal carcinoma. However, despite initial good results, some tumors were able to develop different mechanisms to adapt to the new conditions and continue growing. Thus, resistance to the antiangiogenic drugs appeared. Moreover, preclinical studies showed that some tumors increased their invasive and metastatic capacity after the therapy. Different murine orthoxenografts models, derived from patients with renal carcinoma, were developed to characterize the response to the antiangiogenic treatment. Both drugs used, DC101 and Bevacizumab, produced a reduction of the tumor growth and its volume, as well as a reduction of the number of vessels. However, when tumor invasion was evaluated, it could be observed that not all tumor models responded equally. While some tumors showed a higher metastatic capacity and an increase in invasiveness and aggressiveness after the treatment, others did not show any alteration of their characteristics.

To study the mechanisms involved in the increase of tumor malignization, different assays comparing the gene expression of non-invasive and pro-invasive tumors after the antiangiogenic treatment were developed. These analyses generated a list of candidate genes that could be responsible for the invasive process, with CD44 among them.

In this thesis, we have studied the role of CD44 in the tumor invasion and migration processes using *in vitro* and *in vivo* models of renal carcinoma. We have explored the signaling pathway that could be induced due to the CD44 activation. The Src signaling route was possibly shown to be involved in the invasive process of cancer cells. The mechanism responsible for CD44 activation has also been investigated. Between different candidates, Serglycin appeared as a possible ligand and inducer of CD44. Thus, this thesis opens different study ways to determine the molecules responsible for tumor invasion after antiangiogenic treatment and develop new different strategies to overcome the resistance.

RESUM

L'aparició de les teràpies antiangiogèniques va suposar un gran avenç en el tractament de diferents tipus de tumors, com és el cas del carcinoma renal. Tot i els bons resultats que presentaven inicialment, els tumors han estat capaços de desenvolupar diferents mecanismes per tal d'adaptar-se a les noves condicions i continuar creixent. D'aquesta manera, a la llarga acaba apareixent resistència als fàrmacs antiangiogènics. A més, estudis pre-clínic han demostrat que alguns tumors presenten un increment de la seva capacitat invasiva i metastàtica després de la teràpia.

Diferents models murins d'ortoxenoempelts derivats de pacients amb carcinoma renal es van desenvolupar per caracteritzar la resposta al tractament antiangiogènic. Ambdós fàrmacs utilitzats, DC101 i Bevacizumab, van produir una reducció del creixement i del volum tumoral, així com una reducció en el nombre de vasos sanguinis. Tot i així, en el moment d'avaluar la invasió tumoral, es va veure que no tots els models responien de la mateixa manera. Mentre uns tumors mostraven un caràcter més invasiu i agressiu després del tractament juntament amb un increment de la capacitat metastàtica, un altre grup de tumors no presentava cap alteració de les seves característiques.

Per estudiar el mecanisme implicat en aquest increment de la malignització tumoral, es van dur a terme diferents assajos per comparar l'expressió gènica dels tumors pro-invasius abans i després del tractament. Aquests anàlisis van generar un llistat de gens candidats a ser responsables del procés invasiu, d'entre els quals s'hi trobava CD44.

En aquesta tesi s'ha estudiat el paper de CD44 en el procés d'invasió i migració tumoral utilitzant models *in vitro* i *in vivo* de carcinoma renal. S'ha estudiat la via de senyalització induïda per l'activació de CD44 i s'ha vist que la via de Src podria estar involucrada en el procés invasiu de les cèl·lules cancerígenes. També s'ha intentat dilucidar el mecanisme responsable de l'activació de CD44. D'entre diferents candidats, la Serglicina ha aparegut com a possible lligand i inductor de CD44. Així doncs, amb aquesta tesi diferents fronts d'estudi s'han obert per determinar els responsables de la invasió tumoral després del tractament antiangiogènic i desenvolupar noves estratègies per combatre-la.

INTRODUCTION

1. CANCER

Every year, 14 million new cases of cancer are detected globally and 9.6 million people die from the disease. In Europe, more than 3.7 million new cases of cancer are diagnosed annually and it is responsible for 1.9 million deaths. Cancer is the second leading cause of death and morbidity after cardiovascular diseases (“World Health Organization,” 2020). Given these adverse statistics, it has never been more important to understand and fight against cancer.

Cancer is described as a set of diseases with a common characteristic: the uncontrolled growth of cells. Under normal physiological conditions, cells grow and divide. This generates new cells that will replace the oldest ones when they die or become damaged (“Instituto Nacional del Cancer,” 2020).

During cancer progression, this balance is disturbed and becomes out of control. New unnecessary cells are generated while the oldest cells do not die. This instability leads to the formation of an abnormal cellular mass and eventually a tumor mass (“Instituto Nacional del Cancer,” 2020).

The genetic modification of cells is the main cause of cancer. These alterations can be inherited genetically or can appear due to errors during cellular division processes or DNA damage caused by environmental exposure (Pearson & Van Der Luijt, 1998). Each type of cancer from each individual patient presents unique genetic changes, complicating their treatment (Pearson & Van Der Luijt, 1998).

Genetic changes that contribute at the onset of cancer normally affect three principal types of genes: proto-oncogenes, tumor suppressor genes, and DNA repair genes. These genes are implicated in the regulation of cell growth and division, and in the DNA damage repair that could occur in some cells (Pearson & Van Der Luijt, 1998).

Epigenetic alterations can also activate the oncogenes and/or inhibit the tumor suppressor genes, increasing the cell proliferation ratio and reducing the apoptosis of malignant cells (Baeriswyl & Christofori, 2009).

Moreover, cancer cells can detach from the mass of origin and migrate to distal organs through the circulatory or lymphatic system. In the new organ, these cells can proliferate and generate a new tumor with the same molecular features of the primary tumor. This process is known as metastasis and is the main cause of death in patients suffering from cancer (“Instituto Nacional del Cancer,” 2020).

1.1 RENAL CELL CARCINOMA

According to the National Cancer Institute (NCI), renal cancer is the eighth most common type of cancer (“National Cancer Institute,” 2020).

When the tumor is localized in the kidney and detected at the initial stages of the disease, the 5-years relative survival rate of patients is about 74,8%. However, as the tumor progresses, the survival rate of patients is drastically reduced (“National Cancer Institute,” 2020).

Renal cell carcinoma (RCC) includes a heterogeneous group of cancers, which have different molecular and genetic alterations from the epithelial cells of the renal tubules (Capitaniao & Montorsi, 2016; Hsieh, Le, Cao, Cheng, & Creighton, 2018). Although it can be a sporadic or hereditary disease, in both cases there is a common structural alteration of chromosome 3, specifically in its short arm (Capitaniao & Montorsi, 2016).

Patients suffering from RCC normally present flank pain, hematuria, and a palpable abdominal mass. Other symptoms such as fatigue, weight loss, and anemia can also appear. All these manifestations are useful for tumor detection (Cohen & McGovern, 2005).

The incidence of RCC increases with age and men are at higher risk than women of developing the disease (Hsieh et al., 2017). Other risk factors associated with RCC include smoking, obesity, and hypertension (Cohen & McGovern, 2005). Chronic kidney disease, hemodialysis, kidney transplantation, acquired kidney cystic disease, and diabetes mellitus are other medical conditions associated with RCC (Hsieh et al., 2017).

The initial tumor mass is usually localized in the kidney. However, due to blood flow, cells can migrate and colonize other distal organs, leading to metastasis. The most frequent sites where metastasis occurs are lungs, bones, and brain. In some cases, the adrenal glands, contralateral kidney, and liver can also be affected. At the moment of diagnosis, more than 17% of patients show metastasis, which compromises their prognostic (Capitanio & Montorsi, 2016).

1.2 CLASSIFICATION OF RENAL CELL CARCINOMA

RCC comprises of more than 10 subtypes of renal cancers (Table 1). The World Health Organization (WHO) classifies the different subtypes of renal cancer according to their cytology, architectural, immunohistochemical, cytogenetic, and molecular features (Hsieh et al., 2018).

Subtypes of Renal Cell Carcinoma
Clear cell renal cell carcinoma
Multilocular cystic renal neoplasm of low malignant potential
Papillary renal cell carcinoma
Hereditary leiomyomatosis and renal cell carcinoma associated renal cell carcinoma
Chromophobe renal cell carcinoma
Collecting duct carcinoma
Renal medullary carcinoma
MiT family translocation renal cell carcinomas
Succinate dehydrogenase deficient renal cell carcinoma
Mucinous tubular and spindle cell carcinoma
Tubulocystic renal cell carcinoma
Acquired cystic disease-associated renal cell carcinoma
Clear cell papillary renal cell carcinoma

Unclassified renal cell carcinoma
Papillary adenoma
Oncocytoma

Table 1. WHO Classification of RCC. Table adapted from Moch, Cubilla, Humphrey, Reuter, & Ulbright, 2016.

The most common subtypes of RCC are clear cell renal cell carcinoma, papillary renal cell carcinoma, and chromophobe renal cell carcinoma. These three pathologies represent 85-90% of all renal malignancies (Capitanio & Montorsi, 2016).

1.2.1 Clear cell Renal Cell Carcinoma (ccRCC)

83% of RCC cases are represented by ccRCC, the most common subtype of the disease. It is believed that cells responsible for the ccRCC originate from the renal proximal epithelial cells, but the origin and differentiation process that occurs is still unknown (Tun et al., 2010).

Histologically, ccRCC is characterized as showing clear cell morphology due to the accumulation of lipid and glycogen inside the cytoplasm of cells, as shown in Figure 1 (Tun et al., 2010). Typically, this type of tumor is highly vascularized (Hsieh et al., 2018). ccRCC cells are different from the normal epithelial cells of the kidney. These malignant cells have lost the differentiation capacity required to adopt the necessary functions for the proper functioning of the kidney. Histologically, it can be observed by a lack of the tubular architecture typical from the epithelial cells (Tun et al., 2010).

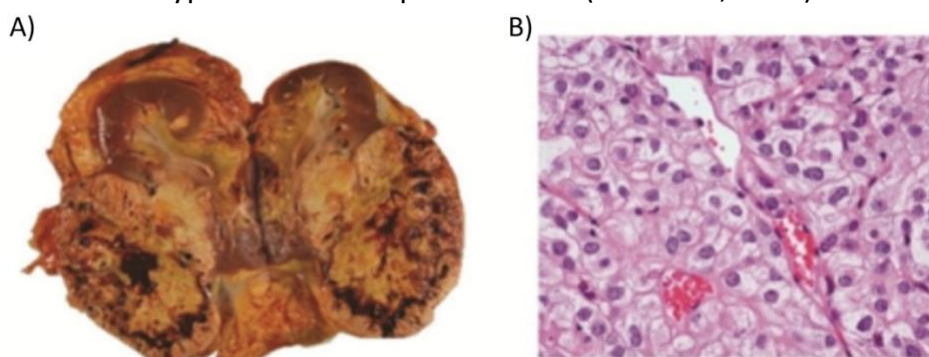


Figure 1. clear cell Renal Cell Carcinoma (ccRCC). A) Picture of a human kidney with a tumor. B) Image of Hematoxylin-Eosin staining of a ccRCC tumor at 20X.

The most important biological alterations in ccRCC are: the loss of renal function; the downregulation of various metabolic pathways, which alters normal renal function; and the activation of immune pathways (Tun et al., 2010).

This type of cancer is also characterized by presenting particular genomic mutations. The von Hippel-Lindau (VHL) gene is a tumor suppressor gene that presents somatic or epigenetic mutations in more than 80% of ccRCC cases (Capitanio & Montorsi, 2016). VHL gene codifies for VHL protein, responsible for inhibiting the hypoxia-inducible gene (HIF). HIF protein is activated under low oxygen stress conditions, promoting the activation of its target, responsible for regulating encoding proteins involved in angiogenesis, cell growth, glucose uptake, and acid-base balance. In the absence of VHL protein, HIF proteins accumulate. Consequently, these processes are uncontrolled and the proliferation of epithelial cells is favored (Cohen & McGovern, 2005; Arjumand & Sultana, 2012). For that reason, mutations in the VHL gene contributes to tumorigenesis, even under normoxic conditions (Linehan & Zbar, 2004).

1.3 HISTOLOGICAL CLASSIFICATION OF RCC

Over the years, various different systems have been proposed to classify RCC. The most frequently used was the Fuhrman Grading System (FGS) proposed in 1982. This system classified tumors depending on the nuclear size, shape and nucleolar prominence of their cells. However, this grading method did not take into account the chromophobe RCC and the new subtypes of renal carcinomas. For that reason, in 2016 WHO in accordance with the International Society of Urological Pathology (ISUP), proposed another grading system valid for the majority of renal cell carcinoma subtypes (Table 2). However, it has not yet been validated for tumors with few reported cases (Moch et al., 2016).

WHO/ISUP grading system for RCC	
Grade	Description
Grade 1	Nucleoli absent or inconspicuous and basophilic at 40X
Grade 2	Nucleoli not prominent at 10X but visible and eosinophilic at 40X
Grade 3	Nucleoli conspicuous and eosinophilic at 10X
Grade 4	Extreme nuclear pleomorphism, multinucleated cells, rhabdoid or sarcomatoid differentiation

Table 2. Nuclear grade classification of Renal Cell Carcinoma. Table adapted from Moch et al., 2016.

1.4 CLINICAL CLASSIFICATION OF RCC

In the clinics, RCC is classified in different stages depending on the results obtained during a physical exam, biopsy and imaging test or -if surgery takes place- by examining the tissue removed (“American Cancer Society,” 2020).

The most common staging system to classify solid tumors (including RCC) is the American Joint Committee on Cancer (AJCC) TNM system. It is based on the information of three principal tumor features:

- T from tumor → the size and extent of the main tumor.
- N from nodes → the extension to adjacent lymph nodes.
- M from metastases → the extension to distant organs.

Each letter is provided with a number indicating the progression of the disease. The higher is the indicator value, the more advanced is the disease (“American Cancer Society,” 2020).

Classification of RCC is important for the prognosis and treatment of the disease. There are four different stages based on the tumor size, the extent of the invasion into the

kidney, the involvement of lymphatic nodes, and the distant metastasis (“American Cancer Society,” 2020) (Table 3).

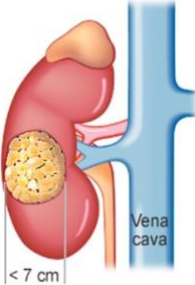
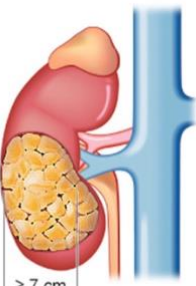
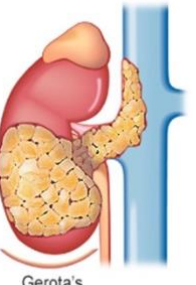
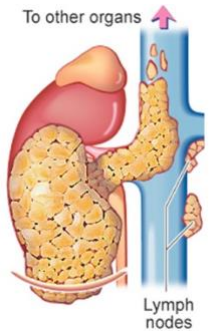
Stage	Description	Schematic representation
Stage I	Tumor is found only in the kidney and is 7cm or smaller	
Stage II	Tumor is found only in the kidney and is larger than 7cm	
Stage III	Tumor has spread from the kidney to the surrounding tissue or nearby lymph nodes	
Stage IV	Tumor has spread outside the kidney to multiple lymph nodes and/or other organs	

Table 3. Stages of Renal Cell Carcinoma (RCC). RCC tumors are classified in four different stages depending on the progression and extension of the disease. Images are adapted from “New Health Advisor,” 2020.

1.5 RCC TREATMENT

Surgery is the fold treatment of choice in RCC. This is because it is only in re-sectioning the tumor mass that it is possible to cure the disease completely. The surgery is comprised of a partial or radical nephrectomy (Hsieh et al., 2018; Ljungberg et al., 2007). However, this procedure can only be executed when the tumor is localized, locally advanced, or has limited metastasized (Grimm, Wolff, Zastrow, Fröhner, & Wirth, 2010). Tumors bigger than 7cm and those presenting local invasion have more potential to become malignant and invade other organs through the vascular system (Rini, Campbell, & Escudier, 2009). Approximately 30% of patients will present metastasis at the time of diagnosis and another 30% of the cases previously subjected to surgery will eventually develop metastasis (Hsieh et al., 2018).

The concern around metastatic renal cell carcinoma (mRCC) means that different therapeutic strategies are required to beat the disease. These therapeutic strategies are divided according to the chemical features of the compounds and the targets they are guided to. The different treatments against mRCC are explained in section 2.

2. ANGIOGENESIS

Tumors, like other tissues and organs, need the support of nutrients and oxygen to feed their cells. Once the tumor mass reaches a critical size, the normal vasculature of the organism is not enough to feed all their cells. The apoptosis and necrosis processes are initiated, which leads to a reduction of tumor growth. However, they can overcome the situation and continue proliferating. Tumors are able to take advantage of pre-existing blood vessels and generate new ones, which are responsible for the uptake of oxygen and nutrients necessary to feed their cells. This process is known as tumor angiogenesis (Baeriswyl & Christofori, 2009; Bergers & Benjamin, 2003). Moreover, these new blood vessels not only contribute to tumor growth and maintenance, but also provide tumor cells with an escape route to colonize other organs and give rise to metastasis (Baeriswyl & Christofori, 2009).

Angiogenesis is a balanced process between the expression of pro-angiogenic and anti-angiogenic factors. When this balance is in favor of pro-angiogenic factors, the “angiogenic switch” occurs (Bergers & Benjamin, 2003). The “angiogenic switch” refers to the transition from pre-vascular hyperplasia to highly vascularized and progressively outgrowing tumors (Baeriswyl & Christofori, 2009). This process can happen during different stages of tumor progression; it depends on the expression of different pro-angiogenic factors, such as the tumor type and its environment (Bergers & Benjamin, 2003). Figure 2 shows the different pro- and anti-angiogenic factors involved in the angiogenic switch.

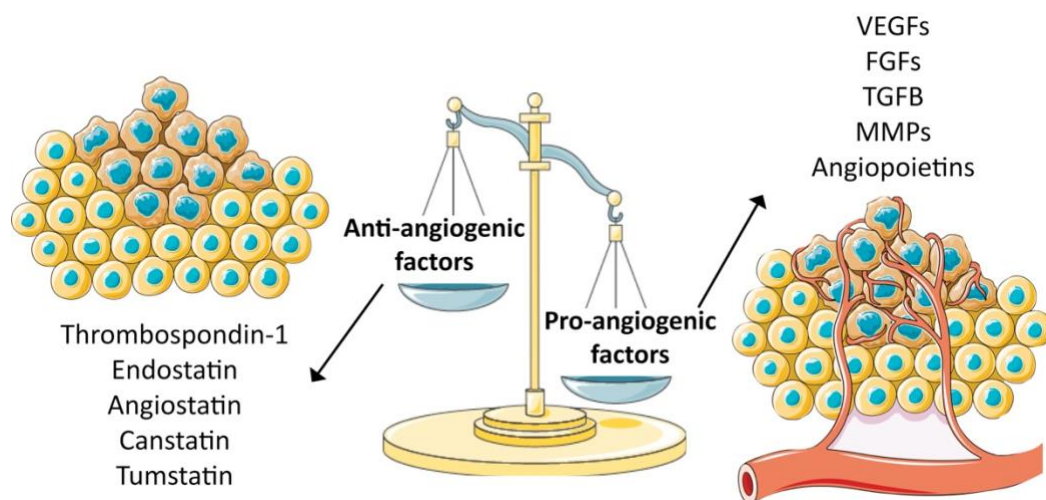


Figure 2. Representation of the angiogenic switch. Image representing the different anti- and pro-angiogenic factors involved in the regulation of the angiogenesis process. When the balance bends to the pro-angiogenic factors, the angiogenic switch happens producing an increase in the vascularization, growth and metastatic potential of tumor cells.

Angiogenesis is required during physiological events such as the recovery of damaged tissue or pregnancy. Blood vessels created during these conditions are mature and quickly become stable, finding the equilibrium between the pro- and anti-angiogenic secreted factors. In tumors, this balance does not exist. Blood vessels fail to mature but instead continue to grow at an uncontrolled rate. These new blood vessels have irregular shapes, increased permeability, vessel dilatation, abnormal spacing and decreased or abnormal pericyte coverage. Moreover, they show mixed features of venules, arterioles and capillaries (Bergers & Benjamin, 2003; Carmeliet, 2000; Ellis & Hicklin, 2008).

There are different pro-angiogenic factors that can contribute to tumor angiogenesis. The most important one is VEGFA (commonly called VEGF (Vascular Endothelial Growth Factor)), which belongs to a gene family that includes PLGF (Placental Growth Factor), VEGFB, VEGFC and VEGFD (Baeriswyl & Christofori, 2009; Ferrara, Gerber, & LeCouter, 2003).

VEGF expression is induced during physiopathological events due to the lack of oxygen production. The main hypoxia response mediator factor and consequently the most studied is HIF-1. Accumulation of this factor, in particular of HIF-1 α , stimulates the transcription of VEGF among other growth factors. This process, as explained in Section 1.2.1, is characteristic of pathologies where the VHL gene is mutated and consequently unable to degrade HIF-1 α , such as ccRCC (Baeriswyl & Christofori, 2009; Iyer et al., 1998; Semenza, 2007).

However, VEGF expression can also be upregulated by other factors like TGF- α and - β (Transforming Growth Factor), EGF (Endothelial Growth Factor) or IGF-1 (Insulin-like Growth Factor) (Ferrara et al., 2003).

VEGFR-1 and VEGFR-2 are the main receptors of VEGF. VEGFR-3 also exists, but it is not the receptor for VEGF (Ferrara et al., 2003).

Other important factors that contribute to angiogenesis are FGF-1 (Fibroblast Growth Factor) and -2 and PDGF-B (Platelet Derived Growth Factor) and -C. These factors induce proliferation and migration of endothelial cells (Baeriswyl & Christofori, 2009). Angiopoietin-2 also helps the angiogenic process avoiding the maturation of blood vessels, so they can continue growing (Baeriswyl & Christofori, 2009).

The discovery of the role of angiogenesis in RCC and the subsequent emergence of antiangiogenic therapies was a turning point in the treatment of this type of cancer.

2.1 ANTIANGIOGENIC THERAPIES

Tumor reliance on angiogenesis and the contribution of the stroma to its growth were big steps to develop new therapeutic strategies. These therapies aimed at targeting the cells that support the tumor, rather than the cells belonging to the tumor mass (Jiménez Valerio & Casanovas, 2013; De Falco, 2014).

This has led to the production of different antiangiogenic drugs, which target the endothelial cells that contribute to tumor development. Recently, there have been found to be some drugs that target other cell types from the microenvironment of the tumor, such as pericytes, which cover the blood vessels and contribute to their maturation and stability (Jiménez Valerio & Casanovas, 2013).

Antiangiogenic drugs can be classified into two groups depending on their mechanism of action: drugs with a direct effect and drugs with an indirect effect.

On the one hand, direct drugs affect the proliferation and migration of endothelial cells avoiding those effects. Moreover, they also prevent cell death in response to the expression of different proangiogenic proteins. On the other hand, drugs with an indirect effect prevent the expression or block the activity of proteins that contribute to the activation of angiogenesis (Al-Husein, Abdalla, Trepte, DeRemer, & Somanath, 2012).

There are antiangiogenic drugs with different targets. As previously described, VEGF is the main factor involved in the angiogenic process. For that reason, VEGF and its receptor (VEGFR) are the most interesting targets for tumor treatment. Bevacizumab is an example of a human monoclonal antibody against VEGF ligand. It inhibits the activation of its receptors expressed in endothelial cells surface (Rini et al., 2009; Harshman & Srinivas, 2010). This drug was the first to show clinical benefits on the treatment of mRCC (Harshman & Srinivas, 2010; Jiménez Valerio & Casanovas, 2013).

Furthermore, there are inhibitors of multiple tyrosine kinase receptors, which includes VEGFR. Sorafenib and Sunitinib are two drugs targeting this kind of receptors that show the best antiangiogenic activity. This is why they became the most used in the clinic

(Jiménez Valerio & Casanovas, 2013). Sorafenib is a small molecule inhibitor of multiple kinases. It mainly inhibits the Raf family non-receptor kinase, but can also act by blocking the activation of VEGFR2 (VEGF receptor 2), VEGFR3, Flt-3, c-KIT, B-RAF and PDGFR (PDGF receptor) (Rini et al., 2009; Larkin & Eisen, 2006). Sunitinib is another tyrosine kinase inhibitor with antitumor effects. This small molecule targets VEGFR1 and 2, Flt-1 and 3, PDGFR, c-KIT and RET kinase 1 (Rizzo & Porta, 2017; Ljungberg et al., 2007).

Other approved inhibitors of tyrosine kinases that are used as first and second-line treatments for mRCC include: Pazopanib, Azitinib, Lenvatinib, and Cabozantinib (Hsieh et al., 2017).

FGF, PDGF and ECGF and their respective receptors FGFR, PDGFR and ECGFR are also important targets to inhibit in order to achieve a reduction of the antiangiogenic activity of tumors. These growth factors are important for the functionality of organs and the normal vasculature. It was seen that genetic alterations of them (or their receptors) enhance tumor growth. For that, inhibitors of multiple tyrosine kinase receptors are more effective than those with a unique target (De Falco, 2014).

The superfamily of semaphorins is also reported to be involved in angiogenesis and tumor progression. Not only do semaphorins control different processes such as proliferation, survival, adhesion, and invasion of tumor cells, but they can also be implicated in migration and survival of endothelial cells, contributing to tumor dissemination. Inhibitors of some of these glycoproteins are used as antiangiogenic therapies (Al-Husein et al., 2012; De Falco, 2014).

Finally, there are growth factors that promote angiogenesis, stabilizing and helping the new blood vessel to form from pre-existing ones. They also take part in the vascular maturation. These factors are angiopoietins. Angiopoietin-2 cooperates with VEGF, stimulating angiogenesis and tumor progression. This means that antibodies capable of neutralizing it also came out as a good therapy (Jiménez Valerio & Casanovas, 2013; Al-Husein et al., 2012).

Despite their involvement in angiogenesis, targeting drugs against semaphorins and angiopoietins are not the most common antiangiogenic therapies. Table 4 shows a summary of the antiangiogenic drugs most commonly used in the clinic and their main indications.

Drug	Inhibitor type	Indication
Bevacizumab (Avastin)	Monoclonal antibody targeting VEGFA or VEGF	<ul style="list-style-type: none"> → Metastatic colorectal cancer (1st/2nd line) → Non-small cell line cancer (1st line) → Recurrent glioblastoma (1st line) → Metastatic renal cell carcinoma (1st line) → Wet age-related macular degeneration (off-label)
Sorafenib (Nexavar)	Tyrosine kinase inhibitor targeting VEGFRs, PDGFRs, FGFR1, KIT, RAF	<ul style="list-style-type: none"> → Metastatic renal cell carcinoma (1st line) → Unresectable hepatocellular carcinoma (1st line)
Sunitinib (Sutent)	Tyrosine kinase inhibitor targeting VEGFRs, PDGFRs, KIT, FLT3	<ul style="list-style-type: none"> → Metastatic renal cell carcinoma (1st line) → Gastrointestinal stromal tumor (2nd line) → Unresectable pancreatic neuroendocrine tumors (1st line)
Pazopanib (Votrient)	Tyrosine kinase inhibitor targeting VEGFRs, PDGFRs, KIT	<ul style="list-style-type: none"> → Metastatic renal cell carcinoma (1st line) → Advanced soft tissue sarcoma (2nd line)
Cabozantinib (Cometriq)	Tyrosine kinase inhibitor targeting VEGFRs, RET, MET	<ul style="list-style-type: none"> → Progressive medullary thyroid cancer (1st line)

Table 4. List of the most common antiangiogenic drugs used in the clinic. Antiangiogenic drugs that are usually used in the clinic describing their targets and their main indications. Table adapted from De Falco, 2014.

2.2 OTHER THERAPIES

Although antiangiogenic therapies are the gold treatment in the clinics to beat RCC, there are new therapeutic strategies currently being explored.

2.2.1 Immunotherapy

Some cytokines such as Interleukine-2 (IL-2) and Interferon-alpha (INF- α) were the first standard treatment for mRCC patients. However, both therapeutic agents only benefit a defined group of patients. Moreover, their administration can produce toxic side effects (Ljungberg et al., 2007).

Later, a new generation of immunotherapeutic drugs called T cell immune checkpoint inhibitors came out. Some examples are Avelumab and Atezolizumab, two antibodies against the cell death protein-1 ligand (PDL-1). Other antibodies against the programmed cell death protein-1 (PD-1) such as Nivolumab and Pembrolizumab were also discovered (Hsieh et al., 2017).

The cytotoxic T lymphocyte-associated protein 4 (CTLA4) became another target to treat mRCC. Antibodies such as Ipilimumab, responsible for lymphocyte T activation through blocking CTLA4 are other immunotherapeutic strategies that have recently appeared (Hsieh et al., 2017; Motzer et al., 2019).

2.2.2 Targeted therapies

As previously explained, antiangiogenic drugs are the main targeted therapies. Nevertheless, understanding the molecular biology of RCC and other tumor types, allowed the mTOR pathway inhibitors (indicated for breast cancer) such as Temsirolimus and Everolimus to also be suitable for the treatment of some mRCC (Ljungberg et al., 2007; Rini et al., 2009).

2.2.3 Combined therapies

The previously described treatments have not always been effective. This is why recently, a combination of different strategies have been studied in order to improve the

progression-free survival (PFS) and the overall survival (OS) of the patients (Hsieh et al., 2017).

In Figure 3 there is a representation of the different treatments approved to treat metastatic renal cell carcinoma that appeared over time.

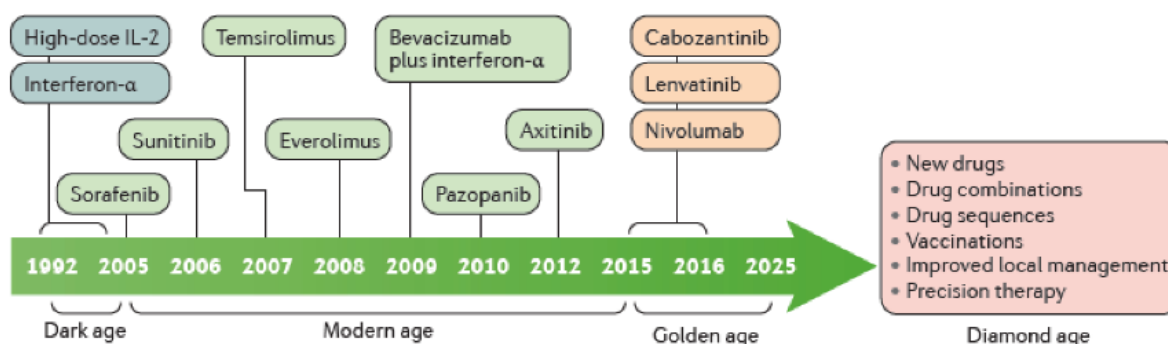


Figure 3. Treatment evolution of metastatic renal cell carcinoma over time. First treatments were basically immunotherapy. Since 2005 some new drugs appeared enhancing the treatment and the survival of patients. Finally, the golden age was characterized by the discovery of some monoclonal antibodies important for the cancer therapy. Nevertheless, new drugs are being investigated to overcome the limitations of the existing therapies. Figure extracted from Hsieh et al., 2017.

Despite the big effort of existing therapeutic strategies to treat mRCC, there still exists a great variability in treatment response. This is due to the heterogeneity that exists between tumors and even between different parts of the same tumor (Hsieh et al., 2018).

Election of the treatment will depend on the existing benefit-risk ratio of the different therapies for each tumor and individual patient. Selected drugs will provide the major benefit and minimize the side effects. The purpose of the treatment is always to increase the likelihood of patient survival and maximize their quality of life (Rini et al., 2009).

2.3 RESISTANCE TO ANTIANGIOGENIC THERAPIES

Drug resistance or resistance to therapy is commonly described as the progression of the disease according to RECIST criteria (Response Evaluation Criteria in Solid Tumors) despite treatment (Bielecka, Czarnecka, Solarek, Kornakiewicz, & Szczylik, 2013).

Tumors are sensitive to treatment when their survival depends on the signaling pathway targeted by that drug. Resistance to the therapy appears when tumors can grow independently from the activity of the pathway targeted by the therapy. This occurs due to some genetic alterations that inhibit the interaction between the drug and its target. Furthermore, sometimes the activation of other signaling pathways or the expression of some proteins that compensate the effect produced by the therapy are responsible for the resistance (Bielecka et al., 2013).

When antiangiogenic therapies were first established, they were considered so innovative and it was widely believed tumors would not show resistance to them. After all, these drugs do not target the genetically unstable tumor cells, but instead affect the endothelial cells responsible for the sustenance of the tumors. However, after pre-clinical studies, it was observed that tumors can become resistant to those therapies as well (Moserle, Jiménez-Valerio, & Casanovas, 2014).

There are two different types of resistance to antiangiogenic treatment: intrinsic resistance and acquired resistance (Jiménez Valerio & Casanovas, 2013).

2.3.1 Intrinsic Resistance

Intrinsic resistance is the failure of a tumor to respond to the therapy from the beginning of the treatment. In these cases, the tumors continue to grow normally and never respond to the therapy (Jiménez Valerio & Casanovas, 2013). Figure 4 shows a representation of the intrinsic resistance.

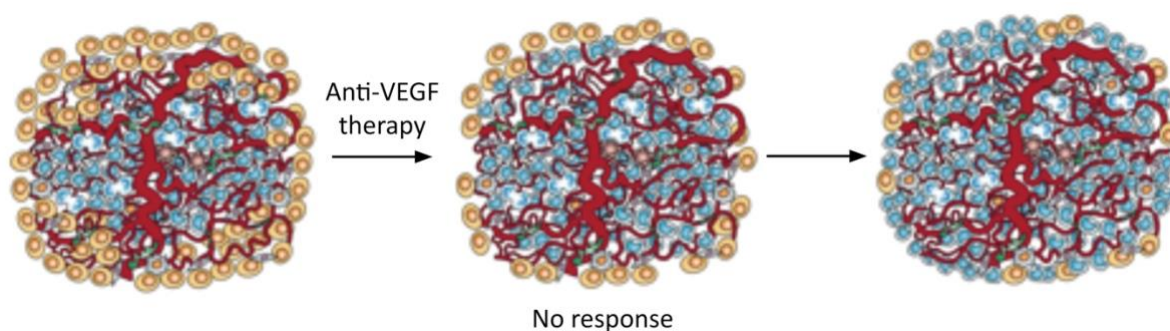


Figure 4. Representation of the intrinsic resistance. This type of resistance is a pre-existing condition characterized by the lack of a response to the antiangiogenic treatment. Tumors grow and progress as if they were not treated. Figure adapted from Bergers & Hanahan, 2008.

This type of resistance has been observed in tumors that, during their development and due to some microenvironment factors, displayed evasive mechanisms of resistance that were already activated. No type of response to the treatment is observed. There is no reduction of tumor growth, not even of its volume. Neither benefits of patient survival nor an improvement of their quality of life are noticed after the treatment (Bergers & Hanahan, 2008).

Intrinsic resistance to antiangiogenic treatment in ccRCC is not so common, but it can occur (Bielecka et al., 2013). It can be due to the dysregulation of the HIF pathway. HIF is usually activated in RCC and some genes codifying for pro-angiogenic factors controlled by this pathway are expressed, producing the reduction of the antiangiogenic therapy efficacy (Bergers & Hanahan, 2008; Jiménez Valerio & Casanovas, 2013).

Furthermore, some tumors have mechanisms independent of angiogenesis to maintain their growth. These mechanisms include: the co-option of pre-existing vessels;

vasculogenic mimicry; mosaic vessels; and the mobilization of latent vessels (Jiménez Valerio & Casanovas, 2013).

2.3.2 Acquired Resistance

The main difference between intrinsic resistance and acquired resistance is that the latter develops progressively, whereas for the former, tumors are resistant from the very beginning (Jiménez Valerio & Casanovas, 2013).

Acquired resistance has been described in mRCC after long term therapy with VEGFR inhibitors (Moserle et al., 2014).

Tumors showing acquired resistance, respond to the therapy at first, but after an initial period of effectiveness, they adapt to the treatment, overcome its effects and continue growing. Acquired resistance to antiangiogenic therapies is characterized as indirect and evasive. The activation of alternative mechanisms switches on angiogenesis processes, despite the treatment. Nevertheless, these mechanisms are reversible once therapy is discontinued (Jiménez Valerio & Casanovas, 2013; Bielecka et al., 2013). Figure 5 shows a representation of the acquired resistance.

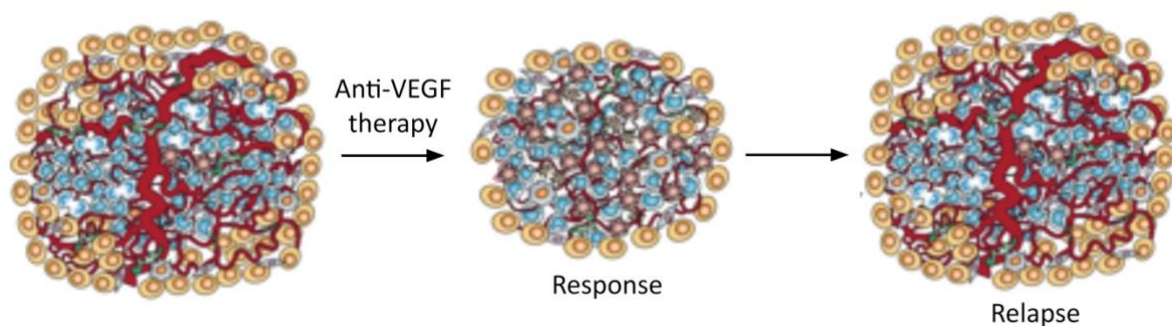


Figure 5. Representation of the acquired resistance. This type of resistance is characterized by an initial phase of response to the antiangiogenic treatment showing a reduction of the tumor grow, but after that period tumors relapse and regrows. Figure adapted from Bergers & Hanahan, 2008.

There are believed to be four different adaptive mechanisms that lead to tumors becoming resistant to antiangiogenic therapies. These mechanisms are: activation of alternative pro-angiogenic signaling pathways inside the tumor; recruitment of proangiogenic cells derived from the bone marrow; increase of the pericyte coverage of tumor vasculature to enhance its integrity; and activation and improvement of invasive and metastatic processes to reach the vasculature of normal tissue with no dependence of neovascularization processes (Bergers & Hanahan, 2008; Bielecka et al., 2013).

2.4 STRATEGIES TO OVERCOME ANTIANGIOGENIC RESISTANCE

Different clinical strategies have been investigated and are still being investigated to overcome resistance to antiangiogenic therapies.

The first suggestion to overcome resistance was to use a combination of drugs. This includes the combination of several targeting-drugs against different signaling pathways implicated in the angiogenic process, such as VEGF and FGF. There is also the possibility of using a unique drug with different targets (Moserle et al., 2014; Casanovas, Hicklin, Bergers, & Hanahan, 2005).

The combination of drugs to avoid the resistance induced by the hypoxia produced in the tumor has also been studied. Therefore, the usage of antiangiogenic drugs together with inhibitors of HIF-1 -which is the main responsible for tumor hypoxia- is another treatment strategy (Moserle et al., 2014).

As previously described, resistance to antiangiogenic treatment, in particular to acquired resistance, is reversible. Once treatment has stopped and time has elapsed, tumors can become sensitive to that treatment again. This observation led to thought about sequential treatments. The idea arose to use an antiangiogenic drug followed by the treatment with a non-antiangiogenic drug or chemotherapy. This would let the tumor re-sensitized and respond to the third treatment with another antiangiogenic drug (Moserle et al., 2014; Casanovas et al., 2005).

Combining different drugs or changing treatment once signals of resistance appear have shown benefits and improved the RCC treatment. These considerations have also helped to delay the emergence of resistance. Nevertheless, in some groups of patients, those therapies still fail (Moserle et al., 2014).

3. TUMOR MALIGNIZATION: INCREASE AGGRESSIVENESS AFTER ANTIANGIOGENIC THERAPY

As antiangiogenic therapies target blood vessels that nourish tumors, it was thought that these therapies would not only affect tumor volume and growth, but they would also produce a reduction of metastasis. Nevertheless, different studies have demonstrated that long-term treatment with antiangiogenic drugs produces an alteration of the tumor's nature. It not only causes the emergence of resistance, but makes tumors more invasive, and leads to an increase of lymphatic and hematologic metastasis (Moserle et al., 2014).

In some studies, using animal models, the increase of the invasion process after one week of antiangiogenic treatment was observed. However, this effect was even more notable when the treatment was maintained for four weeks. Moreover, the more aggressive the antiangiogenic therapy, the more intense the induced invasion (Pàez-Ribes et al., 2009).

It was observed that these tumors, which initially were encapsulated or showed micrometastases, were able to break the capsule and invade the acinar tissue surrounding them. There was seen to be an increase in their metastatic capacity and the lesions produced were bigger (Pàez-Ribes et al., 2009).

It was also noticed that the metastatic lesions showed hypoxia markers, suggesting the role of hypoxia in the tumor malignization process. However, it was observed that other mechanisms alternative to hypoxia could be involved in increased aggressiveness of tumors in response to antiangiogenic treatment (Moserle et al., 2014).

3.1 METASTATIC PROCESS

Metastasis is a multistep process through which cancerous cells, in groups or individually, disseminate from the primary tumor to a secondary organ or tissue (Deryugina & Quigley, 2006).

In order to reach the metastatic organ, tumor cells have to escape from the primary tumor, migrate through the surrounding tissue until the bloodstream, circulate inside it, arrive at a second organ, extravasate, and establish the metastatic locus in the new organ (process represented in Figure 6) (Deryugina & Quigley, 2006).

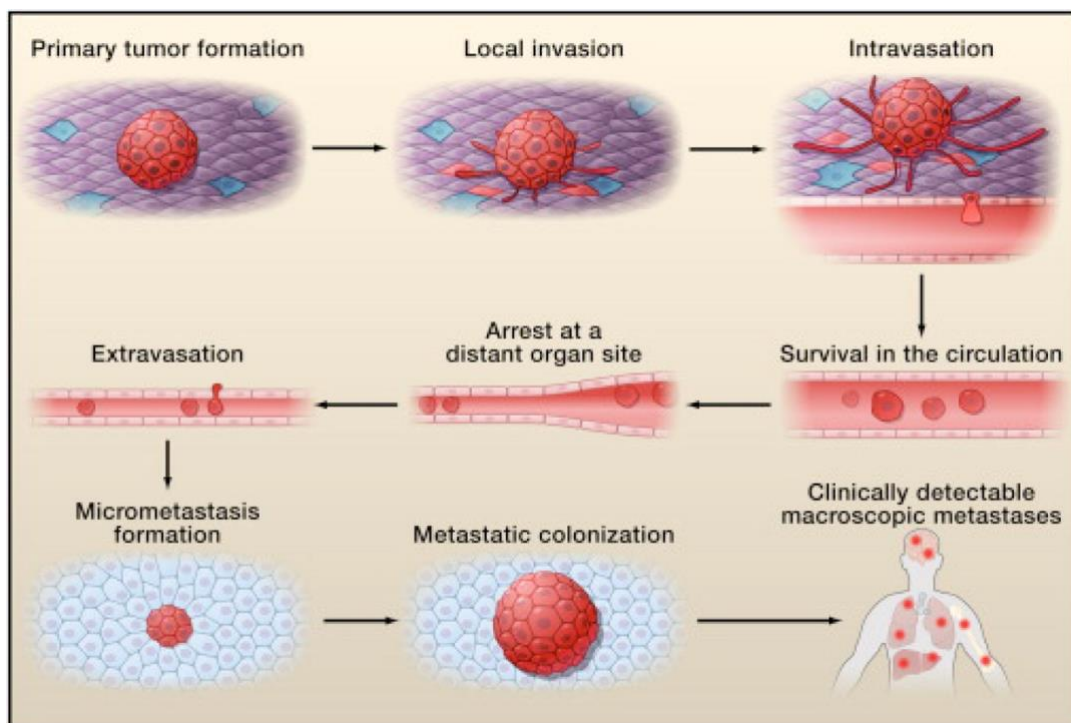


Figure 6. Representation of the metastasis cascade. To metastasize, tumor cells have to leave the primary tumor, survive in the circulation and finally colonize a second distant organ. Image adapted from Valastyan & Weinberg, 2011.

To carry out all those steps, cells have to suffer different genetic and epigenetic alterations and collaborate with other non-neoplastic cells from the stroma that help them to produce metastasis (Valastyan & Weinberg, 2011).

The first step to initialize metastasis is local invasion. In this process, tumor cells have to leave the primary tumor, invade the surrounding stroma, and consequently break the basement membrane (BM). The normal architecture of the epithelial tissue acts as a barrier that cells need to overcome to proceed with metastasis (Valastyan & Weinberg, 2011).

Then, cells have to be able to reach the bloodstream or lymphatic circulation to disseminate. This process is known as intravasation. Molecular changes have to be produced ease the crossing of cancerous cells through pericytes and endothelial cells that form the blood vessels. The neoangiogenesis process is also stimulated, which consists of the formation of new blood vessels in the local microenvironment to favor intravasation (Valastyan & Weinberg, 2011; Reymond, D'Água, & Ridley, 2013).

Once tumor cells are in the circulation (called then Circulating Tumor Cells or CTC), they have to survive to disseminate. Inside the bloodstream, cells overcome different stressful situations such as exposure to apoptosis, the damage produced by the hemodynamic forces in the circulation and the attack of the immune cells. For this reason, tumor cells cooperate with platelets that cover and protect them (Valastyan & Weinberg, 2011).

Afterwards, cells reach the organ of metastasis from the bloodstream, and the extravasation process has to be developed. Cells can eventually form a microcolony able to break the walls of the vessels and reach the new organ. They can also seep through endothelial cells and pericytes as in the intravasation process. To overcome the barriers and reach the destiny organ, primary tumors can secrete different factors that will arrive before tumor cells to the metastatic loci increasing vascular permeability to assist the extravasation process (Reymond et al., 2013).

Once cells have extravasated, they have to survive in the microenvironmental conditions of the metastatic loci, which tend to be quite different from the primary tumor. During the adaptation to the new metastatic organ, cancer cells set the “pre-metastatic niche” in order to get used to the new stromal cells, the components of the extracellular matrix

(ECM) and the growth factor and cytokines (Valastyan & Weinberg, 2011; Reymond et al., 2013). Primary tumors can secrete different growth factors at different possible metastatic locus. In response to these factors, tumor-associated cells such as hematopoietic progenitor cells and macrophages assemble to form the pre-metastatic niche, which will help the arrival of tumor cells through adhesion and invasion processes (Fidler, 2003).

The last step of metastasis is the colonization. It is known that not all tumor cells that reach a distal organ will produce metastasis. Moreover, it seems that most cells that produce metastasis could stay for weeks or even months forming microcolonies in a dormancy state until the moment they receive a stimulus that activate them (Valastyan & Weinberg, 2011).

It was observed that there exists biologic heterogeneity among cells of a single metastasis (intralesional heterogeneity) and among different metastasis (intralesional heterogeneity). These genetic and phenotypic variations of the cells are responsible for the different tumor growth, evolution, and target organ of metastasis. Nevertheless, metastasis is not only characterized by tumor cells features, but also by their microenvironment (Fidler, 2003).

There are some aspects and processes that are essential for metastasis. One of these is the endothelial to mesenchymal transition (EMT). During this process, epithelial cells lose polarity and cell-cell contact, and an intense modification of its cytoskeleton is produced. Thus, tumor cells lose epithelial cell features and adopt characteristics of the mesenchymal cells, improving migration processes (Kang & Massagué, 2004).

A group of pleiotropically acting transcription factors (TFs) carry out the EMT process, commonly known as EMT-TFs. Some of these TFs are Slug, Snail, Twist, ZEB1, and ZEB2. EMT-TFs play an important role in primary tumor growth and they are also important in invasion, dissemination, metastasis, and colonization of distal organs (Valastyan & Weinberg, 2011; Brabletz, Kalluri, Nieto, & Weinberg, 2018).

Nevertheless, once tumor cells reach the metastatic loci, in order to generate the secondary tumor, they must show epithelial cells characteristics. Therefore, mesenchymal to endothelial transition (MET) is produced, reversing the effects of EMT. EMT-MET are reversible processes that allows cells to express endothelial or mesenchymal features according to their situation (Brabletz, 2012).

3.2 ROLE OF EXTRACELLULAR MATRIX IN TUMOR MALIGNIZATION

The extracellular matrix (ECM) is an important component of the local microenvironment of the tumor. It is formed by a complex network of macromolecules that have different physic, biochemical, and biomechanical properties. During cancer development, this matrix is deregulated and disorganized affecting to the progression of the disease (Lu, Weaver, & Werb, 2012).

During normal development and tissue function of an organ, some mechanisms are responsible for the regulation of production, degradation and remodeling processes of ECM. When there is a disequilibrium of those processes, ECM is disorganized and consequently, there is an abnormal homeostasis and organ function (Lu et al., 2012).

ECM plays an important role in cancer among other diseases. It determines the behavior of the cells. Moreover, the deregulation of ECM compromises the physical barrier function of the basement membrane and promotes EMT, making tumor cell invasion easier (Lu et al., 2012). Some responsible agents for the alteration of ECM are stromal cells, including cancer-associated fibroblasts (CAFs) and immune cells. But there are also other cell types involved in this transformation, such as epithelial cells and mesenchymal stem cells (MSCs) (Psaila & Lyden, 2009).

Modifications of the ECM especially affects its biochemical properties. They potentiate the oncogenic effects of the different growth factors and modify the behavior of cells. Moreover, there is a change in the matrix architecture, that allows the differentiation of ECM from the normal stromal tissue (Lu et al., 2012).

To reiterate an earlier point, tumor cells have to survive, grow and invade. Thus, they lose their differentiation status and polarity, disrupt tissue integrity and corrupt stromal cells to grow and survive away from the primary tumor. Furthermore, some components of the ECM help them to evade the apoptotic process (Lu et al., 2012; Psaila & Lyden, 2009).

ECM also has an important role in tumor angiogenesis. Some fragments of the matrix collaborate with pro- or anti-angiogenic factors to determine the formation of vascular branches. The most important enzyme contributing to this process are matrix metalloproteinases (MMP), which degrade the vessel basement membrane improving cell invasion (Lu et al., 2012; Deryugina & Quigley, 2006).

The activity of ECM proteases is normally under very strict control, but cancerous cells can use some mechanisms to alter them and take advantage of their proteolytic properties on the basement membrane and interstitial extracellular matrices (Gupta & Massagué, 2006).

ECM not only has an important role in the primary tumor but it is also important in the pre-metastatic niche, contributing to hematopoietic progenitor cells recruitment (Lu et al., 2012; Psaila & Lyden, 2009).

4. PREVIOUS RESULTS

4.1 TUMOR MALIGNIZATION AFTER ANTIANGIOGENIC THERAPIES

As discussed in Section 2.1, antiangiogenic treatment emerged as a useful innovative strategy for the treatment of different types of tumor, such as Renal Cell Carcinoma. Thanks to this therapy it was possible to achieve an improvement of the PFS of the patients, defined as the period of time that a patient lives with a disease, but without progression (while it is being treated or after the treatment). It also demonstrated an increase in the objective response rate (ORR), defined as the percentage of patients with a tumor that is reduced or disappeared after the treatment (Rini et al., 2008; Motzer et al., 2009).

Despite the improvement in the treatment and the survival rate of cancer patients, tumors were able to overcome the therapy and continue to grow. Moreover, preclinical studies performed using murine models of different tumor types such as pancreatic neuroendocrine or glioblastoma, showed that, after treatment, tumors became more aggressive increasing their invasive capacity (Pàez-Ribes et al., 2009).

These results made us question whether renal tumors treated with antiangiogenic drugs would respond similarly. For this reason, a primary test using the ccRCC murine model 786O- was performed. A tumor piece derived from a patient with this tumor type was implanted orthotopically in the kidney of mice. Once grown, animals were divided into different treatment groups. One group was treated with DC101 (murine anti-VEGFR2), another group was treated with Bevacizumab (human anti-VEGF) and the third group did not receive any treatment (used as a control). All antiangiogenic treated mice showed a significant decrease in tumor growth, as expected. However, it also demonstrated an increase in the invasion and metastasis comparing both treatment groups with the control one. Obtained results (Figure 7) were similar to those previously observed with other tumor models.

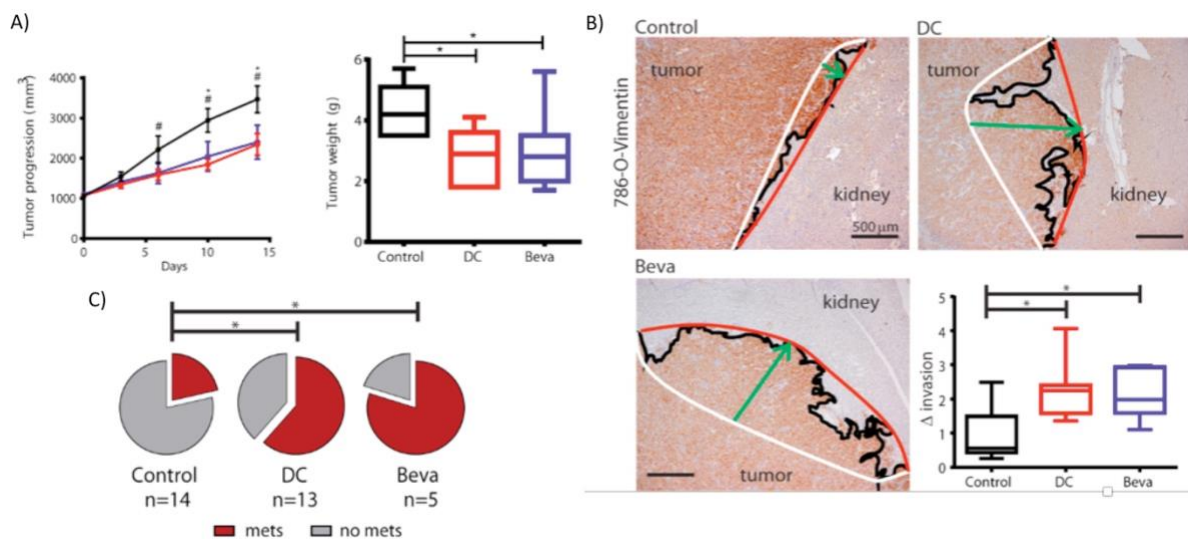


Figure 7. Effect of antiangiogenic therapy on tumor progression, invasiveness and metastatization in 786O- orthoxenograft tumor model. A) Evaluation of the antiangiogenic effect after 14 days of treatment through tumor progression during treatment and tumor weight at sacrifice. B) Representation of the invasive front of 786O- control and treated tumors. The graphic shows the quantification of the invasion. Mann Whitney test $p < 0,05^*$. C) Evaluation of the incidence of lung micrometastasis. Mann Whitney test $p < 0,05^*$. Image adapted from Moserle, L. et al. in preparation.

To get closer to the clinics and to validate this issue, different mice tumor models from renal tumor pieces derived from different patients were generated. Hence, it was possible to generate a set of primary tumor lines known as Ren-PDOX. They were able to recreate the same features as the original tumor pieces and they also maintained the metastatic properties. Another trait of the Ren-PDOX was that, when tumor pieces were implanted, human stroma was replaced by murine stromal components.

Once the Ren-PDOX lines were generated, four of them were selected to test and validate the effect of the antiangiogenic treatment. These lines were Ren13, Ren86, Ren50, and Ren28.

Mice implanted with these tumor models were treated with the two antiangiogenic drugs mentioned above, DC101 and Bevacizumab.

4.1.1 Efficacy of the antiangiogenic treatment

All animals treated with the antiangiogenic drugs showed a decrease in tumor growth noticed by palpation and loss of tumor weight as represented in Figure 8.

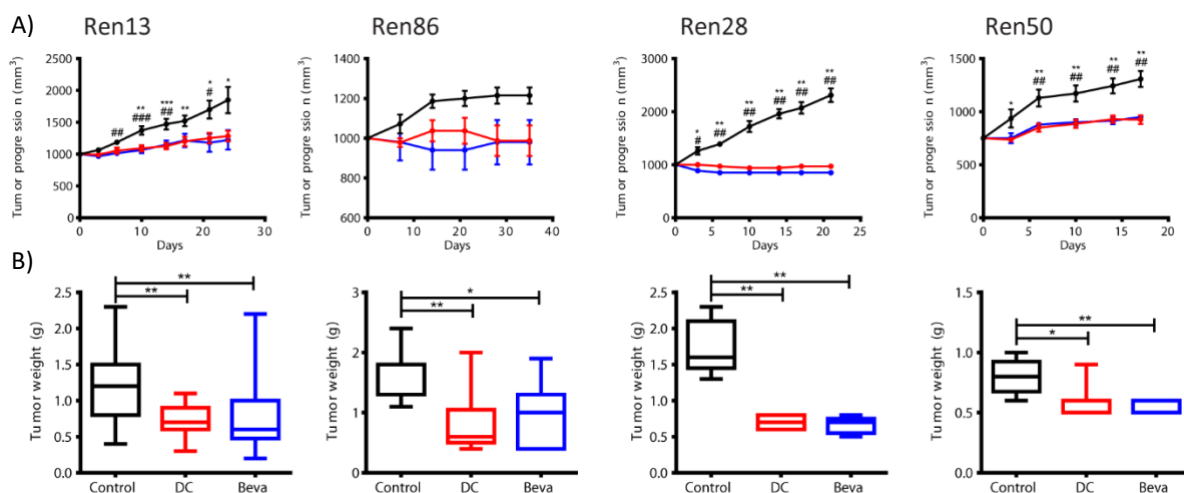


Figure 8. Effects of antiangiogenic drugs in REN-PDOX tumor models. Representation of tumor progression (A) and tumor weight at sacrifice (B) in control and tumors treated with DC101 and Bevacizumab. Mann Whitney test $p < 0,05$ * $p < 0,01$ ** . Image adapted from Moserle, L. et al. in preparation.

In addition, the number of blood vessels were analyzed. These were shown to be decreased in treated groups. The necrotic area of treated tumors, regarding the control ones, was also expanded.

A survival comparison between antiangiogenic treated and non-treated animals was performed, and in this case, not all mice models exhibited the same results. While Ren28 and Ren50 tumors treated with antiangiogenics showed an increase in survival compared with the untreated tumors, Ren13 and Ren86 did not show any differences.

These results suggested that, in all likelihood, tumor lines would not all respond equally to the antiangiogenic treatment.

4.1.2 Increase invasiveness after antiangiogenic treatment

Once the efficiency of the antiangiogenic treatment was evaluated, changes in the invasion process after the therapy were studied. This was done by evaluating the infiltration of tumor cells into the normal renal parenchyma. Two different responses to the antiangiogenics were found. On the one hand, Ren50 and Ren28 tumors did not show any differences in their invasive ability. On the other hand, Ren13 and Ren86 tumors treated with DC101 or Bevacizumab showed an increase in the local invasion compared with the control tumors.

Furthermore, it was also evaluated the metastatic capacity of tumors. According to the obtained results of the invasion, tumors that became more invasive after treatment also showed an increase in their metastatic ability.

Figure 9 represents the different responses of the tumor models at antiangiogenic treatment.

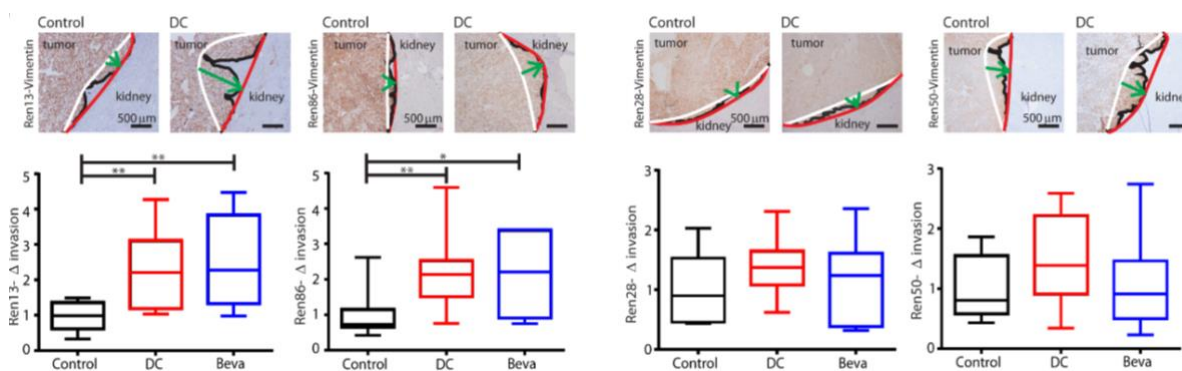


Figure 9. Effect of antiangiogenic therapies on the local invasion of Ren-PDOX. Images of the invasive front of controls and treated samples of Ren13, Ren86, Ren28 and Ren50 tumors. Quantification of the invasion is represented in the graphics. Mann Whitney test $p < 0,05^*$ $p < 0,01^{**}$. Image adapted from Moserle, L et al. in preparation.

These results confirmed the suspicion that not all tumors, although of the same type, would show the same response to the therapy.

4.2 PRO-INVASIVE CANDIDATES AFTER ANTIANGIOGENIC TREATMENT

In order to discover the mechanisms involved in the different responses to the antiangiogenic treatment, a whole-genome RNA sequencing (RNAseq) was developed. This analysis compared the gene expression of three samples of Ren13 tumors treated with DC101 and three non-treated Ren13 tumor samples. In this way, it was possible to evaluate the genes that were differentially expressed due to the antiangiogenic treatment. Moreover, this analysis let us to distinguish the stroma from the tumor, since stroma was codified by murine transcripts while tumor by human transcripts.

Next, from the 62 candidate genes obtained through the RNAseq, the 44 genes that were more upregulated and the 12 that were more downregulated, shown in Figure 10, were selected. These selected genes were validated through TLDA (TaqMan Low Density Analysis). This analysis consists on a high-throughput quantitative RT-PCR with high

sensitivity, specificity, reproducibility, robustness and efficiency. Moreover, it did not require the validation of data (Kodani et al., 2011).

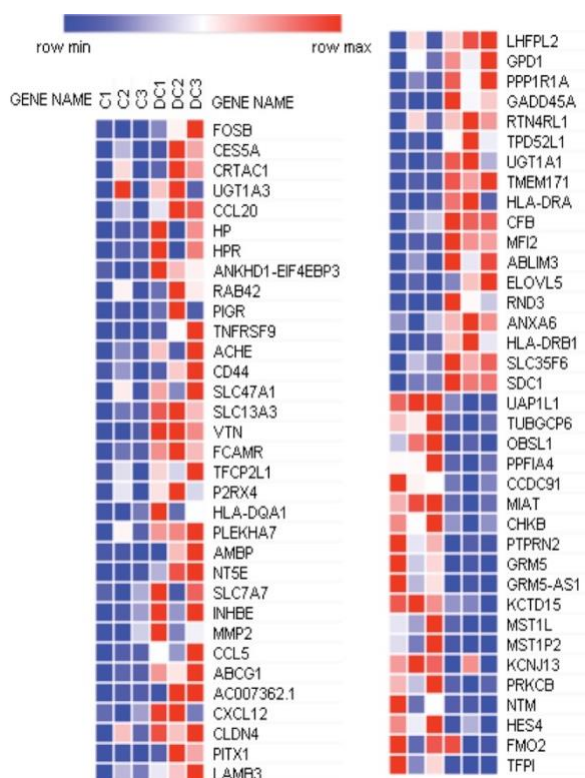


Figure 10. Whole-genome RNA sequencing. Representation of the 44 genes upregulated (in red) and the 12 genes downregulated (in blue) obtained from the RNAseq assay comparing three samples of Ren13 tumors treated with the antiangiogenic drug DC101 (DC1, DC2 and DC3 samples) with three samples of Ren13 non-treated tumors (C1, C2 and C3).

Once analyzed, a correlation between the results obtained of the RNAseq and the TLDA was performed. This correlation reduced the number of candidates from 62 to 27 genes. However, these genes were only validated in one tumor model, Ren13. Hence, it was decided to check its expression in two other pro-invasive tumor models, Ren86 and Ren13M (a high invasive tumor line becoming from the implantation of the brain metastasis of the Ren13 patient into the kidney of a mouse to generate the primary line). Validation was carried out through TLDA and the number of candidates was reduced to 13 genes.

Then, through the cBioportal and the GEO profile platforms, the expression of the candidate genes was analyzed in different renal cancer patients to determine if they were overexpressed and which were associated with patients' survival. These analyses allowed for reducing the candidates from 13 to 9. Through literature research, two genes were discarded and finally, the seven remaining candidates were *EPDR1*, *ABLIM3*, *LHFPL2*, *PDCH1*, *INHBE*, *SDC1*, and *CD44*.

Each of these genes was validated at the protein level through Western Blot and Immunohistochemistry analyses in Ren13, Ren13M, and Ren86 tumors.

Results obtained from the gene expression, the correlations made through TLDA assays, and the protein validation performed in the three pro-invasive tumor models, as well as the information obtained from the bibliography, suggested that *CD44* could be a possible gene involved in the malignization and invasiveness process of tumors after the antiangiogenic treatment.

4.2.1 Implication of CD44 in tumor invasion

As explained in Section 4.2, *CD44* arose from a set of *in silico* analyses using Ren13, Ren13M and Ren86 tumor samples, which were tumor models that demonstrate pro-invasive features after the antiangiogenic treatment.

Evidence of the implication of this gene in the malignization process was first obtained when the gene expression of *CD44* was compared between Ren13/Ren13M control and antiangiogenic treated tumor samples, as shown in Figure 11. As represented, samples of tumors treated with the antiangiogenic drug (DC101) showed higher expression of *CD44* than the untreated or control tumor samples.

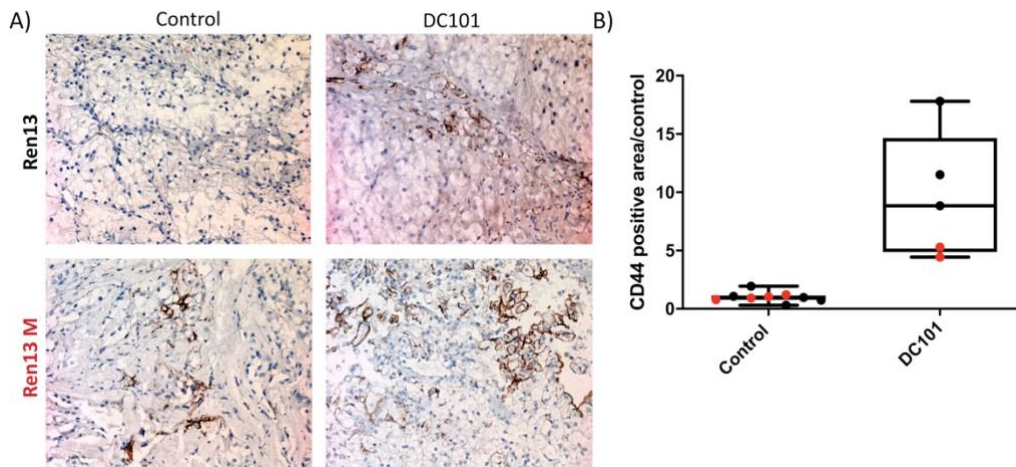


Figure 11. Immunohistochemistry evaluation of CD44 expression. A) Representative images of the CD44 immunohistochemistry performed in Ren13 and Ren13M tumor samples treated with DC101 and non-treated. Images were taken at 20X. B) Quantification of the CD44 positive area relative to the control. Black dots represent Ren13 tumor samples and red dots represent Ren13M tumor samples.

Moreover, the relative expression of CD44 in the three tumor models obtained by TLDA correlated with the invasion produced by each tumor (Figure 12).

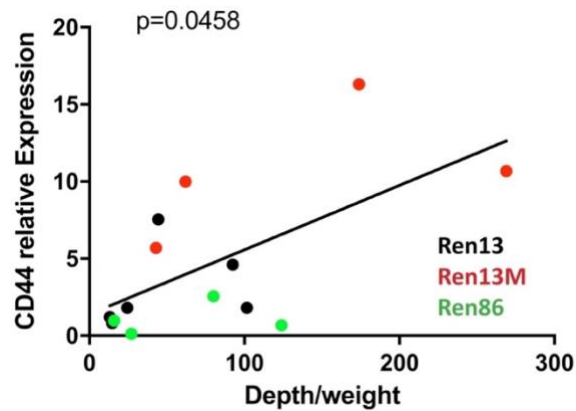


Figure 12. Correlation of CD44 expression with invasion. Correlation of CD44 expression obtained through TLDA analysis with tumor invasion determined as depth/weight. Correlation was performed in three pro-invasive tumor models. Black dots represent Ren13 tumor samples, red dots represent Ren13M tumor samples and green dots represent Ren86. Spearman correlation $p=0,0458^*$

4.2.2 CD44

CD44 is a transmembrane glycoprotein encoded on the short arm of chromosome 11 (Negi et al., 2012). It is expressed on the surface of different mammalian cell types such as endothelial and epithelial cells, fibroblasts, keratinocytes and leukocytes among others (Basakran, 2015; Jordan, Racine, Hennig, & Lokeshwar, 2015). Together with integrins and cadherins, CD44 belongs to the cell adhesion molecules family of CAMs (Orian-Rousseau, 2010). There exist more than 20 different isoforms of CD44 due to an RNA alternative splicing process (Basakran, 2015). These are called variant isoforms (CD44v).

Moreover, CD44 and its isoforms are subjected to some post-translational modifications such as massive N-linked and O-linked glycosylation and glycosaminoglycan (GAG) attachments. These modifications are responsible for the different protein size, that can vary from 85-90KDa until 200KDa or more (Wang et al., 2005; Naor, Nedvetzki, Golan, Melnik, & Fajelson, 2002). The smallest isoform and the most commonly expressed is the standard (CD44s), also called hematopoietic (CD44H). All isoforms contain a constant region, a transmembrane domain, and a cytoplasmic domain (Basakran, 2015; Orian-Rousseau, 2010). Figure 13 represents the structure of the CD44 receptor and its isoforms.

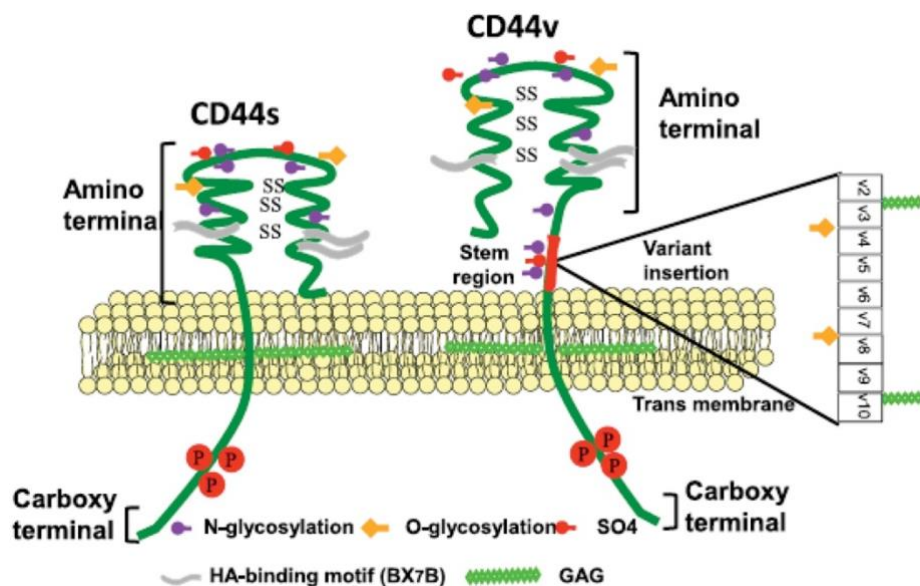


Figure 13. Representation of CD44 and its isoforms. Structural representation of CD44 with its different regions and modifications, including the variant insertion region. Image adapted from Misra et al., 2015.

The principal ligand of CD44 is Hyaluronic Acid or Hyaluronan (HA), but it can also bind to other components of the extracellular matrix such as fibronectin, collagens type I and IV, laminin and osteopontin (OPN). These bindings are produced through the extracellular region of CD44. By the transmembrane region, some members of the galectin family can also bind to CD44. Through the intracellular region it can interact with Ankyrin and Ezrin-Radixin-Moesin (ERM) protein families (Hertweck, Erdfelder, & Kreuzer, 2011).

Despite the interaction of CD44 with a huge variety of the extracellular matrix components, their principal activities are due to its interaction with Hyaluronic Acid. Furthermore, all CD44 isoforms can bind to this ligand, as they have the specific binding site for Hyaluronan (S. J. Wang & Bourguignon, 2011).

CD44 is responsible for cell signaling and for regulating different biological processes between cells. Its involvement in the hematogenic spread of tumor cells has also been described. Its role as an adhesion molecule in the cell-cell and cell-extracellular matrix interactions mediates the lymphocyte homing, hemopoiesis and cell migration (Fujisaki et al., 1999; Orian-Rousseau, 2010). Besides, CD44 activation can modify the bio-

environment of fast proliferating cells facilitating its detachment from the substrate (Negi et al., 2012).

Some CD44 isoforms are implicated in different diseases such as cancer, inflammatory alterations, autoimmune and vascular diseases and infections produced by pathogens (Basakran, 2015; Jordan, Racine, Hennig, & Lokeshwar, 2015). Also described is their role in signaling and metastatic processes of some types of tumors, as ovarian, colon and breast cancer among others (Zou et al., 2013; Draffin, McFarlane, Hill, Johnston, & Waugh, 2004; Fujisaki et al., 1999). Additional functions assigned to CD44 activation are induction of cell motility, activation of cell survival responses and promotion of cell adhesion (Draffin, McFarlane, Hill, Johnston, & Waugh, 2004; Naor et al., 2002).

Moreover, CD44 has been associated with resistance to some chemotherapeutic agents in some tumor types, as is the case of some renal carcinomas (Mikami et al., 2015).

In cancer, the overexpression of CD44 does not always correlates with a bad prognostic and an increase of tumor aggressiveness. In some tumor types such as neuroblastoma and prostate cancer, the lack of CD44 correlates with tumor aggressiveness (Orian-Rousseau, 2010).

It has also been observed that CD44 plays a role as a negative regulator of angiogenesis. CD44 constrains the proliferation of the endothelial cells, thus, in the absence of CD44, there is an increase of the angiogenic response (Pink, Skolnaja, Paell, & Valkna, 2016; Zou, Yi, Song, Wei, & Zhao, 2014).

HYPOTHESIS

AND

OBJECTIVES

Previous results aforementioned demonstrated that not all tumors respond equally to antiangiogenic therapy. While some tumors such as Ren50 and Ren86 didn't show changes in their invasive and metastatic behavior after antiangiogenic treatment, other tumors like Ren13 and Ren86 showed an increase in their invasive and metastatic capacities. In order to determine the mechanisms involved in the tumor malignization, some assays comparing the gene expression of the pro-invasive tumors before and after the antiangiogenic treatment were performed. CD44, among others, emerged as one of the most differentially expressed genes.

Hence, we hypothesized that CD44 activation contributes to the malignization process inducing an increase in the migration and invasion capacity of tumor cells after the antiangiogenic treatment.

To demonstrate this hypothesis, we proposed the following objectives:

1. Investigate and determine the role of CD44 in tumor cell migration and invasion *in vitro* using different renal cell carcinoma models.
2. Elucidate the mechanisms through which CD44 is capable of increasing the invasive behavior of tumor cells after the antiangiogenic treatment using *in vitro* systems. Upstream and downstream regulators of CD44-dependent invasiveness will be identified.
3. Validate the functional and mechanistic results obtained *in vitro* performing *in vivo* experiments using clear cell renal cell carcinoma mouse models.
4. Validate the importance of CD44 expression in the survival of patients suffering from renal carcinoma.

**MATERIALS
AND METHODS**

1. IN VITRO

1.1 CELL CULTURE

1.1.1 Cell Lines

In this thesis, different cell lines with human kidney origin were used and are summarized in Table 5. pVHL-deficient 786O- was provided by *B. Jiménez* (Instituto de Investigaciones Biomédicas CSIC-UAM, Madrid, Spain). HEK293FT, used for the lentiviral production, was supplied by *R. Alemany group* (ProCure, ICO-IDIBELL, Barcelona, Spain). Remainder cells were provided by *F. Setién* from the cell culture facility of the Programa d'Epigenètica i Biologia del Càncer (PEBC).

Cell line	Disease	Medium
RCC4-	Renal Cell Carcinoma	RPMI 1640
SN12C	Renal Cell Carcinoma	DMEM
786O-	Renal Cell Adenocarcinoma	RPMI 1640
ACHN	Renal Cell Adenocarcinoma	DMEM
HEK293FT	Human Embryonic Kidney	DMEM

Table 5. List of cell lines derived from human tissue used.

1.1.2 Primary Cell Lines

Two different primary cell lines derived from Ren-PDOX were generated. They are summarized in Table 6.

Primary cell line	Tumor origin	Medium
Ren13	E101/16 B1DC	RPMI 1640
Ren86	E42/15 D2	RPMI 1640

Table 6. List of primary cell lines derived from PDOX.

To generate the primary cells, fresh tumor pieces from mice were disrupted with a scalpel and tweezers with 5ml of RPMI medium in a plate. Depending on tumor firmness, some were incubated with 200 U/ml of Collagenase IV (Sigma) at 37°C during 10min.

Then, it was filtered using a 70µm cell strainer (Falcon) to obtain single cell suspension. The suspension was centrifuged at 250G during 5min. If there were presence of erythrocytes in the pellet, cells were incubated for 1min with 2ml of ACK (Lonza) and centrifuged 5min at 250G.

At last, cells were resuspended in their culture media and seeded in a 6-well plate. Once grown, primary cells were amplified and cryopreserved.

1.1.3 Cell Line Maintenance

Two different media shown in Table 7 were used to maintain renal cell cultures. Both medias were supplemented with 10% of fetal bovine serum (FBS) (Gibco) previously inactivated during 30min at 55°C. 50U/ml of penicillin, 2mM of L-glutamine, 50µg/ml of streptomycin sulfate, 1% of pyruvate, 1% of non-essential aminoacids and 10mM of HEPES (all from Gibco) was added to both media. 10ng/ml of EGF (ReproTech) and 1x Insulin (Lilly) was also added to the primary media. Cells were maintained at 37°C under humidified conditions with 5% CO₂.

Medium	Reference	Manufacturer
RPMI Medium 1640	#31870-025	Gibco (Thermo Fisher Scientific)
Dulbecco's Modified Eagle Medium (DMEM)	#BE12614F	Lonza

Table 7. Mediums used for cell culture.

1.1.4 Mycoplasma Test

Cells were routinely tested from mycoplasma contamination through PCR using the oligonucleotides described in Table 8.

Oligonucleotide	Sequence
MICO-1	5' - GGCGAATGGGTGAGTAACACG - 3'
MICO-2	5' - CGGATAACGCTTGCGACTATG - 3'

Table 8. Oligonucleotides used for the detection of mycoplasma contamination.

As a template for the PCR, it was used the media from cell incubated in overconfluence in absence of antibiotics for 5 days at least. If there was contamination a treatment with Plasmocin™ at 25µg/ml for 2 weeks was performed and then cells were tested again.

1.1.5 Cell Counting

A manual counting method using trypan blue (Sigma) dying exclusion test was used to determine cell concentration.

Cells adhere to the plate were detached by incubation with pre-warmed trypsin-EDTA (Gibco) at 37°C for 5min. Then, using fresh medium supplemented with FBS trypsin was inactivated. Cells were centrifuged during 5min at 250G and resuspended with fresh full medium.

For the counting, cells were diluted in trypan blue (1:1) and manually counted using a Neubauer chamber. The number of cells per ml was calculated using the following formula:

$$\text{Concentration (cells/ml)} = \text{Mean viable cells per quadrant} \times \text{Dilution factor} \times 10^4$$

1.1.6 Cell Freezing and Cryopreservation

Cells were trypsinized and centrifuged as previously described, then resuspended in cold freezing medium (90% FBS and 10% DMSO from Sigma) in a ½ dilution of a p100 plate.

The suspension of cells was distributed in cryotubes at 1ml/tube and placed in a cell freezing container filled with 2-propanol at -80°C for at least 24h. After that, cryotubes were stored in a liquid nitrogen tank.

To defrost cells, cryotubes containing cells were quickly transported into dry ice to a warm bath at 37°C. Then, cells were diluted in pre-warmed medium (1/10) and trespassed to a Falcon tube. Cells were centrifuged and pellets were resuspended in fresh medium. Finally, they were plated onto a p100 plate to have a high confluence and recover.

1.1.7 Cell Line Treatment

CD44 downregulation was produced through doxycycline induction at 2,5µg/ml (Sigma).

Ren13 primary cells were treated with different inhibitors described in Table 9, and also with different fragments of Hyaluronic Acid described in Table 10.

Inhibitor	Activity	Reference	Manufacturer	Concentration
Bosutinib	Src inhibitor	B-1788	LC Laboratories	0,1µM / 1µM
Ruxolitinib	JAK inhibitor	R-6600	LC Laboratories	0,2µM / 2µM
Perifosine	AKT inhibitor	P-6522	LC Laboratories	2µM / 5µM
Hyaluronidase	HA degradation	H3631	Sigma-Aldrich	20U/mL
IM-7	CD44 blocking antibody	14-0441-82	Invitrogen	5µM / 10µM

Table 9. Inhibitors used for in vitro assays.

Hyaluronan oligosaccharide	Molecular weight (g/mol)	Manufacturer	Concentration
HA4 ^{AN}	776,2	Contipro group	10 μ M
HA6 ^{AN}	1155,3	Contipro group	10 μ M
HA8 ^{AN}	1534,5	Contipro group	10 μ M
HA10 ^{AN}	1913,6	Contipro group	10 μ M
HA12 ^{AN}	2292,7	Contipro group	10 μ M
HA14 ^{AN}	2671,8	Contipro group	10 μ M
HA16 ^{AN}	3050,9	Contipro group	10 μ M
HA18 ^{AN}	3430,0	Contipro group	10 μ M

Table 10. Hyaluronic Acid oligosaccharides used for in vitro assays.

1.2 MOLECULAR ANALYSIS

1.2.1 RNA Detection

1.2.1.1 RNA Extraction from Cells

Cells were washed with PBS (0,15M NaCl, 0,9mM Na₂HPO₄ and 0,1mM KH₂PO₄) and trypsinized for 5min at 37°C. Then, trypsin was inactivated with FBS supplemented fresh medium. Cells were centrifuged during 5min at 250G. The pellet was washed with PBS, centrifuged and stored at -80°C until the day of the RNA extraction. RNA was extracted using the RNeasy Plus kit (Qiagen) following the manufacturer's instructions.

Once RNA was extracted it was quantified using the spectrophotometer NanoDrop TM1000 (Thermo Scientific). The quality of the RNA was validated by loading 500ng of RNA in a 1% agarose gel using 1kb Plus DNA ladder (Invitrogen) as a molecular weight marker.

1.2.1.2 Getting cDNA from RNA

First, 2µg of each sample of RNA was diluted in sterile water to reach a total volume of 20µl. The solution was placed into a microcentrifuge tube and incubated at 65°C for 10min.

Then, it was used the High Capacity cDNA Reverse Transcription kit (Applied Biosystems) to prepare the retrotranscription mix: 1µl of RNase inhibitor, 3µl of RT buffer, 3µl of random primers, 1,2 µl of ddNTPs, 1µl of reverse transcriptase and 0,8µl of sterile water. 10µl of the mix was added to each sample previously warmed. Then, the reverse transcription was performed under the following conditions: 10min at 65°C, 2h at 37°C, 5 min at 85°C and ∞ at 4°C. cDNA obtained was stored at -20°C until use.

1.2.1.3 Real-Time Quantitative PCR

To detect RNA expression, Real-Time quantitative PCR (RT-qPCR) analyses were performed using TaqMan® Technology (Applied Biosystems). First, 25ng of cDNA from the different cells was added into each well of a 384-well plate (Roche) and mixed with 5µl of TaqMan® Universal PCR Master Mix (Applied Biosystems), 0,5 µl of the TaqMan® probe of interest (Table 11) and ddH₂O to a final volume of 10 µl. Once mixed, the plate was read with LightCycler®480II (Roche). Obtained results were analyzed using the RQ Manager 1.2.1 and SDS 2.4 (Applied Biosystems) software.

Gene	Specie	Dye-Label	Reference
GAPDH	Human	FAM™-MGB	Hs99999905
CD44	Human	FAM™-MGB	Hs00153304
Serglycin	Human	FAM™-MGB	Hs01004159

Table 11. Specific probes used in TaMan® analyses.

The cycle threshold (Ct) obtained for each gene was normalized against the same value of the housekeeping gene, GAPDH. Then, RNA expression for each gene was calculated using next formula:

$$2^{-\Delta Ct} = 2^{-(Ct \text{ gene A} - Ct \text{ housekeeping gene})}$$

1.2.2 Protein Detection

1.2.2.1 Preparation of Protein Lysates from Cell Culture

When cells seeded in a p100 plate reached 90-100% confluence were lysed. They were first washed with PBS and then 150 μ l of RIPA lyses buffer was added to the plate. The RIPA lyses buffer contains: 0,1%SDS, 1%NP-40, 0,5%sodium deoxycholate, 50mM NaF, 5mM EDTA, 40mM β -glycerolphosphate, 200 μ M sodium orthovanadate, 100 μ M phenylmethylsulfonyl fluoride, 1 μ M pepstatin A, 1 μ g/ml leupeptin, 4 μ g/ml aprotinin in PBS at a pH 7,4. The plate was incubated with the lysis buffer during 30min in rotation at 4°C. Then, cells were scraped using a scraper cell (Sarstedt) and the lysate was transferred into a 1,5ml Eppendorf. Lysates were centrifuged during 20min at 4°C. Finally, supernatants were collected and stored at -20°C.

1.2.2.2 Quantification of Protein Extracts

The colorimetric PierceTM BCA Protein Assay Kit (Thermo Scientific) was used for quantifying protein lysates.

First, it was performed a standard curve ranging from 0 to 2mg/ml diluting bovine serum albumin (BSA). Samples of interest were diluted too at 1:10 or 1:5.

Then, 10 μ l of the standard curve and the samples of interest was loaded in a 96-well plate. 200 μ l of BCA Working Reagent (50:1, Reagent A:B) was added to each well and carefully mixed. The plate was incubated during 30min at 37°C. The absorbance was measured at 560nm wavelength by spectrophotometry (Power Wave XS, BIO-TEK) using the KCJr Win Software. Protein concentration was calculated by extrapolation in the standard curve.

To prepare protein lysates for Western Blot, samples were prepared at $1\mu\text{g}/\mu\text{l}$ in loading buffer (Laemmli buffer: 300mM Tris-HCl pH 6,8, 600mM DTT, 12% SDS, 0,6% bromophenol blue, 60% glycerol) and boiled at 95°C during 5min. Finally, they were stored until use at -20°C .

1.2.2.3 Protein Analysis by Western Blotting

To validate and compare proteins expression values of different samples, Western Blot was performed.

To start, it was prepared sodium dodecyl sulphate-polacrylamide gels (SDS-PAGE) for protein separation using 1,5mm glass plates (Bio-rad). They were composed mixing dH_2O , acrylamide-bisacrylamide, Tris-HCl 1,5M pH 6,8 or 8,8, APS and TEMED. Gels had two parts: the stacking gel that had a fixed percentage of acrylamide and the resolving gel which acrylamide percentage ranged from 7,5 to 12% depending on the molecular weight of the proteins of interest.

Then, $40\mu\text{g}$ of lysate and a molecular weight marker (Page Ruler™ prestained, Thermo Scientific) were loaded into the gels and submerged into the running buffer (25mM Tris, 192mM glycine, 0,1% SDS). Protein migration was carried out at a constant voltage of 120V. Next, gels were transferred to a nitrocellulose membrane (Immobilon-P, Merck Millipore) at 100V and 4°C for 90-120min. Membranes were incubated with 5% of skimmed milk (Nestle®) in TBS-T (Tris 50mM, NaCl 150mM, Tween 20 0,1%) during 1h at room temperature (RT) under agitation to avoid unspecific antibody binding. After that, membranes were incubated with the primary antibodies of interest diluted appropriately (Table 12) in TBS-T 1% skimmed milk overnight (O/N) at 4°C in agitation.

After incubation, membranes were washed three times with TBS-T during 10min, and subsequently incubated with 1:5000 anti-rabbit IgG or 1:5000 anti-mouse IgG horseradish peroxidase (HRP) linked antibodies (GE Healthcare) diluted in TBS-T 1% skimmed milk at RT during 1h.

Then, membranes were washed three times with TBS-T for 10min and one last wash with TBS for 10min. Blots were developed with Amersham ECL Select™ Western Blotting Detection Reagent (GE Healthcare Life Sciences) following the manufacturer's instructions. Chemiluminescent signal was detected with ChemiDoc Touch (Bio-Rad) and subsequently analyzed using Image Lab Software (Bio-Rad).

Antigen	Antibody	Specie	Dilution	Manufacturer
CD44	156-3C11	Mouse	1:1000	Cell Signaling
Actin	A5441	Mouse	1:1000	Sigma-Aldrich
Vinculin	V9131, Clone hVIN-1	Mouse	1:1000	Sigma-Aldrich
Tubulin	T6074	Mouse	1:1000	Sigma-Aldrich
Phospho-Src (Tyr530)	Sc-166860	Mouse	1:500	Santa Cruz
Src	2123T	Rabbit	1:1000	Cell Signaling
Phospho-FAK (Tyr397)	Sc-81493	Mouse	1:500	Santa Cruz
FAK	3285	Rabbit	1:1000	Cell Signaling
Phospho-Stat3 (Tyr705)	Sc-8059	Mouse	1:500	Santa Cruz
Stat3	Sc-8019	Mouse	1:500	Santa Cruz
Serglycin	HPA000759	Rabbit	1:250	Sigma-Aldrich
Phospho-ERK (Thr202/Tyr204)	9101S	Rabbit	1:1000	Cell Signaling
ERK	9102	Mouse	1:1000	Cell Signaling

Table 12. Primary antibodies used for Western Blot.

1.2.2.4 Protein Detection by Immunocytofluorescence

To detect proteins and determine their localization, Immunocytofluorescence assays were developed.

Glass coverslips were sterilized with UV during 2h. Then, they were put into a 24-well plate using sterilized tweezers. Cells were seeded on the coverslips until reach a confluence between 80-90%. Afterwards, cells were washed with PBS and fixed with 4% paraformaldehyde (PFA) during 5min.

Once fixed, cells were washed three times with PBS. Then, and in order to avoid unspecific binding of the primary antibody, they were blocked during 30min at RT with 20% goat serum in PBS. Cells were incubated with the primary antibody with appropriate dilutions in 20% goat serum (see Table 13) for 1h at RT.

Antigen	Antibody	Specie	Dilution	Manufacturer
CD44	156-3C11	Mouse	1:100	Cell Signaling
Serglycin	HPA000759	Rabbit	1:50	Sigma-Aldrich

Table 13. Primary antibodies used for protein detection by Immunocytofluorescence.

Afterward, coverslips were washed with PBS three times and incubated with secondary antibodies diluted 1/200 (see Table 14). Finally, they were incubated with DAPI (Sigma) diluted 1/3000 during 5min at RT to stain the nucleus of cells. At the end, using Fluoromount™ Aqueous Mounting Medium (Sigma), coverslips were mounted on slides.

Secondary Antibody	Host	Fluorochrome	Manufacturer
Anti-Mouse	Goat	Alexa Fluor 488	Invitrogen
Anti-Rabbit	Goat	Alexa Fluor 647	Invitrogen

Table 14. Secondary antibodies used for protein detection by Immunocytofluorescence.

Cells could be visualized using Nikon Eclipse 80i microscope. Images were taken with the Confocal Leica SP5 was used to take the pictures.

We also used this technique to detect the presence of Hyaluronic Acid on our cell cultures. During this assay and as a specificity control, some cells were treated with Hyaluronidase (Sigma #H3631) (an enzyme responsible for Hyaluronic Acid degradation) at 20U/mL during 1h at 37°C. After the incubation, cells were washed three times with PBS. Then, coverslips were incubated with hyaluronan-binding protein (HABP) at 2,5µg/mL (Amsbio #AMS.HKD-BC41) in BSA 0,1% for 1h at RT (as the primary antibody).

After that, cells were washed three times with PBS and incubated with Streptavidin A488 diluted 1:200 (Life Technologies #s37354) in PBS for 1h at RT. Then coverslips were incubated with DAPI and mounted on slides as previously described. Images were taken with Nikon DS-Ri1 digital camera using NIS-elements BR 3.2 (64-bit) software and subsequently analyzed using Image J Software.

1.2.2.5 Protein Detection by Flow Cytometry

Flow Cytometry assay was used to determine the efficiency of CD44 downregulation.

Cells were washed with PBS, detached through trypsinization, centrifuged and resuspended in 1ml of FACS buffer (PBS with 5% FBS). Then, they were counted as explained in Section 1.1.5. 200.000 cells were added in a well of a 96-well rounded bottom plate.

After that, they were centrifuged for 5min at 1.600rpm at 4°C and subsequently washed twice with 200µl of FACS buffer. They were incubated with 50µl of anti-CD44 APC antibody (BD Pharmingen #559942) diluted 1:50 in FACS buffer. Incubation was performed on ice during 30min and protected from the light. Then, cells were washed twice with FACS buffer and finally resuspended in 200µl of FACS buffer. Gallios cytometer (Beckman Coulter) was used to detect fluorescence and data obtained was processed using Kaluza Analysis Software.

1.2.3 Inducible Downregulation System

1.2.3.1 Doxycycline Inducible shRNA System

To study the effect of CD44, we decided to downregulate its expression in cells using the Inducible Dharmacon™ pTRIPZ™ Lentiviral short hairpin RNA (shRNA) (GE Healthcare) system (Figure 14). Glycerol stocks of E. Coli containing lentiviral plasmid for doxycycline induced CD44 downregulation (RHS4740-EG960, Dharmacon, GE Healthcare) and resistant to Ampicillin® were kept at -80°C until use.

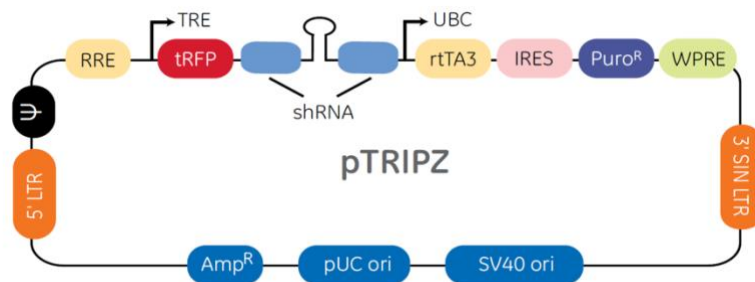


Figure 14. Inducible Dharmacon™ pTRIPZ™ Lentiviral shRNA plasmid.

1.2.3.2 Plasmid Amplification

E. Coli was thawed on ice for 10min. 10µl of the bacteria suspension was added to 5ml of low-salt Lysogeny Broth (LB) (10g Tryptone, 5g NaCl and 5g Yeast Extract in 1L of H₂O) supplemented with 100µg/ml of Carbenicillin® (Sigma) (Ampicillin® analog).

Bacteria were cultured in 15ml bacterial culture tube over day (O/D) at 37°C under shaking conditions. Then, they were diluted in 250ml of low-salt LB supplemented with Carbenicillin® (1:500) in an Erlenmeyer cell culture flask and incubated O/N with shaking at 37°C.

1.2.3.3 Large Scale DNA Preparations

DNA maxi-preparations using Endofree Plasmid Maxi Kit from Qiagen was used to isolate large amounts of plasmidic DNA from E. Coli bacteria culture. It was developed following

manufacturer's instructions. DNA concentration was measured by NanoDrop TM1000 (Thermo Scientific).

1.2.3.4 Lentiviral Production

HEK293FT cells were transfected to produce doxycycline induced CD44 shRNA lentiviruses. They were seeded in a p250 plate until reach a confluence of 60-80%.

First, HEK293FT medium was changed 1h before transfection for 18ml of fresh media. Transfection mixture was prepared by mixing 50µg of plasmid DNA, 37,5µg of pPAX2 packaging vector, 6,25 µg of pMD2-G envelop vector and 400µl of polyethylenimine (PEI) (Polysciences) in 1600µl of 150mM NaCl and incubated during 15min. Then, final volume of 2ml of transfection mixture was added drop by drop to HEK293FT culture while the plate was softly shaking for a homogeneous distribution.

Next day, medium from HEK293FT transfected cells was removed and they were incubated with 2% FBS medium for 48h at 37°C. After two days, it was collected the supernatants with lentiviruses and centrifuged during 10min at 2500rpm. They were filtered using a 0,45µm PES filter (TRP). Then, supernatant and full medium were mixed 1:1 to a final concentration of 10% FBS and 4µg/ml of Polybrene® (Sigma-Aldrich). The remaining supernatant was frozen at -80°C.

1.2.3.5 Lentiviral Infections

Ren13, SN12C and 786O- cells were seeded until reach a confluence between 70-75% at the time of infection. To infect cells with the lentiviruses previously generated, medium of cells was replaced by the mixture described in Section 1.2.3.4 and incubated O/N at 37°C.

Next day, medium was replaced by full fresh medium with 10% FBS. After 48h of the infection, it was added 5µg/ml of puromycin (Sigma) to the cell cultures in order to effectively select infected cells. As a control for antibiotic efficiency, non-infected cells were cultured and treated in parallel in the same way.

Validation of inducible shRNA system was performed treating cells for 48h with 2,5µg/µl of doxycycline. Red fluorescence of cells was confirmed through the inverted Leica DMiL LED microscope. CD44 silencing efficiency was checked at protein and RNA level.

1.3 IN VITRO ASSAYS

1.3.1 Migration Assays

1.3.1.1 Wound Healing Assay

Wound Healing assay was performed to determine the migration capacity of cells under different conditions. In order to generate a precise scratch, 2-well culture inserts (Ibdi®) with a cell-free gap in the middle were used. They were stacked into wells of a 12-well plate.

Cells were washed, detached with trypsin, centrifuged and resuspended in 1ml of fresh medium. Then, they were counted as explained on section 1.1.5. A determined number of cells (depending on their size) were plated inside both compartments of the insert in a final volume of 70µl. 500µl of medium was added around the insert.

After 24h inserts were removed with sterile tweezers leaving a gap between both wells of the insert. Medium of cells were removed and replaced by fresh medium. Pictures of the scratch were taken at 0, 3, 6, 9, 12 and 24 hours depending on cells. Three pictures of each well were taken using an invert microscope (Leica DMi1). Opened area was manually quantified using Image J Software.

Control and experimental groups were performed in parallel in triplicates.

1.3.1.2 Transwell Migration Assay

To determine the directional migration capacity of cells, it was performed a transwell migration assay. 6,5mm inserts with an 8µm polycarbonate membrane of Costar Transwell® Permeable Supports (Corning) were used. 2h before the experiment membranes of the inserts were balanced incubating them with medium at 37°C in a

humidified atmosphere with 5% CO₂. Then, cells were washed, detached from the plate using trypsin and centrifuged. The number of cells placed under the insert was determined for each experiment and cell line. Once seeded, the chamber was incubated during 24h at 37°C in a 5%CO₂ humidified atmosphere.

Next day, using a cotton swab, membranes were wiped to remove non-migrated cells remaining on the upper part of the chamber. Cells were then fixed with methanol during 2min. After fixation, they were washed with PBS and stained with hematoxylin (0,1% Hematoxylin, Merck Millipore, in ethanol 96%) for 1min. At least, the inserts were removed using a blade and mounted on a slide with a drop of sterile water.

Membranes were observed using the Nikon Eclipse 80i microscope and 12 representative pictures of each membrane were taken with a Nikon DS-Ri1 digital camera using NIS-Elements BR 3.2 (64-bit) Software. Migrated stained cell were analyzed counting them manually using Image J Software.

Control and experimental groups were performed in parallel in duplicates.

1.3.2 Invasion Assays

In order to determine the invasive capacity of cells, transwell Matrigel® invasion assay was performed. Inserts of the Corning® BioCoat™ Matrigel® Invasion Chamber with an 8µm polycarbonate membrane were used for the experiment.

The protocol followed to develop the experiment and to take the images was the same as in transwell migration assay (Section 1.3.1.2)

Control and experimental groups were performed in parallel in duplicates.

2. IN VIVO

2.1 ANIMALS AND CONDITIONS

All animal studies were approved by the Ethics Committee for Animal Experimentations from the Biomedical Research Institute of Bellvitge (IDIBELL) and the Generalitat de

Catalunya. They were developed at the IDIBELL Animal Core Facility (AAALAC unit 1155) following the European directives on ethical usage of rodents for animal research (approval DARP #4899).

In this project, all mice used were male athymic nude mice (Harlan Laboratories). They were individually maintained in ventilated cages on constant temperature (20-25°C) in SPF (Specific Pathogen Free) conditions and sterility. Animals were under an artificial circadian cycle (12h light/dark) and received *ad libitum* standard diet and water. Experiments were performed inside a cabinet with vertical laminar flow.

2.2 PATIENT-DERIVED ORTHOXENOGRAFT MOUSE MODEL FROM RCC HUMAN BIOPSY

Orthoxenograft mouse model Ren13 was generated through implantation of a small fresh piece of tissue from a biopsy of a ccRCC patient in the right kidney of a mouse. Resected tissue was obtained from the Hospital de Bellvitge (Barcelona, Spain) under local ethics committee's approved protocols (CEIC approval ref. PR322/11).

Primary tumor line was maintained throughout several passages by orthotopically implantation of a tumor piece into de kidney of another mouse. Mice were normally sacrificed when their survival was compromised.

2.3 CELL LINES MOUSE MODELS

Besides orthoxenograft mouse models, cell lines tumor models were also used to perform *in vivo* experiments.

2.3.1 Kidney Tumors

To develop kidney tumors from SN12C and 786O- human cancer cell lines, 10^6 cells were directly injected into the right kidney of athymic nude mice through a 0,5ml needle (BD Micro-Fine). After 20-30 days of the injection, tumor cells grew in the kidney generating a perceptible tumor. Tumors were perpetuated through successive passages and animals were sacrificed when their survival was compromised.

2.4 TUMOR AND ORGAN COLLECTION

Tumor and other organs from sacrificed mice were collected to further analyses. Tumors, that grew attached to the kidney were divided in two parts. One part of the tumor was fixed using formaldehyde 4% O/N to be included in a cassette for paraffin embedding. The other piece of the tumor was included in OCT (Tissue-TEK® Sakura) and stored at -80°C for further frozen tissue analyses. Some small pieces of the periphery and some pieces from the center of the tumor were frozen directly in cryotubes and maintained at -80°C in order to extract protein or RNA. Lungs, spleen, liver, diaphragm and contralateral kidney were also collected and fixed in formaldehyde 4% to be included in paraffin.

2.5 PARAFFIN INCLUSION

Formaldehyde 4% fixed tissues were rinsed with PBS to eliminate the fixative agent. Then, samples underwent a dehydration process. They were incubated through a battery of alcohols of crescent graduation: 1h in ethanol 70%, 1h in 96% twice and O/N in a new 96%, 1,5h in absolute ethanol thrice and finally submerged into xylene during 1,5h. Tissue samples were then submerged into liquid paraffin at 65°C O/N. The next day, they were embedded in paraffin inside a block sharp and dried at 4°C.

2.6 DETERMINATION OF TUMOR BURDEN

Tumor size (mm²) was measured at the time of sacrifice using a caliper. Tumor weight (g) was determined with a balance and tumor volume (mm³) was measured calculating the PBS volume displaced inside a Falcon tube.

2.7 ANIMAL TREATMENT

During *in vivo* experiments mice were treated with 1mg/dose/mouse of DC101, an anti-mouse VEGFR2 blocking antibody. This antibody was collected from hybridoma culture (ATCC, Manassas, USA), purified and concentrated. Then, it was tested at Leitatz (Parc Científic de Barcelona, Barcelona, Spain) for endotoxin content.

Animals were also treated with doxycycline (400mg/200mL of drinking water) to induce the shRNA system and downregulate CD44 protein expression.

Once tumors grew and were palpable, animals were randomized in four different groups: control, DC101, doxycycline and DC101 plus doxycycline. DC101 was administered intraperitoneally twice a week while doxycycline was dissolved in the drinking water of animals and was changed every week.

In order to study tumor local invasion, the duration of the experiment was calculated based on the median of control lifespan.

2.8 EVALUATION OF TUMOR LOCAL INVASIVENESS

Tumor local invasion was evaluated by image analyses. Vimentin stained sections were used to take 4X images of the tumor-kidney interface through all the invasive front. Then, it was evaluated the widest extension of tumor protrusions into the kidney parenchyma for each image (depth) through calculating the average for each tumor. As there was found a positive correlation between depth and tumor weight in untreated tumors, invasion, determined as depth, was normalized for tumor weight (depth/weight). To compare different experiments, it was calculated the fold-invasion (Δ invasion) that consisted in normalize the invasion of each animal to the average invasion of control groups for each experiment.

2.9 MOLECULAR ANALYSIS

2.9.1 Protein Detection

2.9.1.1 Protein Extraction of Tumor Samples and Quantification.

Tumor pieces stored at -80°C were used for protein extraction. Using RIPA buffer and a glass homogenizer small tumor pieces were mechanically disrupted on ice.

RIPA buffer composition and the protocol used were explained in Section 1.2.2.1.

The colorimetric Pierce™ BCA Protein Assay Kit (Thermo Scientific) was used to quantify protein lysates obtained from tumor pieces as explained in Section 1.2.2.2.

2.9.1.2 Protein Analysis by Western Blotting

Western Blot assay was used to analyze and compare protein levels of tumor tissues. Preparation of samples and development of the experiments were performed as explained in Section 1.2.2.3. Antibodies and concentrations used for protein detection were also described in that section.

2.9.1.3 Immunohistochemistry in Paraffin-Embedded Sections

To determine the expression and localization of proteins in tumors, paraffin-embedded blocks were cut in 3-5µm thick sections. They were deparaffinized by incubation in a battery of 4 xylenes (10min each), 3 absolute ethanol, 3 96% ethanol, 1 70% ethanol and 1 50% ethanol (5min each). Then, sections were rehydrated through submersion in dH₂O.

After that, it was necessary to retrieve the antigens masked during the fixation process. To do that, slides were submerged in a sodium citrate solution (0,38mg/ml) at pH6 under heating conditions for 15min. Then, samples were cooled down inside the citrate solution for 20-30min and washed during 5min with dH₂O.

Endogenous peroxidase activity was blocked incubating tumor slides during 10min with 6% H₂O₂. This process was repeated twice. Then, samples were washed with dH₂O for 5min. Next, they were submerged during 10min in PBS-T in order to permeabilize cell membranes.

Afterwards, to reduce unspecific binding of the primary antibodies, samples were blocked incubating them with 20% of goat serum in PBS for 1h at RT in a humidity chamber. Next step, was to add the appropriate dilution of the primary antibody (Table 15) to the slides and incubate them O/N at 4°C.

The following day, slides were tempered for 20-30min at RT. Then, they were washed with PBS-T three times during 10min each wash. After that, samples were incubated with

the pertinent secondary antibody (anti-mouse or anti-rabbit Envision⁺-System-HRP (DAKO)) for 1h at RT in the humidity chamber.

Antigen	Antibody	Specie	Dilution	Manufacturer
CD44	156-3C11	Mouse	1:200	Cell Signaling
Vimentin	180052 Clone V9	Mouse	1:200	Invitrogen
PCNA	Sc-56	Mouse	1:100	Santa Cruz
HA-BP	H3631	ABC system	1:100	Sigma
CD31	Ab28364	Rabbit	1:50	Abcam
Serglycin	HPA000759	Rabbit	1:100	Sigma-Aldrich

Table 15. Primary antibodies used for protein detection by Immunohistochemistry.

In the case of using the HA-BP to detect Hyaluronic Acid, it was used the ABC system (Vecstatin Elite #PK-6100), which has to be prepared 30min before its usage (for each mL of PBS is necessary 1 drop of reactive A and 1 drop of reactive B). Incubation time is the same as for the previous secondary antibodies.

After incubation, tumor slides were washed three times during 10min with PBS-T. Then they were developed using the chromogenic substrate DAB+ (EnVision™ Kit, Dako) from 30s to 1min, until a brown precipitate appeared. Incubation time depended on the antibody and tissue sample. Reaction was stopped by submerging the slides in tap water for 10min.

Slides were counterstained with Hematoxylin in order to observe the cells and then they were rinsed in tap water to eliminate the liquid excess. Finally, they were dehydrated submerging them in a battery of 1 70% ethanol, 3 96% ethanol, 3 absolute ethanol (5min each) and 4 xylenes (10min each). Slides were covered using coverslips and DPX mounting medium (Merck).

Nikon Eclipse 80i microscope was used to visualize tissue staining and Nikon DS-Ri1 digital camera using NIS-Elements BR 3.2 (64-bit) software was used to take the images that were subsequently analyzed with Image J Software.

2.9.1.4 Immunofluorescence in Paraffin-Embedded Sections

To determine the presence and compare the expression of a protein it was performed Immunofluorescence assay of paraffin-embedded tumor sections.

Paraffin-embedded blocks were cut in 5µm-thick sections and incubated at 65°C O/N to achieve an optimal deparaffination.

Next day, slides were incubated during 15min with pre-heated xylene at 65°C. Then, they were deparaffinized submerging the slides in a battery of xylenes and alcohols (see Section 2.9.1.3) and rehydrated with dH₂O. Antigen retrieval, endogenous peroxidase deactivation, permeabilization and blocking processes were also developed as in Section 2.9.1.3. After that, slides were incubated O/N at 4°C with the primary antibody CD31 diluted 1:50 (Abcam #Ab28364).

The next day, slides were first tempered during 30min at RT. Then, they were rinsed with PBS three times during 5min each. Then, it was applied the secondary antibody Anti-rabbit Alexa Fluor 488 (Invitrogen) diluted 1:200 in 5% goat serum during 1h at RT. After incubation, slides were washed with PSB-T for 5min once and twice with PBS. The, they were incubated with DAPI (1:3000) during 10min and mounted in coverslips using Fluoromount® Aqueous Mounting Media (Sigma).

Fluorescence was visualized using Nikon eclipse 80i microscope and images were taken with Nikon DS-Ri1 digital camera using NIS-Elements BR 3.2 (64-bit) Software and subsequently processed with Image J Software. Quantification were manually performed.

2.9.1.5 Hematoxylin-Eosin Staining in Paraffin Sections

To quantify the invasive front of tumors, it was performed a Hematoxylin-Eosin (HE) staining in paraffin-embedded sections. Deparaffinization and rehydration of the slides were developed as explain in Section 2.9.1.3. Slides were submerged in Hematoxylin 0,1% (Merck) in ethanol 96% during 10min. Then, they were rinsed in tap water in order to remove the excess. After that, slides were submerged for few seconds in HCl 1% and in ammonia water solution (200ml of dH₂O and 1ml of ammonia 30%) until color tissue veered to blue. To finish, tumor sections were counterstained with Eosin (2,5g of eosin in 1L of ethanol 50%) during 2min and mounted using DPX (Merck). Nikon eclipse 80i microscope was used to visualize stained tumor tissue and images of them were taken using Nikon DS-Ri1 digital camera using NIS-Elements BR 3.2 (64-bit) Software.

3. CLINICAL VALIDATION: IN SILICO ANALYSES

3.1 TCGA ANALYSES

Clinical data was extracted from The Cancer Genome Atlas (TCGA). This platform is a project that has generated multidimensional genomics data from 33 types of cancer and 20 thousand patient tumor samples through transcriptome profiling, exome sequencing, copy number alterations profiling and DNA methylation analyses among other techniques (TCGA research network, 2020).

In this thesis, the expression of candidate gene and related pathways were analyzed in the TCGA across the main histological subtype of RCC (TCGA, 2013). We focused the analysis in patients suffering from ccRCC (KIRC-TCGA) and investigated if the overexpression of our candidates correlated between them and the influence in the survival of those patients.

3.2 DATA FROM SUNITINIB-TREATED PATIENTS

From the Gene Expression Omnibus (GEO reference GSE65615) (Stewart et al., 2015) we obtained clinical gene expression data from clear cell renal cell carcinoma Sunitinib-treated patients. This dataset has information about 23 samples of untreated metastatic

ccRCC patients and 23 samples of Sunitinib pre-treated (18 weeks) metastatic ccRCC patients. Some pieces of different parts from each tumor were studied to determine the intratumor heterogeneity, generating 47 samples of untreated patients and 75 samples of Sunitinib-treated patients. Due to the heterogeneity in the different parts of the same tumor, we decided to analyze each sample as an independent tumor. The expression of candidate genes was compared among untreated and Sunitinib-treated samples.

4. STATISTICAL ANALYSIS

GraphPad Prism v8 Software (GraphPad software, Inc. USA) was used to perform all graphs and statistic tests of this thesis.

The majority of the experiments lacked normal distribution of data due to the small sample size, for that reason it was suitable to use a non-parametric test. Continuous variables were analyzed using Mann-Whitney test or t test. Spearman test (non-parametric) or Pearson test (parametric) were used for correlation analyses. The statistical significance was defined as a p value lower than 0.05 (* $p < 0.05$, ** $p < 0.01$, *** $p < 0.001$, **** $p < 0.0001$).

5. FIGURE DESIGN

Graphics elements from Servier Medical Art according to a Creative Commons Attribution 3.0 Unported License guidelines were used in figures designed by the author of this thesis. Figure panels were designed using the Adobe InDesign CS5 software.

RESULTS

1. CD44 AS A PRO-INVASIVE CANDIDATE

Section 4 of the Introduction described some evidence that selects CD44 as a candidate responsible for the increased invasion of tumor cells after antiangiogenic treatment. Moreover, CD44 is a widely-known protein. Its involvement in the migration, invasion, and metastatic processes has been described in some tumor types other than renal carcinoma.

All of this evidence led us to consider studying the role of CD44 in the migration and invasion processes using different cell and animal models of renal cell carcinoma.

1.1 EXPRESSION OF CD44 IN DIFFERENT CELL LINES AND PRIMARY CELLS AND TUMORS

The first step in studying the role of CD44 was to select the most suitable tumor and cell models to work with.

The RNA sequencing and subsequent analysis of where CD44 came from were developed using the Ren13 model. This model was generated from a tumor piece of a patient with renal cancer.

Figure 15 shows the CD44 expression of different Ren13 tumor pieces and cells. The presence of the protein was maintained in cell cultures and also in tumors generated from these cells, although not always at the same expression levels.

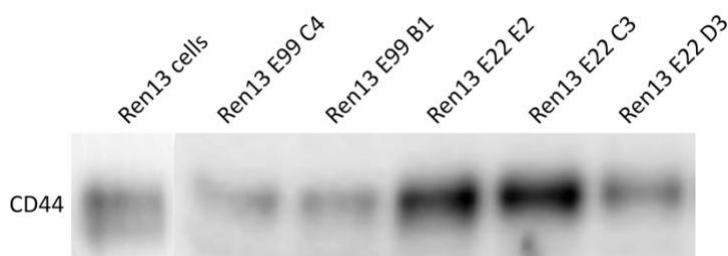


Figure 15. Western Blot of CD44. Expression of CD44 protein analyzed in Ren13 primary cells and different Ren13 tumors originated from the primary cells.

Although we had a good model to develop our study, we decided to select other cells separate to Ren13 to determine the role of CD44 in the invasion process. Figure 16 shows the Western Bot analysis of CD44 expression of the different cells we assessed.

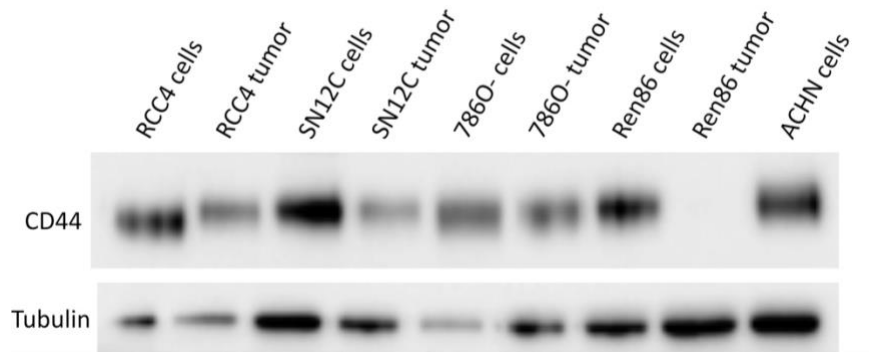


Figure 16. Western Blot screening of different cell lines and their respective tumors. The expression of CD44 from different cell lines and also of their respective tumors was check. Tubulin expression was used as housekeeping.

Among the different tested cells, SN12C and 786O- were two cell lines that distinctly expressed the CD44 protein. They were also very well-known and studied in our research group. Moreover, tumors generated from these cell lines also expressed CD44 protein. Bearing this analysis in mind, we decided to study the role of CD44 in three different models: Ren13, 786O-, and SN12C.

1.2 CD44 DOWNREGULATION

An interesting way to study the role of a protein is to reduce its expression and evaluate the consequences produced at different levels. To do so, we decided to genetically modify SN12C, 786O-, and Ren13 cells through an shRNA system as explained in Section 1.2.3 of materials and methods. This is a tet-on/tet-off system that allows for the reduction of CD44 expression when cells are in the presence of doxycycline. Once doxycycline is removed from the medium, CD44 expression is restored.

One piece of evidence that determines the proper functioning of the shRNA system is that, when doxycycline is administered to the cells, they exhibit red fluorescence, as represented in Figure 17.

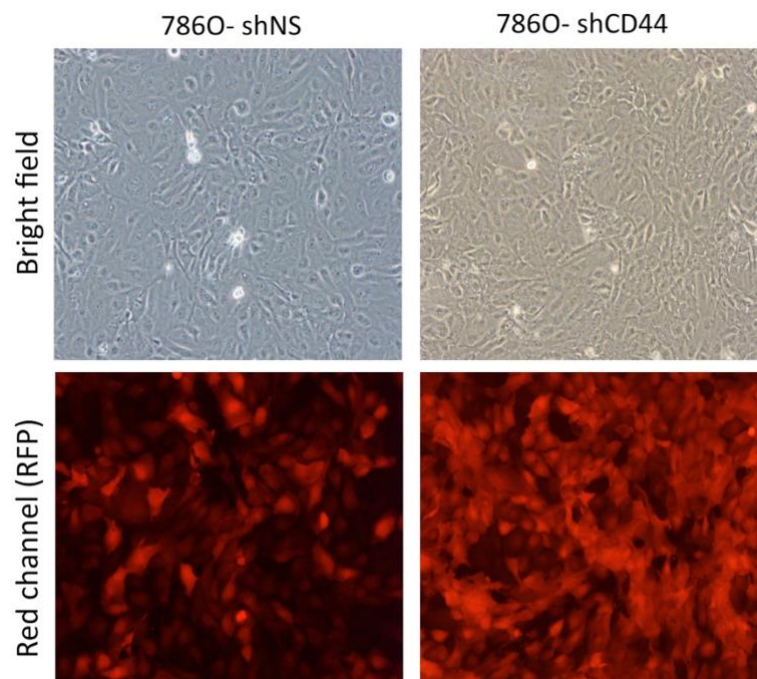


Figure 17. Doxycycline induction of shRNAs system in 786O- cells. From top to the bottom, bright field and red channel (RFP) images of 786O- shNS and 786O- shCD44 cells after doxycycline treatment (2,5 μ M for 48h). Pictures were taken at 20X.

Doxycycline activated the shRNA in the targeted (sh-CD44) and non-targeted (shNS) cells, which is why both cell types expressed RFP. Nevertheless, the silencing of the protein was only produced in the shRNA-CD44 cells.

1.2.1 Validation of shRNAs Functioning

Once the activation of the shRNA system was verified, we wanted to check the reduction of CD44 expression at the protein and RNA levels. We also wanted to determine which shRNA (shCD44-1 or shCD44-2) produced the highest silencing and to confirm that doxycycline did not affect the non-silencing or control cells (shNS). Thus, we performed a Western Blot of the different cell lines treated and non-treated with doxycycline.

As Figure 18 shows, doxycycline did not affect the control cells (shNS), as CD44 expression was maintained in the different cell lines.

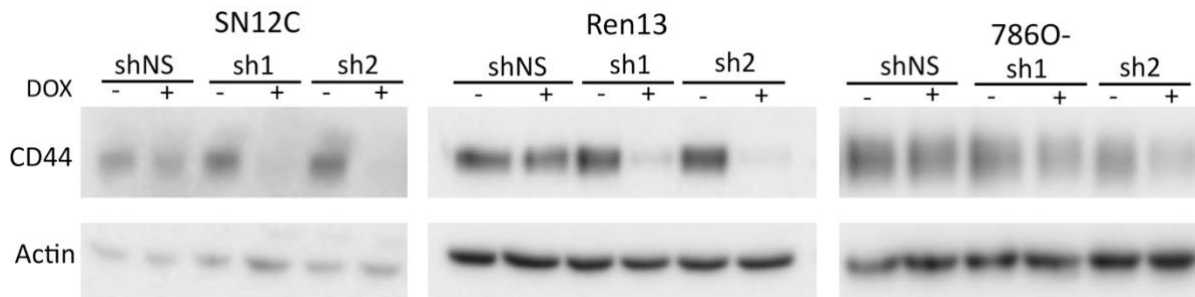


Figure 18. Western Blot of CD44 expression in different cells. Western Blot was developed to check the reduction of the CD44 protein expression in shCD44-1 and shCD44-2 of the three selected cell lines (SN12C, Ren13, and 786O-) when they were treated with doxycycline. shNS cells were used as controls. Actin expression was used as housekeeping. Cells were treated with 2,5µM of doxycycline during 48h.

Regarding the other shRNAs (shCD44-1 and shCD44-2), in all cell lines, a reduction of the CD44 expression after doxycycline treatment could be observed, demonstrating the activation and proper functioning of the silencing system. Nevertheless, in the case of SN12C and Ren13 cells, it seemed that the shCD44-1 produced higher silencing than shCD44-2. Conversely, in the case of 786O- cells, CD44 silencing was greater in the shCD44-2 cells.

Despite these results, we wanted to check the silencing efficiency at the RNA level. To do so, we performed a real-time PCR (explained in Section 1.2.1.3 of materials and methods) of the different cell models induced and non-induced with doxycycline.

Evaluation of the different shRNAs efficacy through Taqman assay demonstrated that doxycycline treatment produced a reduction of CD44 transcription (Figure 19). These data also proved that doxycycline didn't affect the shNS cells, as there were no changes in CD44 expression after administration of the drug.

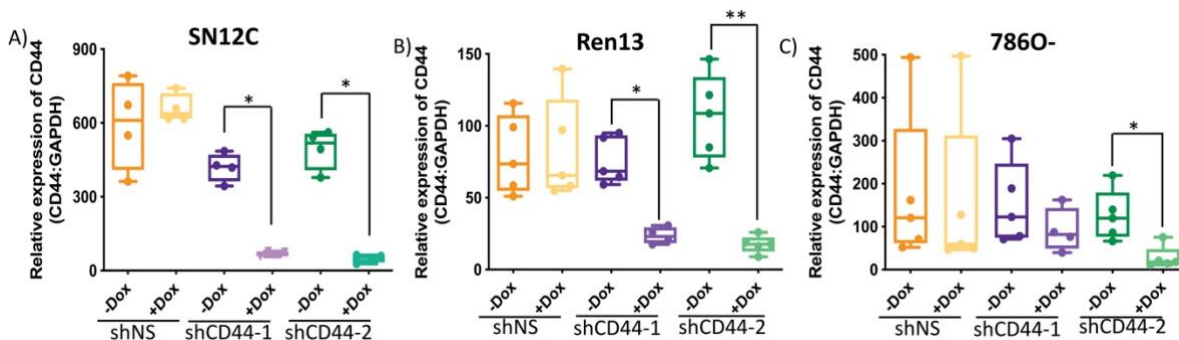


Figure 19. RNA levels of human CD44 in different cells. TaqMan assay was developed to check the CD44 protein reduction when shCD44-1 and shCD44-2 cells of the three selected cell lines (SN12C (A), Ren13 (B), and 7860- (C)) were treated with doxycycline. shNS cells were used as controls. GAPDH expression was determined as housekeeping. Cells were treated with 2,5 μ M of doxycycline during 48h.

To ensure the silencing system was working correctly, we decided to make one last validation assay. The different cells were subjected to a Flow Cytometry analysis (described in Section 1.2.2.5 of materials and methods). The results of the test are represented in Figure 20.

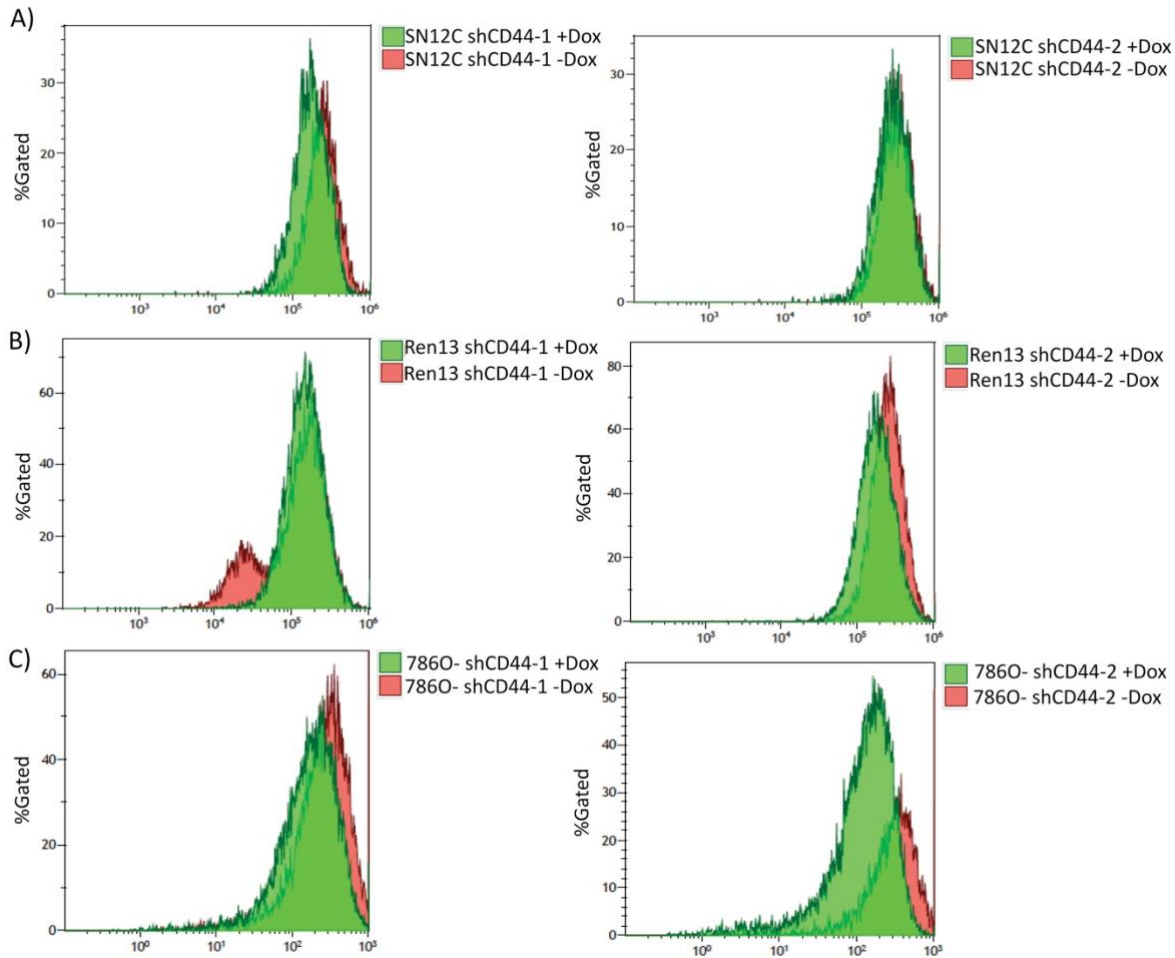


Figure 20. Flow Cytometry analysis of CD44 expression. CD44 protein expression of both shRNAs of SN12C (A), Ren13 (B), and 786O- (C) cells were checked by Flow Cytometry. Control cells (-Dox) were non-treated while doxycycline-treated cells (+Dox) were treated with 2,5µM of doxycycline during 48h.

Through Flow Cytometry assay, we were finally able to verify that shCD44-1 produced a notable CD44 silencing effect in SN12C and Ren13 cells, while shCD44-2 produced a higher downregulation of CD44 in 786O- cells.

For that, considering the results of the different experiments performed to verify the efficacy of shRNAs silencing, we decided to use shCD44-1 for SN12C and Ren13 cells, and shCD44-2 for 786O- cells. In both situations, the selected shRNAs produced a higher silencing of the protein target. Furthermore, shNS cells from all three cell lines were used as controls in all the following experiments.

1.3 FUNCTIONAL VALIDATION OF CD44 DOWNREGULATION IN VITRO

Once cells were selected, we decided to study the functional role of CD44. Our main interest was especially its role in migration and invasion processes. For that, we began to study the effect of CD44 silencing in these two processes *in vitro*.

To study the migration course, we developed Wound Healing and transwell migration assays, as explained in Section 1.3.1 of materials and methods. To determine the effect in the invasion process, we performed transwell invasion assays, detailed in Section 1.3.2 of materials and methods.

1.3.1 Effects of CD44 Knockdown on Cell Migration

SN12C Cells

To determine the role of CD44 in the migration properties of SN12C cells, a Wound Healing assay was performed. Through this experiment, we compared the migration velocity of cells treated and non-treated with doxycycline.

According to our hypothesis, the silencing of CD44 expression should produce a reduction in cell migration. As doxycycline was used to induce the downregulation of CD44, we expected to observe a migration decrease of the SN12C shCD44-1 cells treated with doxycycline compared to the other groups.

Migration process of SN12C cells was followed up until 24h. Figure 21 summarizes the results of the experiment.

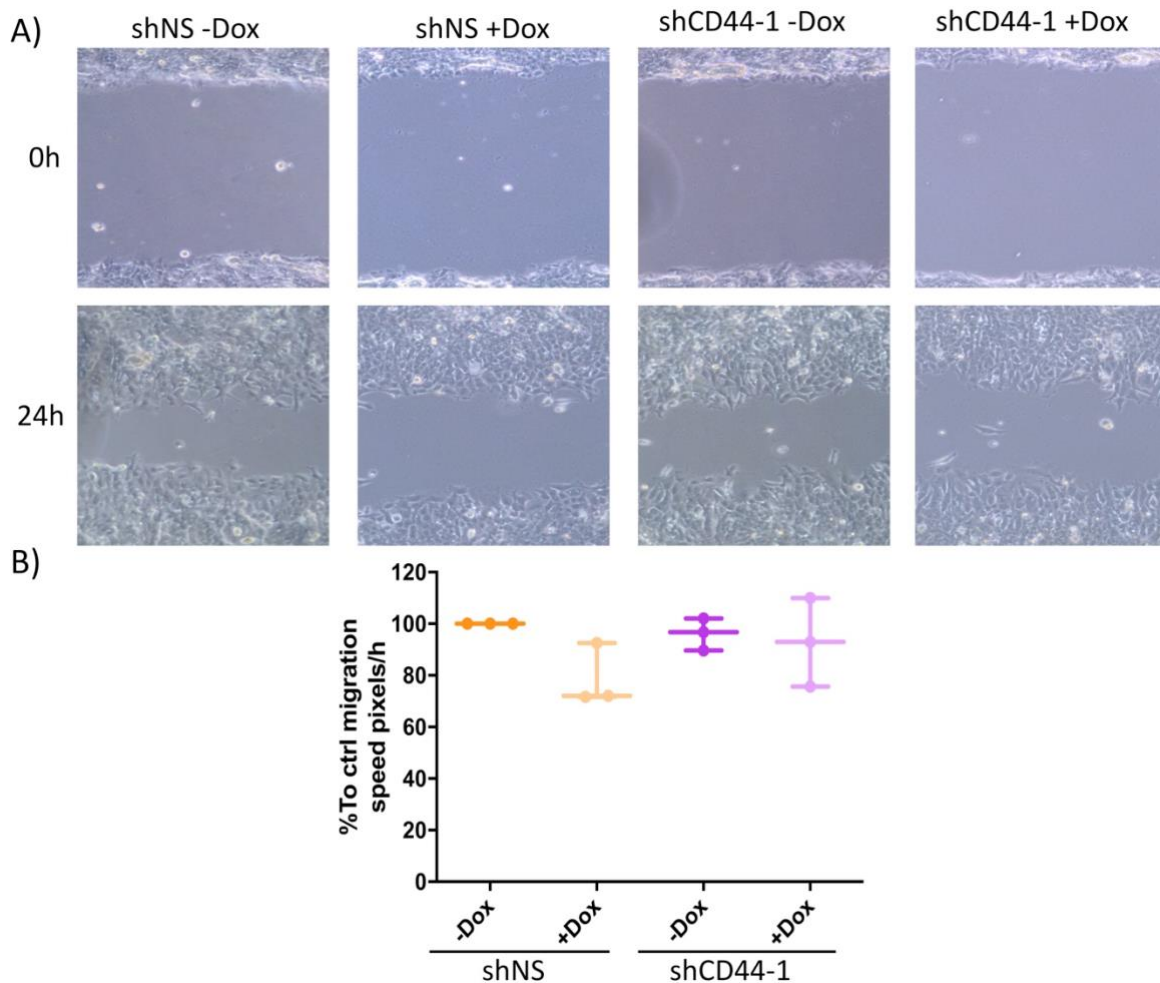


Figure 21. CD44 knockdown did not affect the migration capacity of SN12C cells. Results of Wound Healing assay developed in SN12C cells. Cells were treated with 2,5 μ M of doxycycline during 48h. 75000 cells were seeded in each well of the insert 24h before the experiment. Three images of each well were taken at 10X every 3h. A) Images of the wounds of SN12C shNS and SN12C shCD44-1 cells treated and non-treated with doxycycline at time 0 and after 24h of the experiment. B) Quantification of migration velocity of cells expressed in pixels/h. No differences could be observed between any of the groups.

Represented images, as well as the chart, show that the reduction of CD44 expression did not affect the migration capacity of SN12C cells. In order to confirm these results, we decided to perform another migration assay, but this time using the transwell migration technique (results are represented in Figure 22). This experiment measures the directional migration of cells as they are forced to migrate vertically, whereas in the Wound Healing assay there is no directionality.

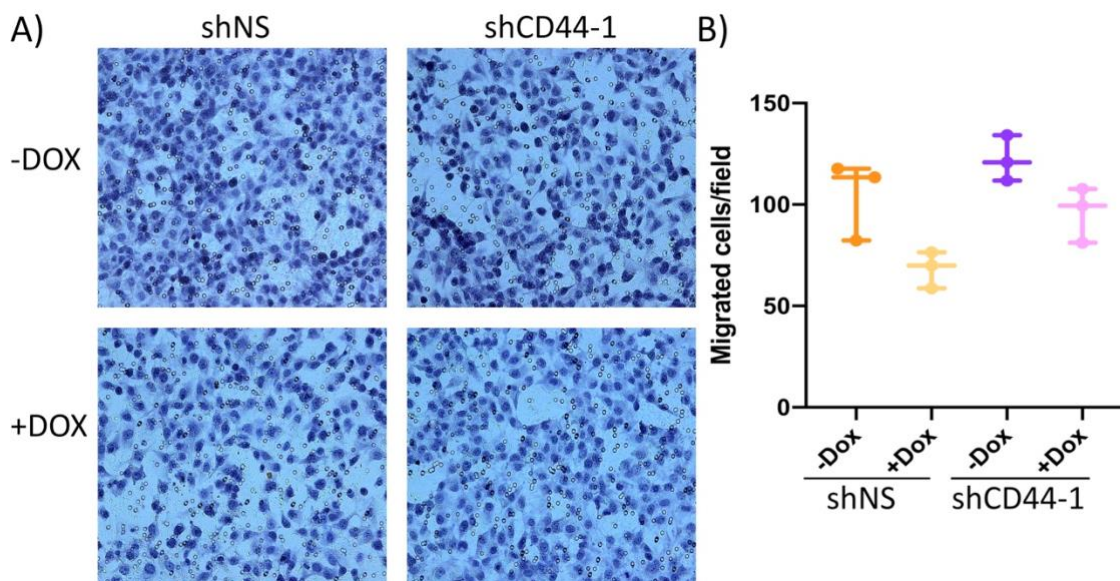


Figure 22. CD44 knockdown did not affect the migration capacity of SN12C cells. Transwell migration assay of SN12C cells. Cells were treated with 2,5 μ M of doxycycline during 48h. 50000 cells were seeded in each transwell. The assay was performed for 24h. Twelve images of each well were taken at 20X and counted manually. A) Representative images of SN12C shNS and SN12C shCD44-1 cells treated and non-treated with doxycycline after 24h of the migration assay. B) Quantification of migrated cells per field. No differences were observed between any of the groups.

Initially, there seemed to be a slight tendency of migration decrease when cells were treated with doxycycline. Nevertheless, as in the previous assay, no statistically significant differences could be observed in the migration ability of cells once CD44 expression was reduced. Both migration assay results suggested CD44 was not involved in the migration process of SN12C cells. However, its role in the invasion process was still undetermined.

Ren13 Cells

Ren13 was the primary tumor model used during the RNA sequencing to define which genes were implicated in the malignization process of tumors. CD44 was one of the candidates that appeared to be overexpressed after the antiangiogenic treatment in this tumor model. Then, considering the previous results, we expected to observe a decrease in the migration ability of cells due to the CD44 silencing. Ren13 cells migrated faster

than SN12C, for that the Wound Healing assay performed to determine differences between untreated and doxycycline-treated groups was monitored for up to 9h.

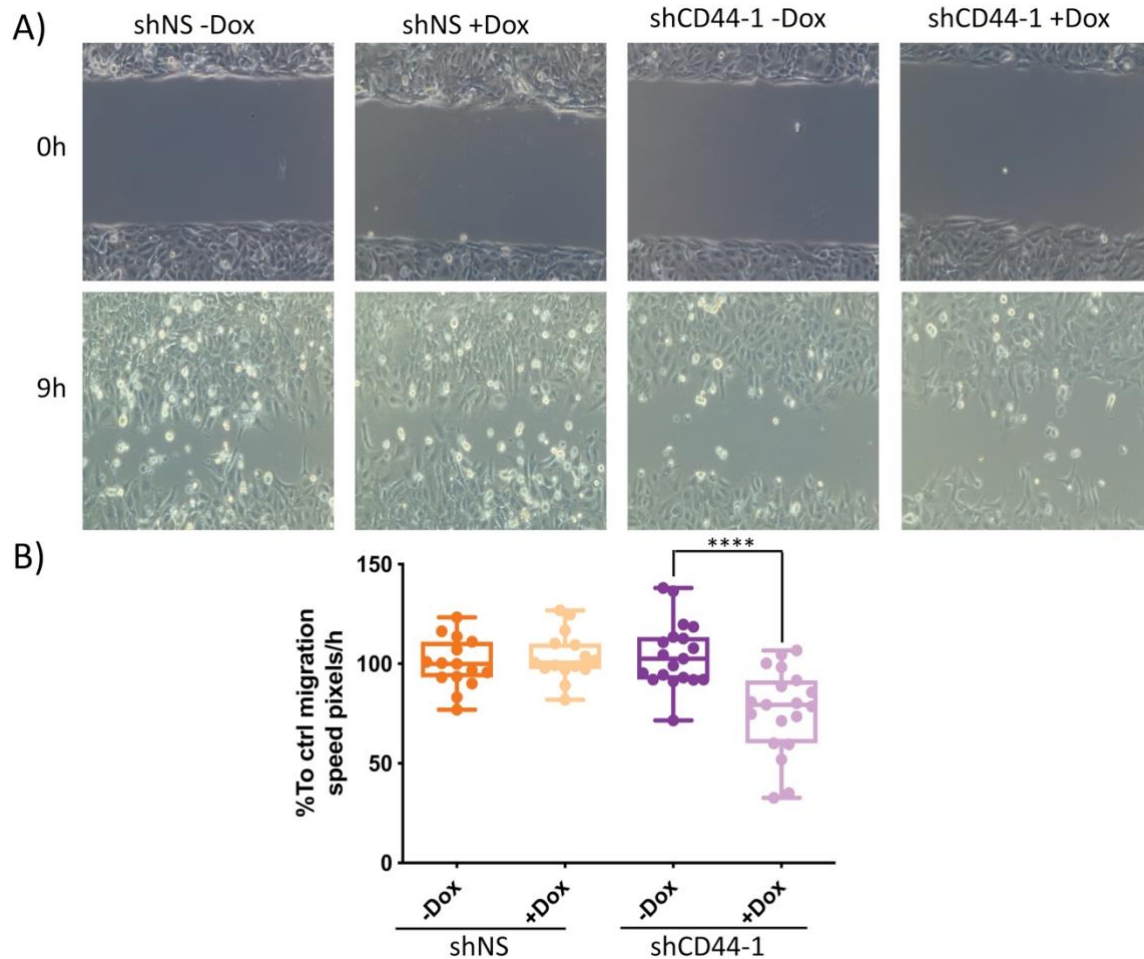


Figure 23. CD44 knockdown produced a reduction of the Ren13 cell migration. Results of the Wound Healing assay developed in Ren13 cells. Cells were treated with 2,5 μ M of doxycycline during 48h. 15000 cells were seeded in each well of the insert 24h before the experiment. Three images of each well were taken at 10X every 3h. A) Images of the wounds of Ren13 shNS and Ren13 shCD44-1 cells treated and non-treated with doxycycline at time 0 and after 9h of the experiment. B) Quantification of migration velocity of cells expressed in pixels/h. (B, Mann Whitney test $p < 0,0001$ ****)

As represented in Figure 23, there was a statistically significant reduction of the migration capacity of shCD44-1 cells when they were treated with doxycycline, which was when CD44 was knocked down. However, shNS cells treated with doxycycline did not exhibit any alteration in their migration capacity, meaning that observed results were specifically due to the reduction of CD44 expression.

To validate the results, we performed a transwell migration assay, as was done with the SN12C cells.

The results of the experiment (Figure 24) confirmed the results obtained with the Wound Healing assay. When Ren13 shCD44-1 cells were induced with doxycycline, and therefore CD44 expression was reduced, there was a statistically significant reduction of the cell migration. It also confirmed that doxycycline did not affect the shNS cells.

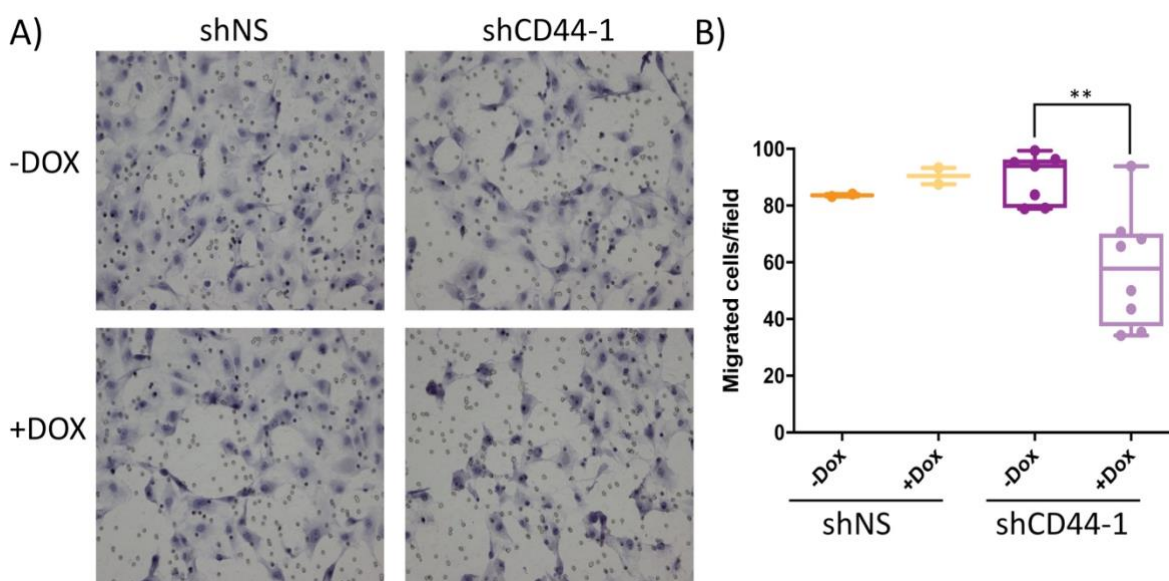


Figure 24. CD44 knockdown produced a reduction of the migration in Ren13 cells. Transwell migration assay of Ren13 cells. Cells were treated with 2,5 μ M of doxycycline during 48h. 10000 cells were seeded in each transwell. The assay was performed for 24h. Twelve images of each well were taken at 20X and counted manually. A) Representative images of Ren13 shNS and Ren13 shCD44-1 cells treated and non-treated with doxycycline after 24h of the migration assay. B) Quantification of migrated cells per field. (B, Mann Whitney $p < 0,01^{**}$)

In accordance with our hypothesis and the results of the RNA sequencing, both assays suggested the role of CD44 in the migration process of the Ren13 tumor model.

786O- Cells

786O- cells were the last selected model to test. The migration ability of those cells was similar to the Ren13 cell model, despite being primary cells. Subsequently, we expected that the migration results obtained with 786O- cells would concur with the Ren13 model.

In order to downregulate CD44 expression, cells were either induced or not with doxycycline over 48h. 24h before the experiment, they were seeded in each well of the insert. The next day, inserts were removed, and the migration process was monitored for up to 9h.

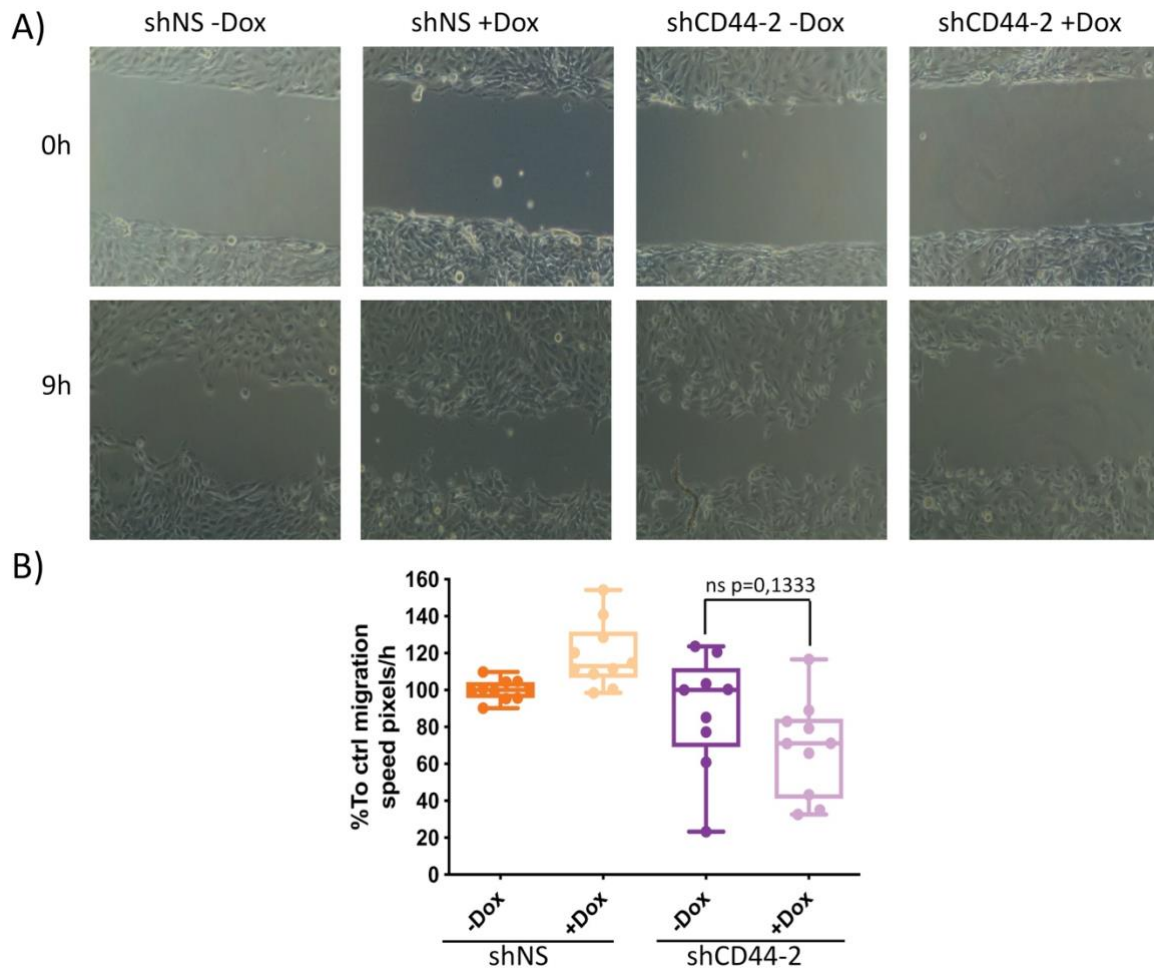


Figure 25. CD44 knockdown produced a slight reduction, but not statistically significant, of the migration in 786O- cells. Results of the Wound Healing assay developed in 786O- cells. Cells were treated with 2,5 μ M of doxycycline during 48h. 30000 cells were seeded in each well of the insert 24h before the experiment. Three images of each well were taken at 10X every 3h. A) Images of the wounds of 786O-shNS and 786O- shCD44-2 cells treated and non-treated with doxycycline at time 0 and after 9h of the experiment. B) Quantification of migration velocity of cells expressed in pixels/h. (B, Mann Whitney test $p=0,1333$)

The results of the experiment are represented in Figure 25. It appears that there was a slight tendency of shCD44-2 cells to decrease their migration capacity after doxycycline treatment, due to CD44 silencing. We could also confirm that doxycycline did not affect

shNS cells and that the migration effect observed was specifically due to the reduction of CD44 expression.

As with the other cell types, a transwell migration assay was performed to confirm the results.

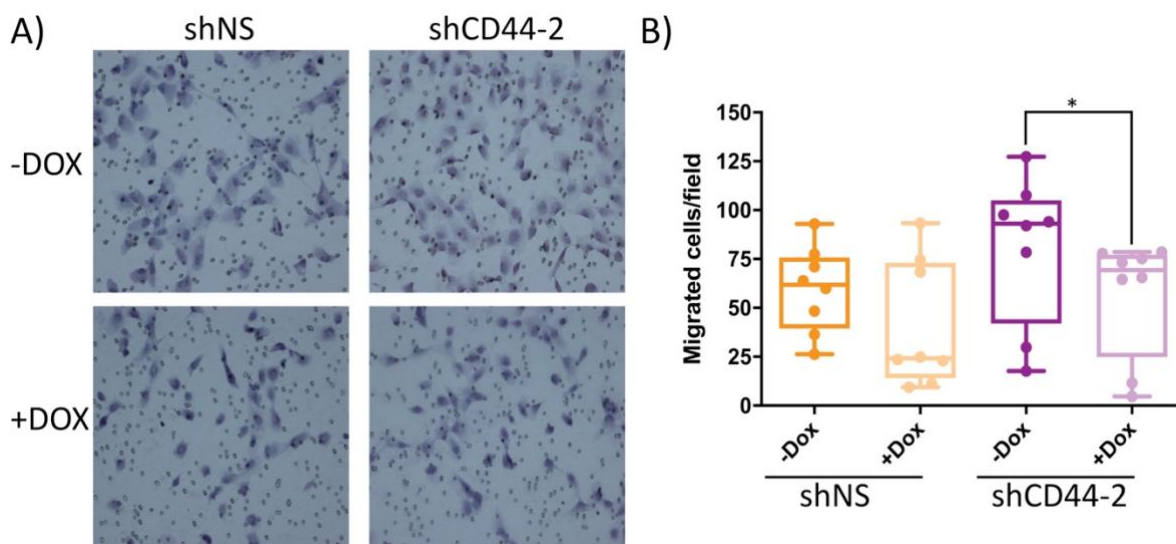


Figure 26. CD44 knockdown produced a slight reduction of the 786O- cell migration. Transwell migration assay of 786O- cells. Cells were treated with 2,5 μ M of doxycycline during 48h. 10000 cells were seeded in each transwell. The assay was performed for 24h. Twelve images of each well were taken at 20X and counted manually. A) Representative images of 786O- shNS and 786O- shCD44-2 cells treated and non-treated with doxycycline after 24h of the migration assay. B) Quantification of migrated cells per field. (B, Mann Whitney test $p < 0,05^*$)

Figure 26 contains the results of the assay. As with the previous experiment, a reduction of the shCD44-2 cell migration when they were treated with doxycycline could be observed. Although this reduction was statistically significant, there was considerable variability in the results.

Both migration assays suggested a role of CD44 in the migration process of 786O-, as expected and demonstrated with Ren13 cell model.

1.3.2 Effects of CD44 Knockdown on Cell Invasion

After studying the CD44 silencing in the migration course of the different cell lines, we decided to determine its role in the invasion process. Subsequently, we performed several transwell invasion experiments.

SN12C Cells

Despite the migration results obtained with the SN12C cells which were not in accordance with what was expected, we decided to test the effect of silencing CD44 in the invasion process of those cells. They were treated with doxycycline for 48h and then the invasion transwell assay was performed.

Contrary to the slow migration capacity that SN12C cells showed previously, they proved to be incredibly invasive. Nevertheless, when invaded cells were counted after 24h, no statistical differences could be observed between the different groups (Figure 27).

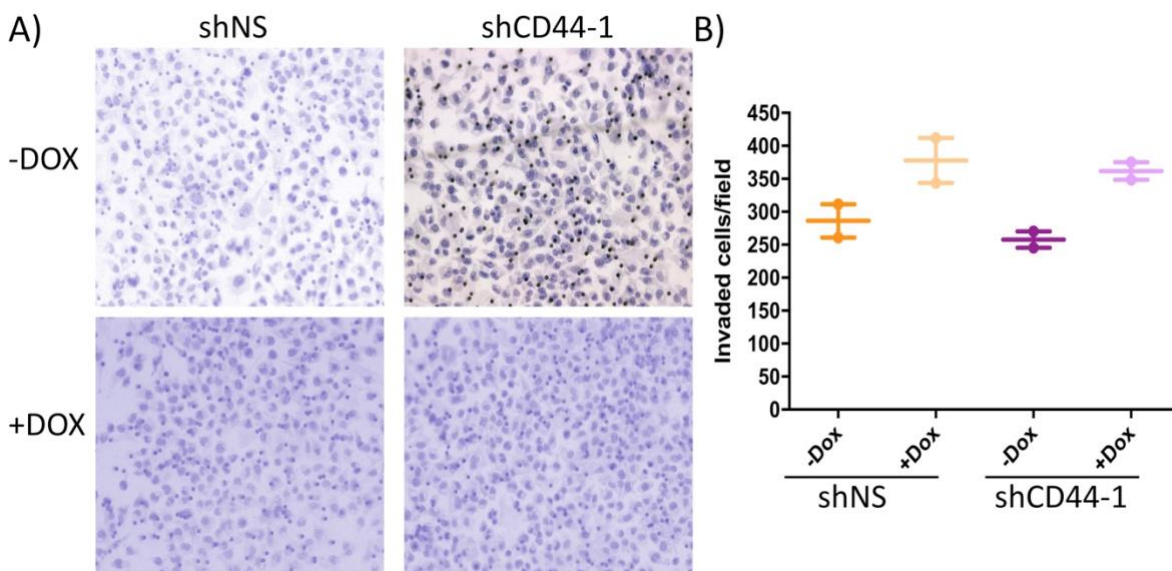


Figure 27. CD44 knockdown did not produce any changes in the invasion capacity of SN12C cells. Transwell invasion assay of SN12C cells. Cells were treated with 2,5 μ M of doxycycline during 48h. 50000 cells were seeded in each transwell. The assay was performed for 24h. Twelve images of each well were taken at 20X and counted manually. A) Representative images of SN12C shNS and SN12C shCD44-1 cells treated and non-treated with doxycycline after 24h of the invasion assay. B) Quantification of invaded cells per field. No differences between any of the groups were observed.

Results obtained in the migration assays together with the invasion ones may suggest that CD44 could not be involved in the malignization process of, at least, SN12C cells.

Ren13 Cells

Ren13 cells previously demonstrated an involvement of the CD44 protein in their migration process. Subsequently, we also expected to observe a reduction of the invasion capacity of cells when CD44 was silenced through doxycycline treatment.

When we studied the invasion ability of those cells after doxycycline induction, the shCD44-1 treated cells were shown to be less invasive than the other groups, as demonstrated in Figure 28. Furthermore, control cells (shNS) were not affected by the treatment, suggesting that the results observed were due to the decrease of CD44 expression.

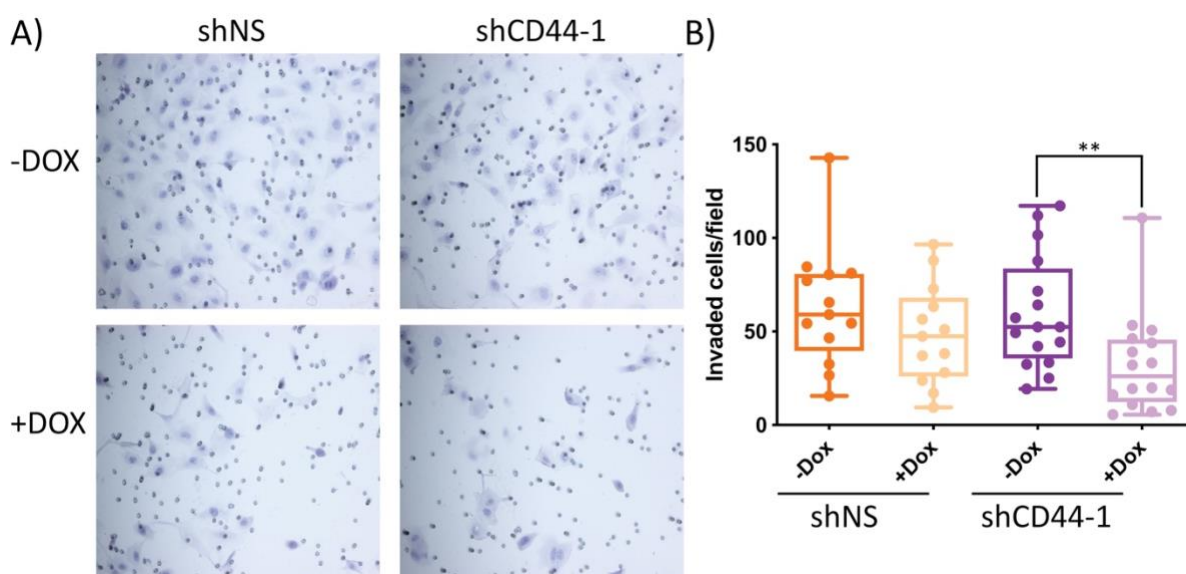


Figure 28. CD44 knockdown produced a decrease in the invasion capacity of Ren13 cells. Transwell invasion assay of Ren13 cells. Cells were treated with 2,5 μ M of doxycycline during 48h. 50000 cells were seeded in each transwell. The assay was performed for 24h. Twelve images of each well were taken at 20X and counted manually. A) Representative images of Ren13 shNS and Ren13 shCD44-1 cells treated and non-treated with doxycycline after 24h of the invasion assay. B) Quantification of invaded cells per field. (B, Mann Whitney test $p < 0,01^{**}$)

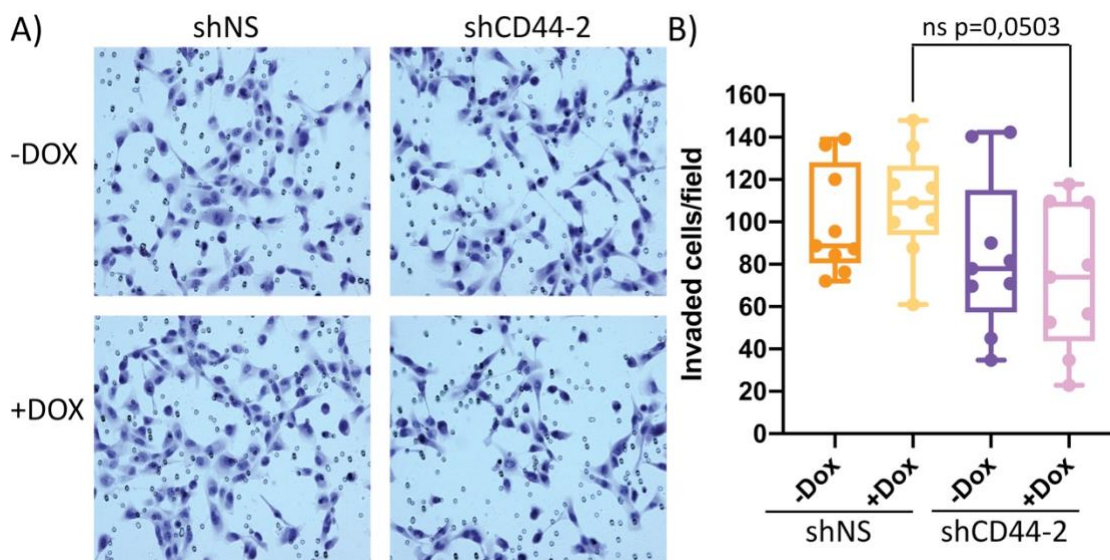
Invasion results were in accordance with the migration response to CD44 downregulation, suggesting the role of this protein in the migration and invasion processes in the Ren13 model.

786O- Cells

As demonstrated with the other cell models, migration and invasion effects were in accordance. Following on from this, and despite the variability in the migration response after silencing CD44 in 786O- cells, we expected to observe a decrease on the invasion process due to the downregulation of the protein.

The invasion assay performed with 786O- cells is represented in

Figure 29. Although there was a degree of variability in the results, there appears to be a slight reduction of the invasion ability of cells when CD44 protein expression was



decreases.

Figure 29. Invasion transwell assay developed in 786O- cells. Cells were treated with 2,5µM of doxycycline during 48h. 50000 cells were seeded in each transwell. Twelve images of each well were taken at 20X and counted manually. A) Representative images of 786O- shNS and 786O- shCD44-2 treated and non-treated with doxycycline after 24h of the invasion assay. B) Quantification of invaded cells per field. (B, Mann Whitney test p=0,0503)

Considering the migration and invasion assays developed in 786O- cells, we could suspect the involvement of CD44 in both processes. Nevertheless, the results were not as conclusive as in the Ren13 cell model.

Once we had evaluated the consequences of silencing CD44 in our three cell models *in vitro*, we could establish that in Ren13 and 786O- cells CD44 protein plays an important role in their migration and invasion properties. As observed when these cells were treated with doxycycline to induce the shRNA, there was a decrease in CD44 expression and consequently, the migration and invasion capacities of cells were reduced. However, the downregulation of CD44 in SN12C cells did not produce any changes in these processes, suggesting that in this tumor model CD44 could not be involved in the malignization process.

1.4 DOWNREGULATION OF CD44 IN VIVO

While *in vitro* experiments were being performed, we started with the *in vivo* assays, as the generation of tumors from genetically modified cells requires some time. Mice models were developed as described in Section 2.3 of materials and methods. Unfortunately, it was only possible to generate tumors from SN12C shCD44-1 cells and 786O- shCD44-2 cells, but not from Ren13 shCD44-1 cells.

In both cases, animals were divided into four groups depending on the treatment (previously explained in Section 2.7 of materials and methods). Animals injected with SN12C shCD44-1 cells were treated for three weeks, whereas animals injected with 786O- shCD44-2 tumors were treated for two weeks.

Once the experimental had finished, animals were sacrificed. Tumors, as well as other organs, were collected for further analysis.

The first and most important thing to verify when the experiments had finished was the proper functioning of shRNAs. We checked whether the tumors of mice treated with doxycycline showed a decrease of CD44 expression. We developed a Western Blot of

different fragments of each tumor. We also performed CD44 Immunohistochemistry of tumor slides to verify the protein reduction and its location.

SN12C shCD44-1 Tumors

The principal objective of the *in vivo* experiments was to study the invasiveness role of CD44, but first it was necessary to validate the proper activation of the silencing system. To verify that doxycycline treatment induced the shRNA and produced the decrease of CD44 protein expression, several pieces of the tumor from each animal were lysate and properly manipulated to perform a Western Blot assay. The results of the experiment are collected in Figure 30.

As the graph indicates, doxycycline produced a decrease in CD44 expression both in antiangiogenic-treated (+DC101) and non-treated (-DC101) groups, validating the *in vitro* results previously shown.

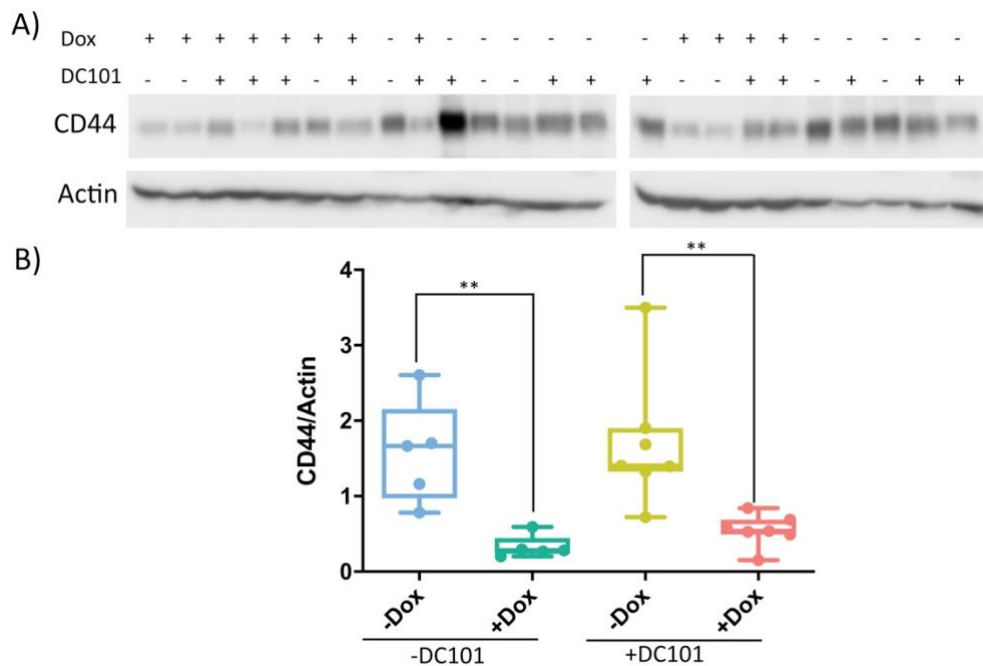


Figure 30. Expression of CD44 protein and its downregulation in tumors generated from SN12C shCD44-1 cells. A) Western Blot of CD44 expression of different tumor pieces. The treatment of each tumor sample is described with + or -. Doxycycline dose was 400mg/200ml of water and 1mg/dose of DC101. Actin expression was determined as housekeeping. B) Quantification of CD44 expression of each tumor piece normalized by the housekeeping. (B, Mann Whitney test $p < 0,01^{**}$)

However, according to our hypothesis, the upregulation of CD44 expression observed in the Ren13 tumor model was due to the antiangiogenic treatment. In the present exposed tumor model (SN12C), the antiangiogenic treatment did not produce the expected increase of CD44 expression (comparison between -Dox-DC101 group and -Dox +DC101 group).

This was more evidence that added to the *in vitro* experiments, questioning the role of CD44 in the SN12C tumor model.

786O- shCD44-2 Tumors

Due to the impossibility of generating tumors from Ren13 cells, we evaluated the *in vivo* effects of silencing CD44 in tumors generated from the 786O- shCD44-2 cells. As was previously demonstrated, 786O- cells proved to respond in a similar way to Ren13 cells when CD44 is silenced *in vitro*. Thus, we expected to confirm our hypothesis and observe a reduction of the tumor invasion when the downregulation of CD44 was induced.

Figure 31 shows the results of the Immunohistochemistry and Western Blot of CD44 developed in 786O- shCD44-2 tumors.

Images of the Immunohistochemistry showed that tumors of animals treated with doxycycline expressed less CD44 protein than the rest. Nevertheless, the loss of protein expression was not absolute. Moreover, there was heterogeneity between the tumors and even different regions of the same tumor; this is the reason why protein expression can oscillate.

The Western Blot of tumor pieces of the mice exhibited a reduction of CD44 expression in those animals that were treated with doxycycline in the antiangiogenic-treated (+DC101) and non-treated (-DC101) groups. According to the Immunohistochemistry results, the protein decrease was noteworthy rather than absolute in affecting the migration and invasion features of tumor cells.

In this tumor model, we could observe an increase in CD44 expression after DC101 treatment, supporting the previous results where antiangiogenic treatment induced the upregulation of CD44 in the Ren13 tumor model.

Thus, 786O- model seemed to fit better than the SN12C in our hypothesis and to replicate the results observed with the Ren13 model.

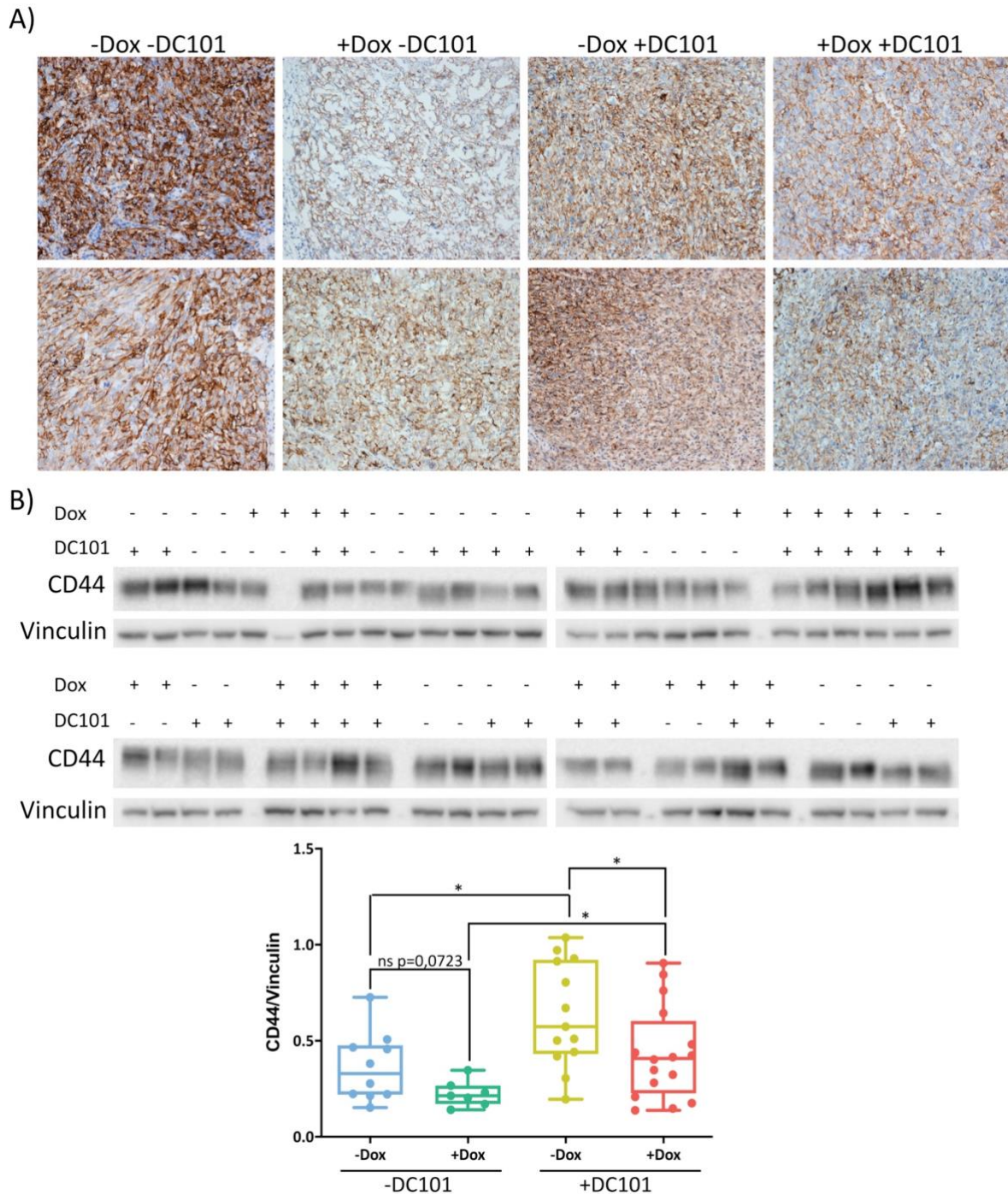


Figure 31. Expression of CD44 protein and its downregulation in tumors generated from 786O- shCD44-2 cells. A) Representative images of CD44 Immunohistochemistry of different tumors. Pictures were taken at 20X. B) Western Blot of CD44 expression of different tumor pieces. The treatment of each tumor sample is described with + or -. Doxycycline dose was 400mg/200ml of water and 1mg/dose of DC101. Vinculin expression was determined as housekeeping. At the bottom, it is represented the quantification of CD44 expression of each tumor piece normalized by the housekeeping. (B, Mann Whitney test $p < 0,05^*$)

1.4.1 Tumor Characterization: Vessel Density and Cell Proliferation

Other important tumor characteristics we wanted to evaluate from the samples were the vessel density and cell proliferation.

On the one hand, we expected to find differences in the number of blood vessels between the groups. Apart from the doxycycline induction of shRNAs, some mice were also treated with DC101, an antiangiogenic drug that targets the murine VEGFR2. Then, if the treatment was successful, we would expect to observe a decrease in the number of vessels of DC101-treated animal tumors.

On the other hand, no changes in cell proliferation of tumor cells were expected between any of the different treatment groups, as antiangiogenic treatment affects the tumor vasculature, not the tumor cells.

SN12C shCD44-1 Tumors

Determination of vessel density was used to evaluate the effectiveness of the antiangiogenic drug, as its administration should produce a reduction in the number of vessels. We also evaluated cell proliferation to determine that DC101 only affected the vessels and not the tumor cells.

In SN12C shCD44-1 tumors, the vessel density was studied through Immunofluorescence using the CD31 antibody. As shown in Figure 32 (A), tumors treated with the antiangiogenic drug (+DC101) had fewer blood vessels, as was expected. However, the results were not statistically significant. In observing the non-antiangiogenic (-DC101) treated tumors, no differences could be observed between the +Dox and -Dox groups.

Figure 32 (B) shows the results of the Immunohistochemistry developed to determine the proliferation of tumor cells through PCNA staining. No differences could be observed between any of the groups.

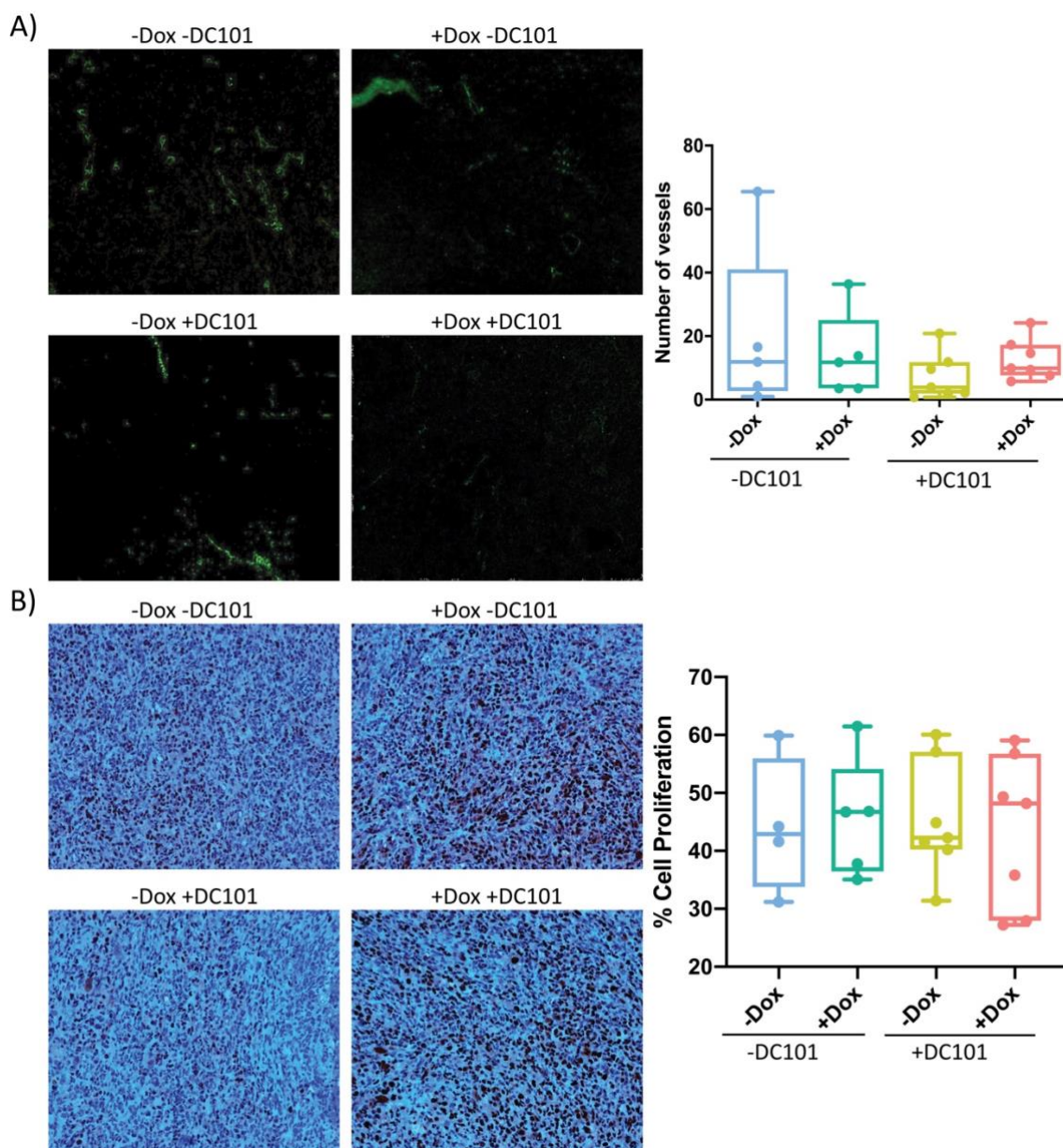


Figure 32. Characterization of SN12C tumors through immunoassays. A) Immunofluorescence of blood vessels using the CD31 antibody. Different images of each tumor were taken at 20X. Quantification of the number of blood vessels was developed manually. B) Immunohistochemistry of proliferative cells using the PCNA antibody. Different images of each tumor were taken at 20X. Quantification of the number of proliferative cells was developed manually. No differences between any of the groups could be observed.

786O- shCD44-2 Tumors

The vessel density and the proliferation of tumor cells were also determined in the *in vivo* assay performed with the 786O- shCD44-2 tumors.

This time the number of vessels was determined through Immunohistochemistry using the CD31 antibody. The results are shown in Figure 33 (A). As expected, antiangiogenic-treated tumors (+DC101) showed fewer blood vessels than the non-treated groups (-DC101), independent of the doxycycline treatment.

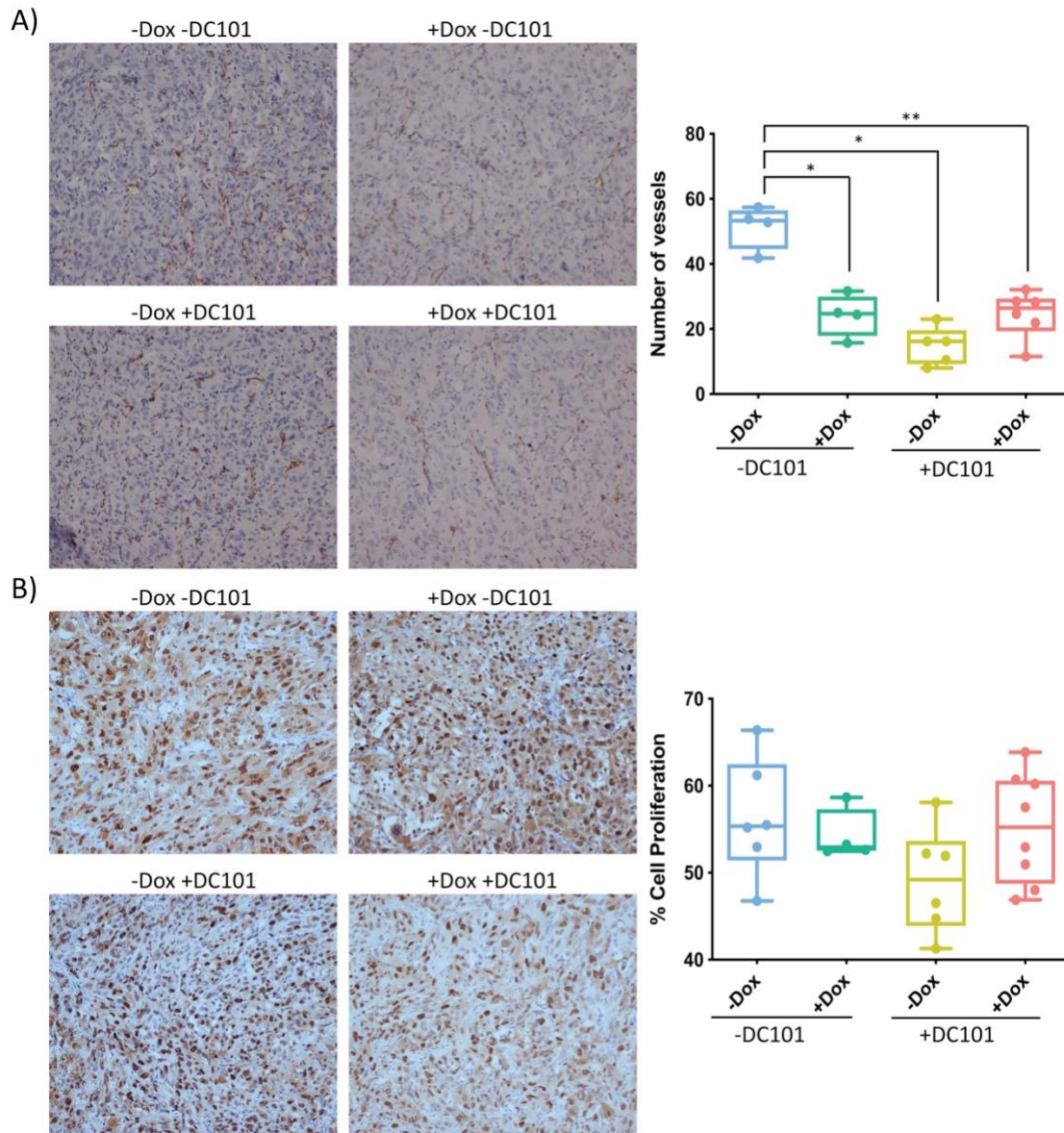


Figure 33. Characterization of 786O- tumors through Immunohistochemistry. A) Immunohistochemistry of blood vessels using the CD31 antibody. Different images of each tumor were taken at 20X. Quantification of the number of blood vessels was developed manually. B) Immunohistochemistry of proliferative cells using the PCNA antibody. Different images of each tumor were taken at 20X. Quantification of the number of proliferative cells was developed manually. (A, Mann Whitney test $p < 0,05$ * $p < 0,01$ **)

There was an unexpected result in the non-antiangiogenic treated group (-DC101): the tumors from animals that received doxycycline showed a decrease in the number of vessels. This suggests CD44 plays a role in angiogenesis.

Figure 33 (B) shows the results of the Immunohistochemistry developed using the PCNA antibody to determine cell proliferation. As can be observed in the quantification, there were no changes in the proliferation of tumor cells between any of the treatment groups.

1.4.2 Effects of CD44 Downregulation on Tumor Invasion

Afterwards, we moved to study invasion, which was the main objective of the *in vivo* experiments. First, Hematoxylin-Eosin staining was developed (as described in Section 2.9.1.5 of materials and methods) in order to distinguish the tumor from the normal renal parenchyma. Next, we proceeded to measure the invasion of tumor cells into the normal renal tissue. This method is described in Section 2.8 of materials and methods.

SN12C shCD44-1 Tumors

The *in vitro* results of the migration and invasion processes suggested CD44 was not implicated in these processes in SN12C tumor cells, as its silencing did not produce any changes. Thus, we did not have many expectations about the *in vivo* evaluation of the CD44 involvement in the invasion process in this tumor model. However, given *in vivo* and *in vitro* results do not always coincide, we decided to carry on with the assay.

Section (A) of Figure 34 shows an example of how the invasion measurement was performed. Section (B) shows the quantification of the invasion expressed as depth/tumor weight.

On the one hand, there was a slight tendency to increase the invasive potential of tumors treated with the antiangiogenic drug, which is the -Dox +DC101 group. Nevertheless, the number of samples was too low to confirm that. However, this result would confirm the observations explained in the previous results: that the antiangiogenic treatment is

responsible for the malignization process producing an increase of the invasive potential of tumors.

On the other hand, according to our hypothesis, CD44 was implicated in the increase of tumor invasion after antiangiogenic treatment. Hence, tumors of animals treated with doxycycline should present a reduction of their invasive capacity, as we would be blocking the mechanism through tumors become more aggressive. Unfortunately, the silencing of CD44 expression did not have any effect on tumor invasion. These results were in accordance with the *in vitro* analysis of SN12C cells, where CD44 knockdown did not affect the migration and invasion processes too.

One of the main issues of SN12C tumors was the highly aggressive and metastatic potential they showed from the beginning of the experiment. In some cases, tumors destroyed completely the kidney, thwarting the study of the invasion and reducing the number of samples.

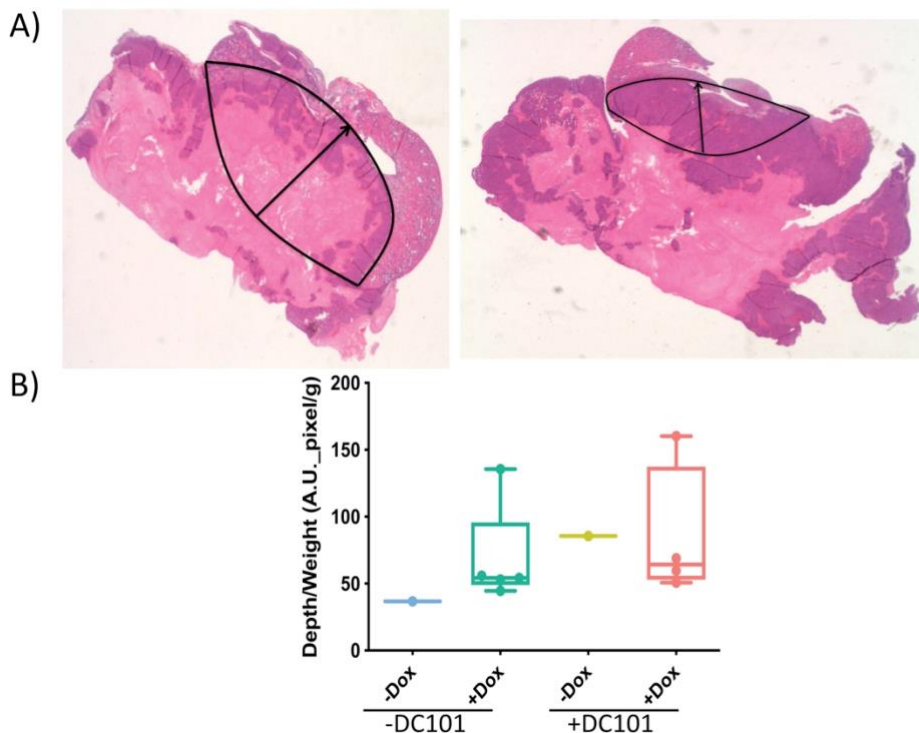


Figure 34. Determination of the invasion in tumors generated from SN12C shCD44-1 cells. A) Representative images of Hematoxylin-Eosin staining used to distinguish the tumor from the kidney to determine the invasion. B) Quantification of tumor invasion expressed as depth/tumor weight. No invasion differences could be observed between any of the groups.

786O- shCD44-2 Tumors

Using the same method as before, invasion of tumors generated from 786O- shCD44-2 cells were determined. This time, if the migration and invasion *in vitro* results obtained with those cells were reproduced, we would be able to confirm our hypothesis of the role of CD44 protein in the malignization process of some tumors. At the same time, we would be demonstrating there are different types of tumors that differ in the antiangiogenic response, as its post-treatment malignization is not performed through the same mechanisms.

Figure 35 shows representative images of how the invasion was measured and also its quantification expressed as depth/tumor weight.

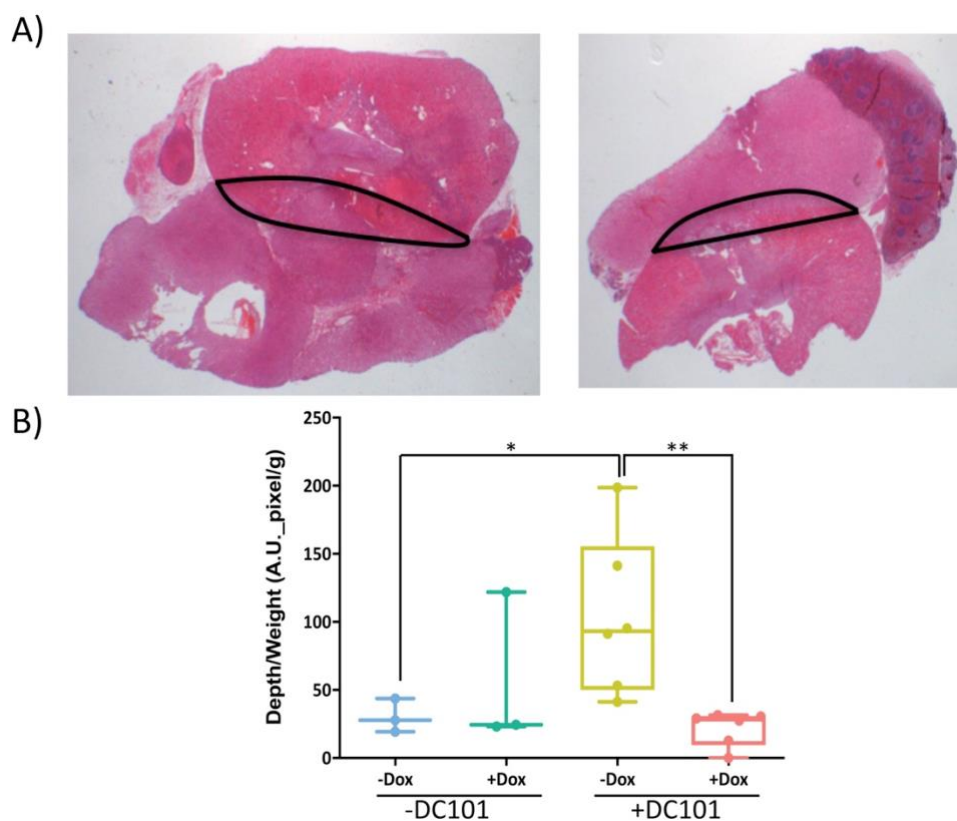


Figure 35. Determination of the invasion in tumors generated from 786O- shCD44-2 cells. A) Representative images of Hematoxylin-Eosin staining used to distinguish the tumor from the kidney to determine the invasion. B) Quantification of tumor invasion expressed as depth/tumor weight. (B, Mann Whitney test $p < 0,05$ * $p < 0,01$ *)

In this case, the increase of invasion of those tumors treated with antiangiogenic was statistically significant. It meant that the DC101 group was more aggressive than the control group (-DC101).

Additionally, mice that received the double treatment (+Dox+DC101) showed a significant reduction of the invasion compared to the group treated with the antiangiogenic drug but not with doxycycline (-Dox+DC101). This result would confirm the hypothesis that CD44 is involved in further invasion produced by the antiangiogenic treatment. When tumors were treated with DC101, CD44 expression increased and consequently, its invasive capacity increased too. However, when CD44 protein expression was reduced through doxycycline treatment, antiangiogenic therapy was not able to increase the tumor invasion, as the mechanism responsible for the malignization was altered.

In summary, the role of CD44 in migration and invasion of renal cancer cells could be demonstrated *in vitro* in Ren13 and 786O- models. However, *in vivo*, we could only demonstrate the involvement of CD44 in tumor invasion after antiangiogenic treatment using the 786O- shCD44-1 tumors, as it was impossible to generate tumors from Ren13 shCD44-1 cells.

Nevertheless, the role of CD44 in tumor invasion and migration using SN12C model could not be determined. It seems probable that some other mechanisms are involved in the malignization of this tumor model which are distinct from CD44.

2. MIGRATION AND INVASION MECHANISMS DOWNSTREAM CD44

Once we had demonstrated the involvement of CD44 in the increased invasion due to the antiangiogenic treatment, we were interested in discovering which signaling pathways downstream CD44 took part in that process. To do so, we carried out in depth bibliographic research. Three different signaling pathways associated with CD44 appeared possibly to be implicated in the migration and invasion processes of cancer cells. Those pathways were: Src, JAK/Stat, and AKT. Thus, we decided to inhibit the

different pathways and study the consequences in the migration and invasion processes. We were also interested in combining the inhibitors with the CD44 knockdown to determine the link between them.

Selected inhibitors to develop the analysis were: Perifosine (AKT inhibitor), Ruxolitinib (JAK inhibitor) and, Bosutinib (Src inhibitor).

2.1 MIGRATION EFFECT OF INHIBITING THE CANDIDATE PATHWAYS DOWNSTREAM CD44

Initially, we performed some migration assays through Wound Healing using different doses of each drug to determine their effect over the cells and choose the appropriate dose to treat them.

To carry out these tests, we decided to use the Ren13 wild type (WT) primary cells, which were the Ren13 cells without any genetic modification. Keeping in mind the results obtained in the *in vitro* and *in vivo* assays, the SN12C model was discarded. There was no evidence that CD44 played an important role in the invasion process in this tumor model. However, in observing the *in vivo* results of the 786O- model, it seemed that CD44 could be implicated in the invasion, although the outcome of *in vitro* experiments showed some variability. Although it was not possible to generate tumors from Ren13 cells, the *in vitro* results of these cells appeared to be similar to 786O- cells, and they were statistically significant. Moreover, the initial experiments were developed with tumors derived from this cell line. For that, we thought that Ren13 would be a good model for the next experiments.

Perifosine

Perifosine is a selective AKT inhibitor with antiproliferative activity. It acts over the cell membrane, concretely over the proliferating cells, and induces growth arrest and apoptosis (Richardson, Eng, Kolesar, Hideshima, & Anderson, 2012).

We tested the drug using the doses described in the literature to produce a high inhibitor effect without damaging cells.

The results from the Wound Healing assay are described in Figure 36.

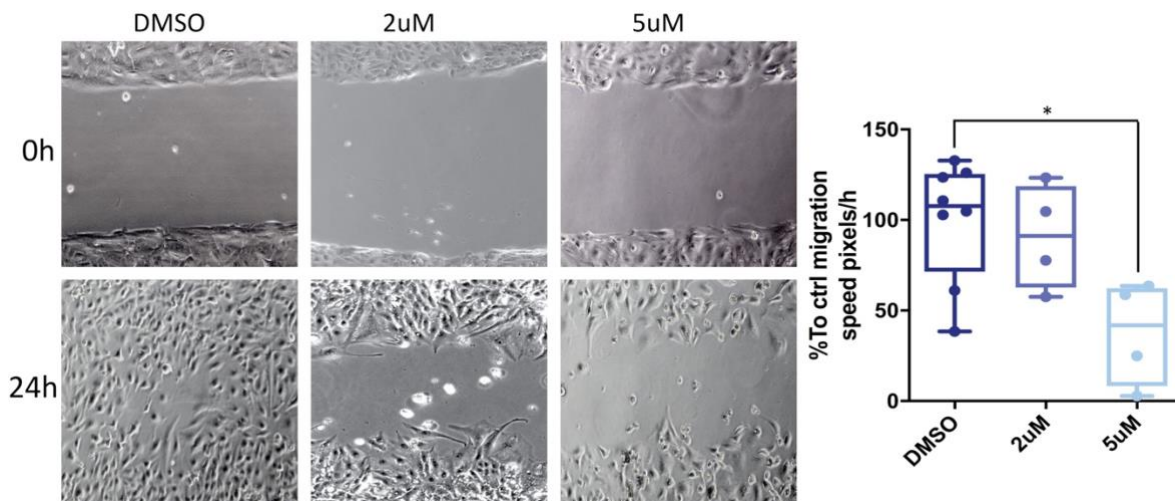


Figure 36. Migration effects of Perifosine in Ren13 WT cells. Wound Healing assay of Ren13 WT cells treated with Perifosine or DMSO. 15000 cells were seeded in each well of the insert. Three images of each well were taken at 10X every 3h. From left to right, representative images of the wounds at time 0h and 24h. Quantification of the migration velocity expressed in pixels/h. DMSO at 0,1% was used as a control treatment. Perifosine was used at 2µM and 5µM and administered to the cells at time 0 of the experiment. (Mann Whitney test $p < 0,01^*$)

The lower dose of Perifosine (2µM) did not have many effects on cell migration. However, the higher dose (5µM) produced a decrease in the migration cell capacity. Nevertheless, in most cases, it produced cell death, and the decrease in migration observed was due to the mortality effect over the cells.

Ruxolitinib

Ruxolitinib is a selective inhibitor of JAK1 and JAK2 kinases with antineoplastic and immunomodulatory activity (Plosker, 2015).

As with Perifosine, we developed some Wound Healing assays using the doses described to produce a solid reduction of cell migration. The results are summarized in Figure 37.

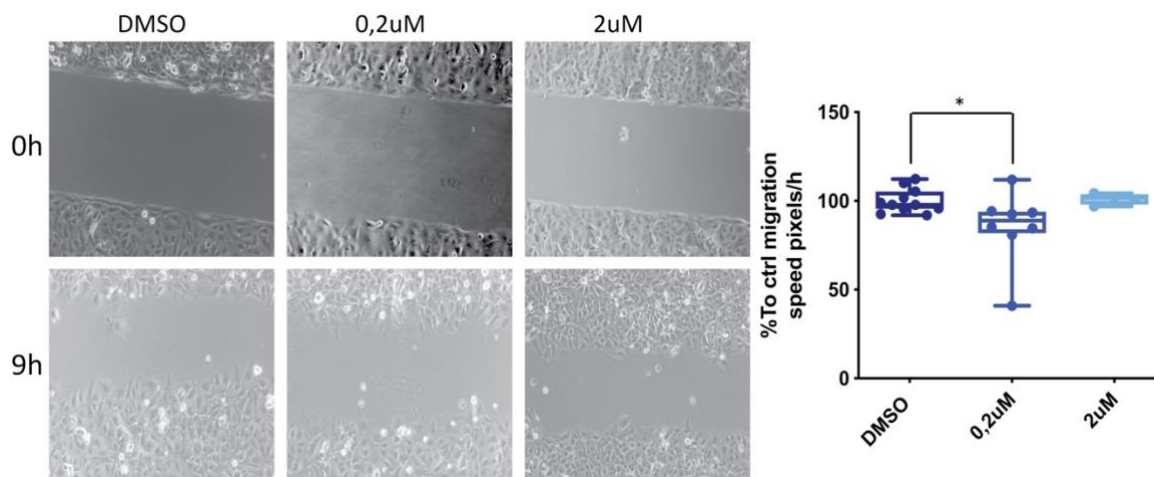


Figure 37. Migration effects of Ruxolitinib in Ren13 WT cells. Wound Healing assay of Ren13 WT cells treated with Ruxolitinib or DMSO. 15000 cells were seeded in each well of the insert. Three images of each well were taken at 10X every 3h. From left to right, representative images of the wounds at time 0h and 9h. Quantification of the migration velocity expressed in pixels/h. DMSO at 0,1% was used as a control treatment. Ruxolitinib was used at 0,2µM and 2µM and administered to the cells at time 0 of the experiment. (Mann Whitney $p < 0,05^*$)

The lower dose (0,2µM) produced a minimum reduction of cell migration, but there was a huge variability in the results. This could explain the statistics. The 2µM dose did not produce any alteration on cell migration. This time, no traces of mortality were observed.

Bosutinib

The last inhibitor tested was Bosutinib, a potent ATP-competitive inhibitor of the Src tyrosine kinase (Boschelli, Arndt, & Gambacorti-Passerini, 2010).

The most common doses described were the ones we tested through the Wound Healing assay. The results of the experiment are shown in Figure 38.

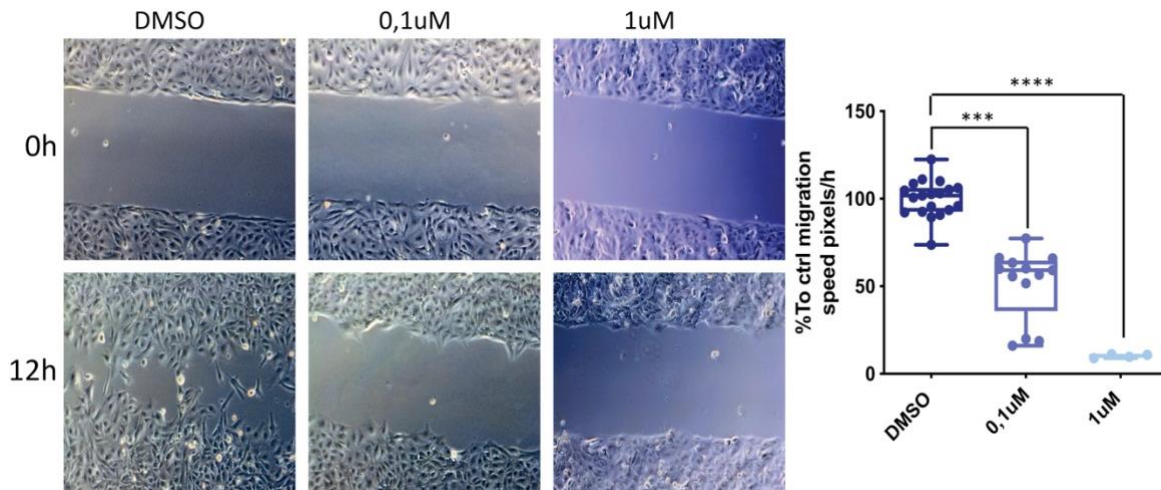


Figure 38. Migration effects of Bosutinib in Ren13 WT cells. Wound Healing assay of Ren13 WT cells treated with Bosutinib or DMSO. 15000 cells were seeded in each well of the insert. Three images of each well were taken at 10X every 3h. From left to right, representative images of the wounds at time 0h and 12h. Quantification of the migration velocity. DMSO at 0,1% was used as a control treatment. Bosutinib was used at 0,1µM and 1µM and administered to the cells at time 0 of the experiment. (Mann Whitney test $p < 0,001$ *** $p < 0,0001$ ****)

The lower dose (0,1µM) produced a statistically significant reduction of cell migration without damaging the cells. Moreover, the higher tested dose (1µM) was too potent and made cells completely immobile.

Bearing in mind the results of these three inhibitors, we decided to continue testing the drugs which had led to better results, namely Ruxolitinib (the JAK inhibitor) and Bosutinib (the Src inhibitor). We discarded Perifosine because of the toxicity produced in the cells.

2.2 DOUBLE INHIBITION OF CANDIDATE PATHWAYS AND CD44

Once we had determined the most effective inhibitors and the appropriate doses to treat our cell cultures, we wanted to study the effect of a double inhibition using doxycycline together with the inhibitors. Cells were treated over 48h with doxycycline to induce the shRNA and consequently reduce the CD44 protein expression. Then, Bosutinib (the most promising inhibitor) and Ruxolitinib were used. The drug combinations were tested through the Wound Healing assay. This time Ren13 shNS and shCD44-1 cells were used to develop the experiments.

2.2.1 Ruxolitinib

The role of JAK/Stat signaling pathway on the migration process of different cancer cells has been described by some authors. Primary test results using Ruxolitinib did not show promising effects, in terms of inhibiting the migration process in our setting. However, we still wanted to test whether doxycycline treatment together with the inhibitor could produce any effect.

Figure 39 shows the results of the Wound Healing assay performed to study the effect of the drug combination.

Focusing on the inhibitory effect, we could observe that, in control cells (shNS) and also in targeted-cells (shCD44-1), Ruxolitinib treatment did not produce any change in the cell migration. This confirms the results previously obtained.

It appears that the doxycycline treatment did not affect the shNS cells, whereas it produced a decrease in shCD44-1 cell migration. This was also observed in previous experiments. These results are detailed further in Section (C) of Figure 39.

While studying the double treatment of Ruxolitinib plus doxycycline, no changes were shown in shNS cells. However, shCD44-1 revealed a decrease in their migration capacity, but it was only due to the doxycycline treatment.

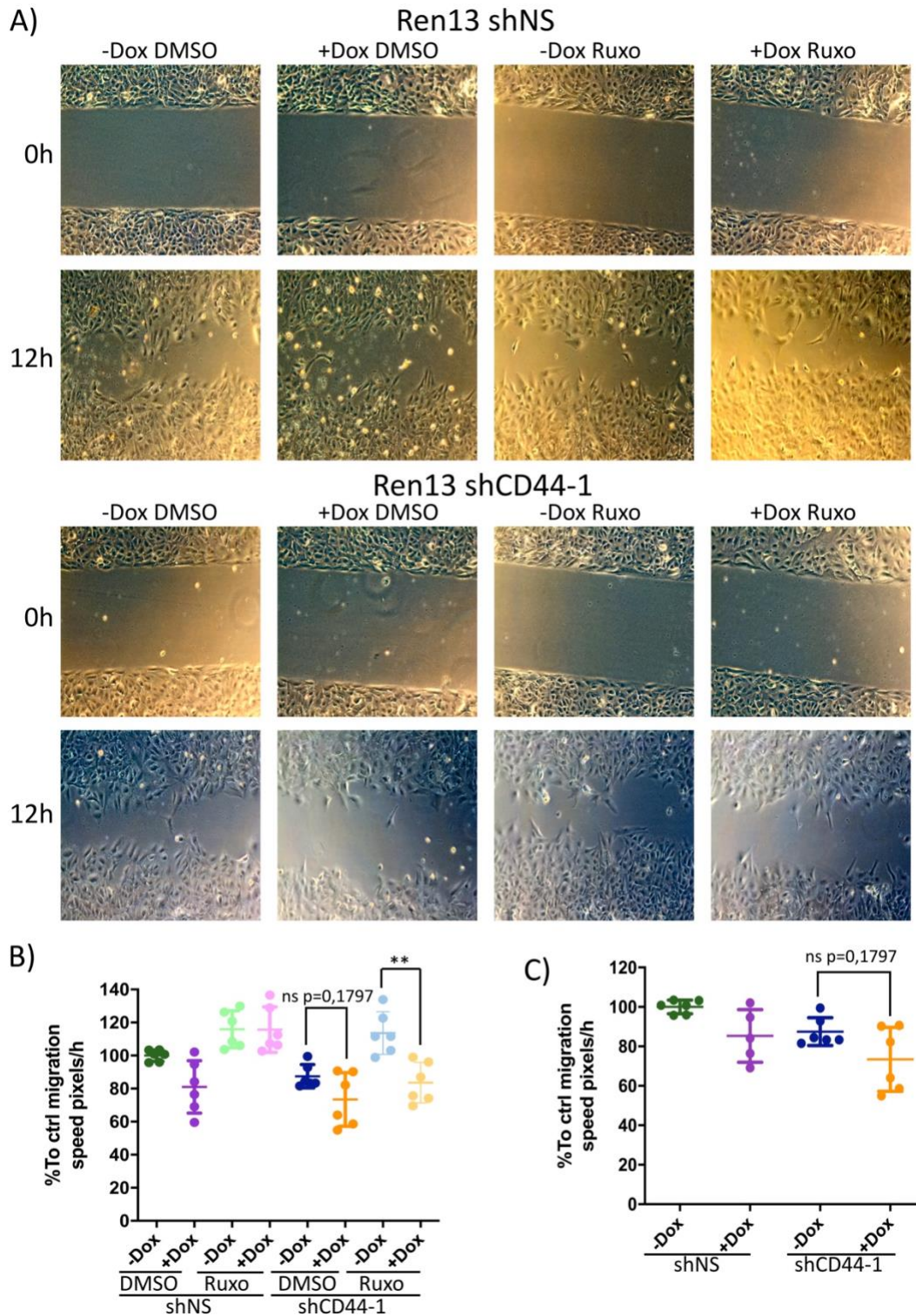


Figure 39. Migration effects of Ruxolitinib and doxycycline in Ren13 cells. Wound Healing assay of Ren13 cells treated or non-treated with doxycycline and/or Ruxolitinib. 15000 cells were seeded in each well of the insert. Cells were treated with 2,5 μ M of doxycycline during 48h and/or 2 μ M of Ruxolitinib at time 0h. DMSO at 0,1% was used as a control treatment. Three images of each well were taken at 10X every 3h. A) Images of the wounds of Ren13 shNS and Ren13 shCD44-1 at time 0 and after 12h of the experiment. B) Quantification of migration velocity of cells to determine the double treatment effect. C) Quantification of migration velocity of cells to determine the effect of doxycycline. (B Mann Whitney test $p < 0,01^{**}$)

The lack of the inhibitor effect in the Wound Healing assay previously exposed could be attributed to: the not involvement of the signaling pathway in the migration process; the dosage being too low; or the bad state of the product. Thus, to confirm that Ruxolitinib was inhibiting the JAK/Stat signaling pathway we decided to treat cells (Ren13 shCD44-1) with the same dose used during the migration assay for different periods and evaluate the state of the proteins implicated in the target pathway. Once samples were obtained, we performed a Western Blot to check the inhibitor effect. The results of the assay are summarized in Figure 40.

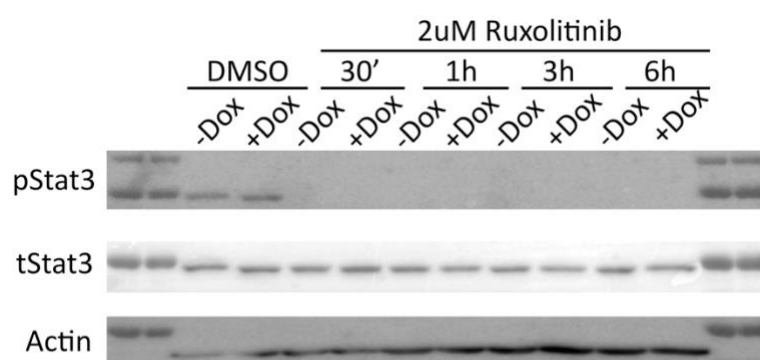


Figure 40. Ruxolitinib inhibited the JAK/Stat signaling pathway. Western Blot of Ren13 shCD44-1 cells (induced or not with 2,5µM doxycycline) treated with 2µM Ruxolitinib during 30', 1h, 3h, or 6h. DMSO at 0,1% was used as a control treatment. Proteins determined in the experiment were pStat3 and tStat3. Actin was determined as housekeeping.

As can be observed, all samples treated with 2µM of Ruxolitinib at every time points, showed a reduction of the Stat3 phosphorylation. However, the expression levels of the total protein were not affected.

These results confirmed that Ruxolitinib was inhibiting the JAK/Stat signaling pathway, as pStat3 in the non-treated samples was expressed. Nevertheless, the lack of migration inhibition may suggest that this pathway was not involved downstream CD44 either in the migration process of our cell model.

2.2.2 Bosutinib

Results obtained with the migration assays using Bosutinib in combination with doxycycline are represented in Figure 41.

If we focus on Ren13 shNS cells, which were our control cells, Bosutinib at a dose of 0,1 μ M produced a decrease of the cell migration, as previously observed. If we focus on the results after doxycycline treatment alone, control cells (shNS) were not affected. The reduction of the migration produced in the Ren13 shNS cells was due to Bosutinib treatment.

Analyzing results obtained with Ren13 shCD44-1 shows that Bosutinib treatment also produced a statistically significant decrease in cell migration. Furthermore, there was a notable reduction of migration due to CD44 silencing through doxycycline treatment, confirming the doxycycline activity. The effect of the CD44 silencing is detailed in part (C) of Figure 41. Finally, the double treatment, as with shNS cells, did not increase the inhibitory potential of Bosutinib. The variability observed in both cases is due to the experimental procedure.

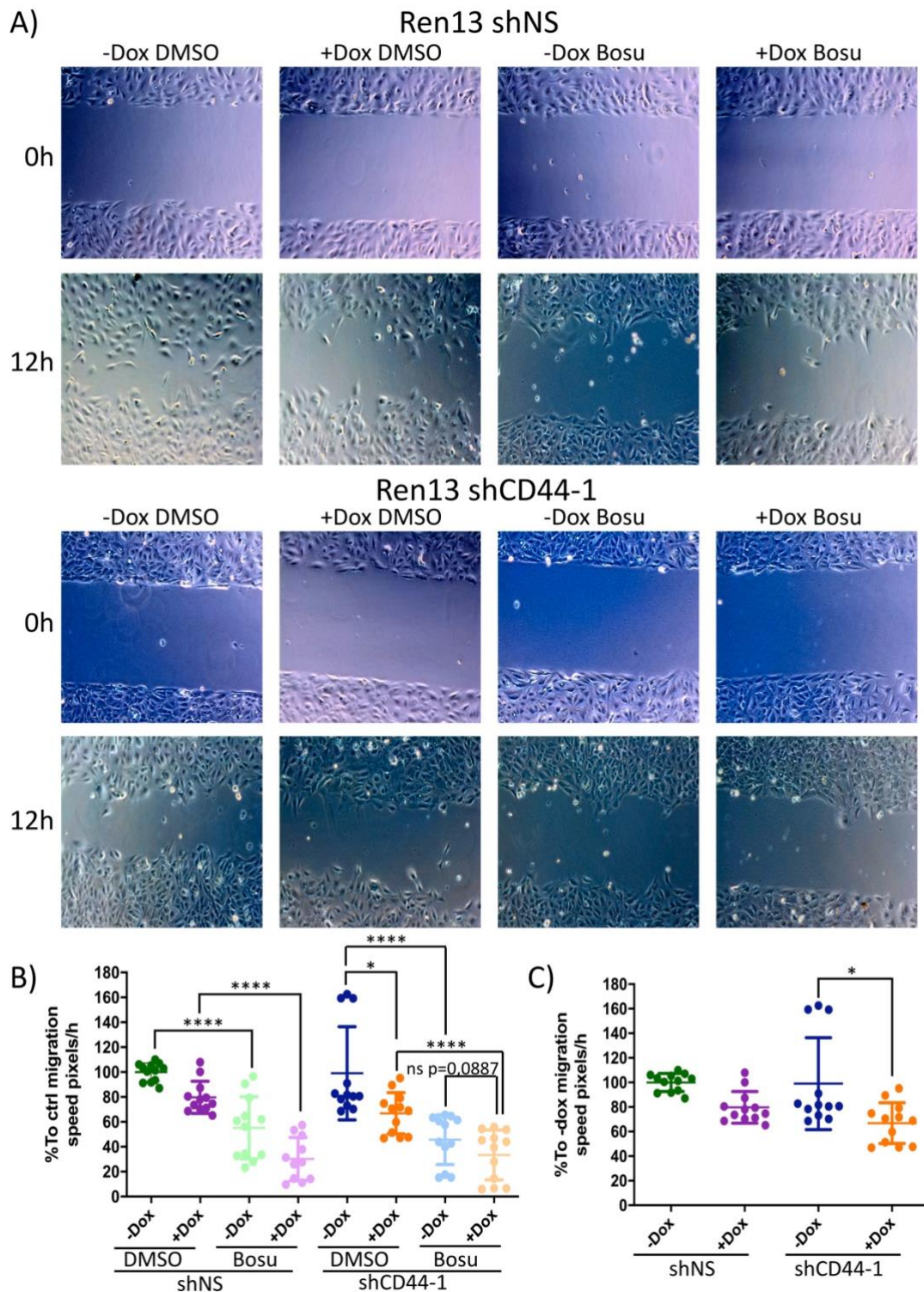


Figure 41. Migration effects of Bosutinib and Doxycycline in Ren13 cells. Wound Healing assay of Ren13 cells treated or non-treated with doxycycline and/or Bosutinib. 15000 cells were seeded in each well of the insert. Cells were treated with 2,5 μ M of doxycycline during 48h and/or 0,1 μ M of Bosutinib at time 0h. DMSO at 0,1% was used as a control treatment. Three images of each well were taken at 10X every 3h. A) Images of the wounds of Ren13 shNS and Ren13 shCD44-1 at time 0 and after 12h of the experiment. B) Quantification of migration velocity of cells to determine the double treatment effect. C) Quantification of migration velocity of cells to determine the effect of doxycycline. (B, C Mann Whitney test $p < 0,0001$ **** $p < 0,05$ *)

On the whole, these results confirmed the effect of Bosutinib over the migration activity of the cells. Moreover, the lack of an additive effect when drugs were combined could indicate that Src and CD44 are in the same signaling pathway. When an important node of a pathway is strongly inhibited, although we try to inhibit another node, the observed effects would be the same, as the pathway was already blocked.

However, the main interest of the project was focused on the role played by CD44 in tumor invasion. For this, we needed to validate the observations during the migration assays produced by Bosutinib treatment alone or in combination with CD44 silencing through an invasion experiment. We performed a transwell invasion assay using the Ren13 shCD44-1 cells.

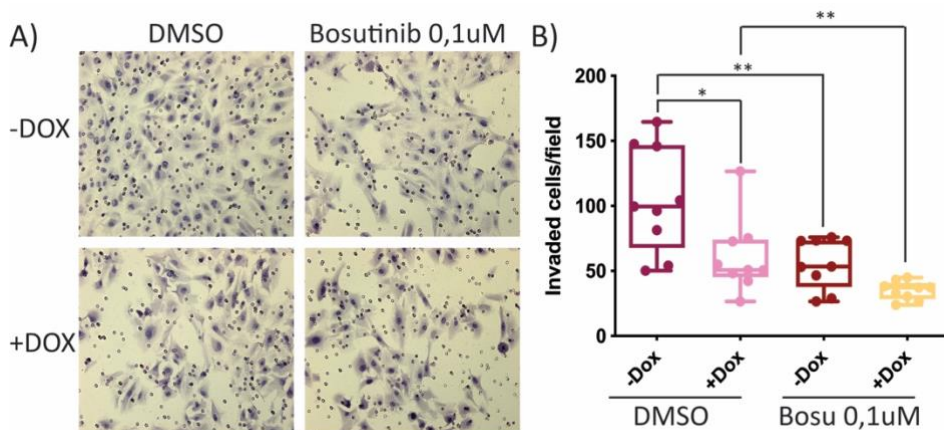


Figure 42. Invasion transwell assay to determine the effect of Bosutinib in Ren13 cells. A) Representative images of Ren13 shCD44-1 treated and non-treated with doxycycline and treated or non-treated with 0,1 μ M of Bosutinib, after 24h of the invasion assay. B) Quantification of invaded cells per field. 50000 cells were seeded in each transwell. Twelve images of each well were taken at 20X and counted manually. Cells were treated with 2,5 μ M of doxycycline during 48h. DMSO at 0,1% was used as a control treatment. (B, Mann Whitney test $p < 0,01$ ** $p < 0,05$ *)

On the one hand, Figure 42 shows that CD44 downregulation caused by doxycycline treatment produced a reduction of the cell invasion, as previously observed. On the other hand, it could be seen that Bosutinib treatment, without considering CD44 silencing, produced a statistically significant reduction in the cell invasion. There also seemed to be a higher reduction of cell invasion when cells were treated with both drugs together,

rather than the ones only treated with Bosutinib. However, this tendency was due to the experimental variability.

Although a reduction in the migration and invasion of cells when they were treated with Bosutinib was observed, we wanted to determine if this effect was due to the inhibition of the Src signaling pathway. Thus, as with Ruxolitinib, we checked the inhibition of Src through Western Blot.

First, we wanted to check the effect of Bosutinib in the different cell lines without inducing them with doxycycline. This time, we treated cells with three different doses of the drug (0,1 μ M, 1 μ M, and 5 μ M) over two different periods of time: 5h and 24h. As observed in Figure 43, Bosutinib treatment produced a reduction of the Src phosphorylation dependent on the dose and treatment time without producing any alteration of the total protein expression.

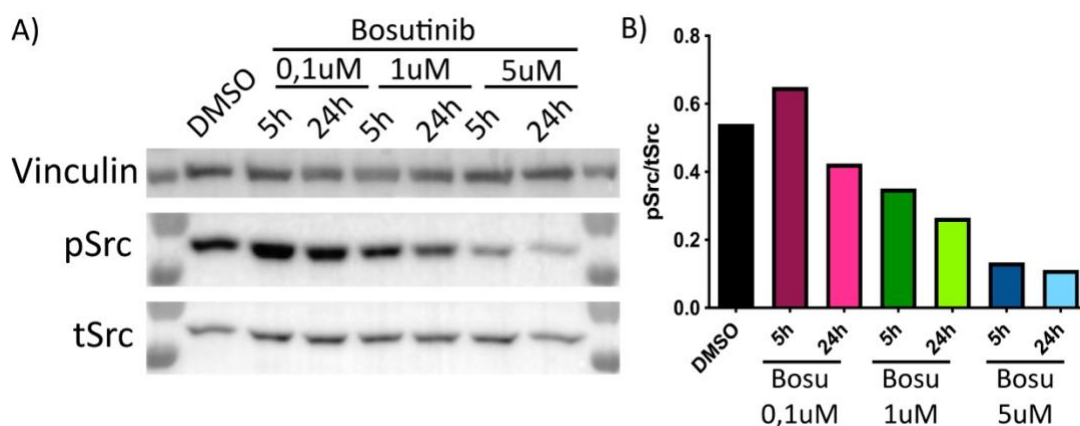


Figure 43. Bosutinib inhibited the Src signaling pathway. A) Western Blot of Ren13 shCD44-1 cells treated with 0,1 μ M, 1 μ M, or 5 μ M of Bosutinib for 5h or 24h. B) Quantification of the Western Blot. DMSO at 0,1% was used as a control treatment. Proteins determined in the experiment were pSrc and tSrc. Vinculin was determined as housekeeping.

Furthermore, we also wanted to check if CD44 silencing produced any change in the Src signaling pathway. Then, we tested whether Bosutinib treatment together with CD44 silencing would increase the inhibition effect. The results of the assay are collected in Figure 44.

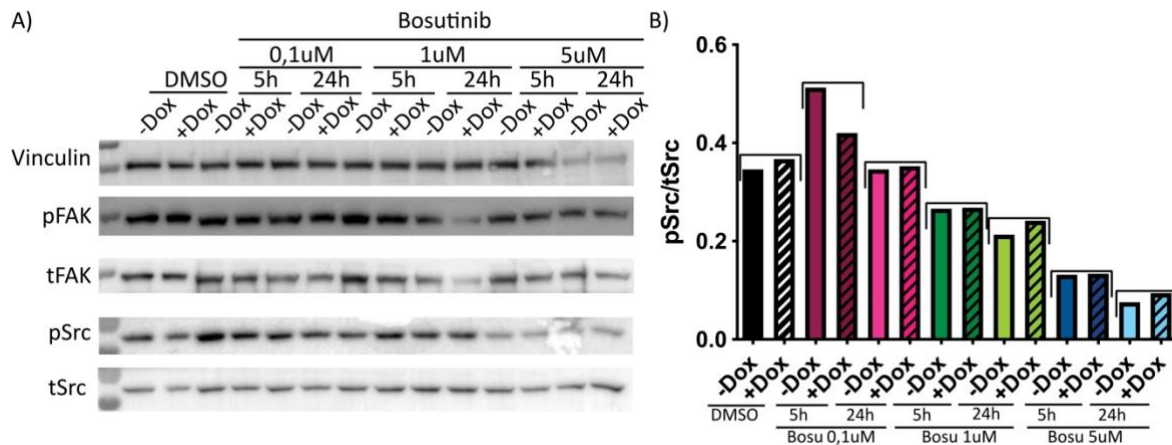


Figure 44. CD44 silencing did not affect the Src signaling pathway. A) Western Blot of Ren13 shCD44-1 cells (induced or not with 2,5 μM doxycycline) treated with 0,1 μM, 1 μM, or 5 μM of Bosutinib for 5h or 24h. B) Quantification of the Western Blot. DMSO at 0,1% was used as a control treatment. Proteins determined in the experiment were pFAK, tFAK, pSrc, and tSrc. Vinculin was determined as housekeeping.

As previously shown in Figure 43, Bosutinib treatment produced a reduction of the Src phosphorylation, effect dependent on the dose and time, demonstrating the proper activity of the inhibitor.

By focusing on the CD44 silencing effect over Src (Figure 44), we could verify that the reduction of the CD44 expression did not produce any change in the phosphorylation of Src, neither of the total protein expression.

We also wanted to check also whether there were changes in the phosphorylation of FAK, as often, in this pathway, there is an autoregulation between FAK and Src proteins. However, in our setting, no changes were observed in pFAK nor in the total protein levels (Figure 44).

The Western Blot results together with the results obtained in the migration and invasion assays suggest that it is possible that the Src pathway plays an important role downstream CD44. Furthermore, it could be responsible for the effects observed in the migration and invasion processes of renal carcinoma cells.

3. UPSTREAM ACTIVATION OF CD44

We discovered that CD44 is responsible for the activation of certain signaling pathways that affect the migration and invasion processes of cells. But who is responsible for CD44 induction?

We proposed to find which were the co-receptors, ligands, or modulators able to induce CD44 activation and consequently trigger the subsequent signaling.

3.1 HYALURONIC ACID

The first candidate we thought might be responsible for CD44 activation was Hyaluronic Acid or Hyaluronan (HA). As previously explained, HA is the principal ligand of CD44. It has been described that in different tumor types HA can activate the CD44 signaling and promote migration and invasion of tumor cells.

Hyaluronic Acid is a glycosaminoglycan composed of the repetition of two disaccharides linked via glycosidic bonds (represented in Figure 45). There are different lengths of HA, and they are classified into two main groups: the low molecular weight fragments (LMWHA) and the high molecular weight fragments (HMWHA).

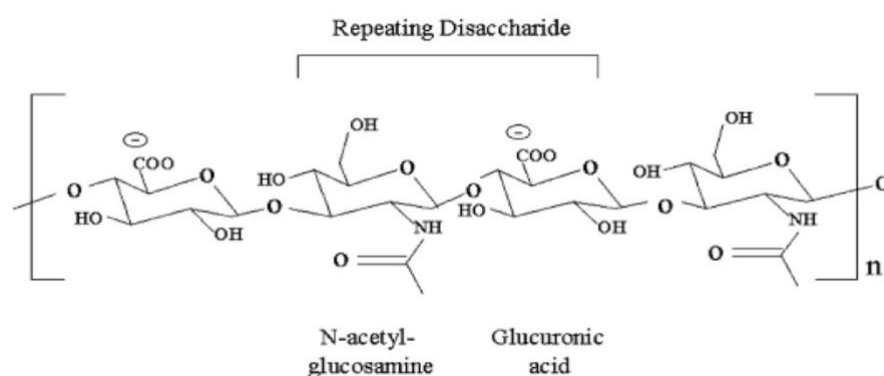


Figure 45. Representation of Hyaluronic Acid. Image of both disaccharides linked by the glycosidic bond to set up the unit of Hyaluronic Acid. Image adapted from Garg, Quinn, Mascarenhas, & Hales, 2004.

These HA fragments can also interact with its receptor. Interaction between the different pieces of HA with CD44 can trigger its activation, but also its inhibition. Some research groups have tried to classify the LMWHA and HMWHA into activators or inhibitors of the receptor but, depending on the tissue and the tumor type, they can act in one way or another.

With all this information in mind, we hypothesized that in our *in vitro* and *in vivo* models, the interaction between HA and CD44 could be responsible for the activation of CD44 and consequently produce the changes previously observed in the migration and invasion processes of the cells (Figure 46).

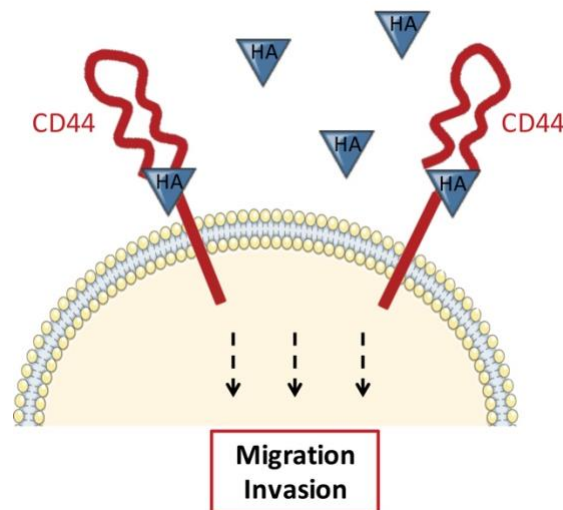


Figure 46. Representation of the interaction between CD44 and Hyaluronic Acid.

3.1.1 Presence of HA in our Cell Models

First of all, we had to confirm the presence of Hyaluronic Acid in our cell models. To do that, we performed an Immunocytofluorescence assay of Ren13 cell cultures.

Given that Hyaluronan is not a protein, we had to use a hyaluronan-binding protein (HA-BP), which is a glycoprotein with a specific affinity toward HA. Subsequently, with Immunocytofluorescence we could detect the glycoprotein bonded to Hyaluronic Acid.

Figure 47 shows the obtained results during the immunoassay. Cells under normal culture conditions expressed Hyaluronic Acid in their cell membrane (Figure 47(A)). To

ensure that the fluorescence signal we were detecting was Hyaluronic Acid and not background noise, we used Hyaluronidase, an enzyme responsible for the polymer degradation. As observed in Section (B) of Figure 47, Hyaluronidase treatment produced the degradation of Hyaluronic Acid without affecting the integrity of the cells.

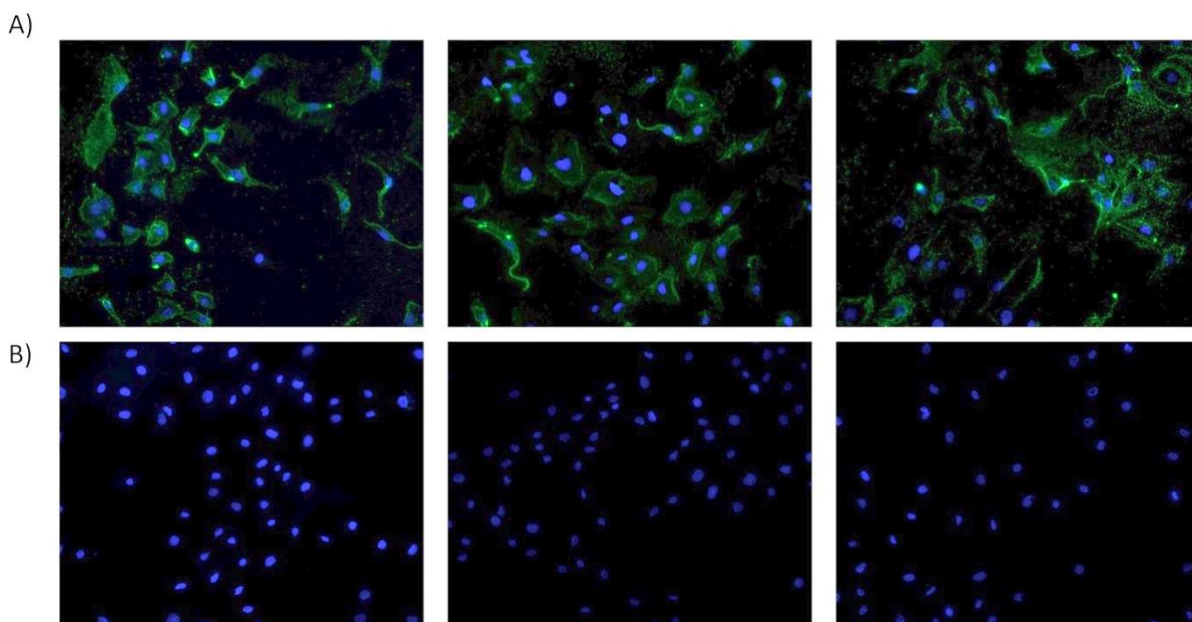


Figure 47. Ren13 cell cultured in normal conditions expressed Hyaluronic Acid. Immunocytofluorescence of Hyaluronic Acid performed in Ren13 cells (A) and after 1h of Hyaluronidase treatment at 37°C (B). 30000 cells were seeded in each well 24h before the experiment. Hyaluronidase was used at 20U/mL. Images were taken at 20X.

This assay allowed us to confirm the presence of Hyaluronan in Ren13 cell cultures.

3.1.2 Presence of HA in our Tumor Models

In addition, we wanted to know if, apart from cells, tumors also expressed Hyaluronic Acid. We performed an Immunohistochemistry assay of the different tumors generated from SN12C shCD44-1 cells and 786O- shCD44-2 cells. As before, we used Hyaluronidase as a specificity control of the antibody.

SN12C shCD44-1 Tumors

An Immunohistochemistry of tissue samples was also performed using the hyaluronan-binding protein. The results obtained with the assay using SN12C shCD44-1 tumor

samples are shown in Figure 48. In Section (A) we can observe that there was a high density of Hyaluronic Acid in the different samples without considering the treatment administered to the animals (doxycycline and/or DC101). Section (B) displays the effect of Hyaluronidase. Hyaluronan staining after Hyaluronidase treatment of the samples was low, but it was still observable. This fact could be due to the fixation of samples and subsequent embedding with paraffin that complicated the Hyaluronidase activity.

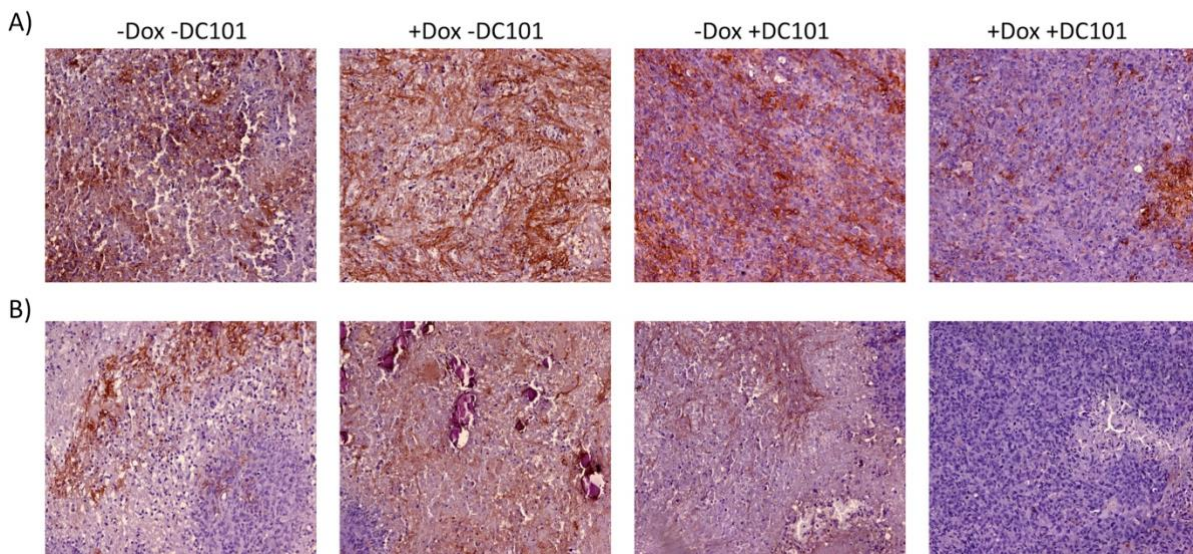


Figure 48. Hyaluronic Acid was expressed in SN12C tumors. Immunohistochemistry of Hyaluronic Acid developed in SN12C shCD44-1 tumor tissues (A) and after 2h of Hyaluronidase treatment at 37°C (B). Hyaluronidase was used at 20U/mL.

786O- shCD44-2 Tumors

The same immunoassay was performed to detect the presence of Hyaluronic Acid in tumor tissues generated from 786O- shCD44-2 cells. Figure 49 shows the results. As in the previous experiment, all the tumors expressed Hyaluronic Acid, regardless of the treatment animals received (section (A) of Figure 49). Hyaluronidase treatment (Section (B) of Figure 49) also produced the degradation of the polymer, but again results were not as conclusive as the results obtained *in vitro*. There always remained some Hyaluronic Acid.

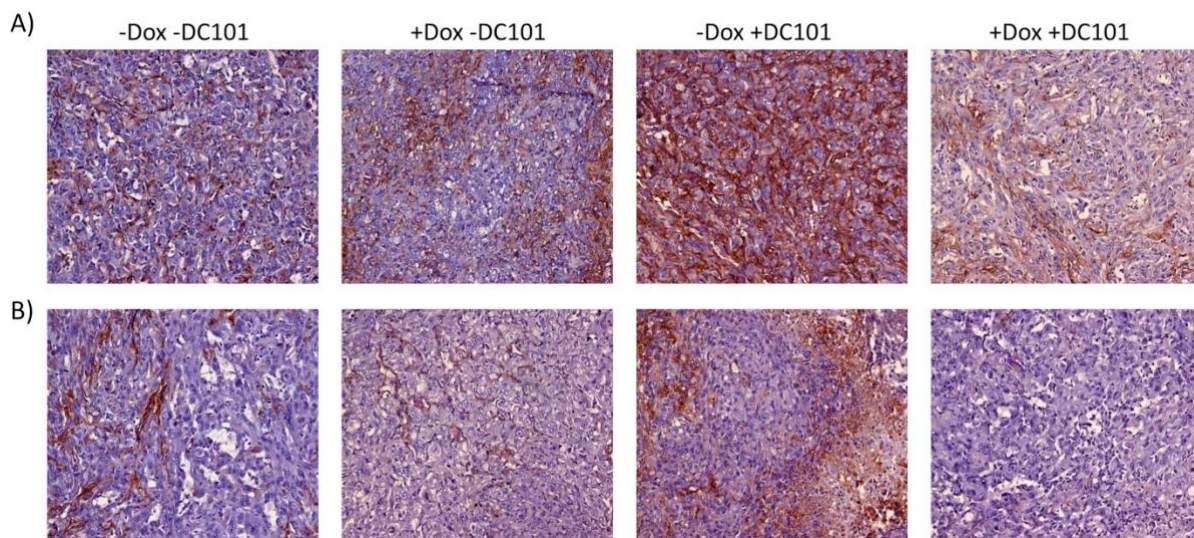


Figure 49. Hyaluronic Acid was expressed in 786O- tumors. Immunohistochemistry of Hyaluronic Acid developed in 786O- shCD44-2 tumor tissues (A) and after 2h of Hyaluronidase treatment at 37°C (B). Hyaluronidase was used at 20U/mL.

3.1.3 Effects of Hyaluronidase on Cell Migration

Once we had demonstrated there was HA both in cell cultures and tumor tissue, we considered what impact its lack or its degradation would have.

According to our hypothesis, the presence or absence of Hyaluronan or its fragments would activate or inhibit CD44, having consequences in the migration process. Thus, the Hyaluronidase treatment would produce the degradation of the polymer existing in our cell culture and would disrupt the migration of the tumor cells.

Following on from this, we decided to treat cells with Hyaluronidase and develop a migration assay to determine the effects of removing HA.

We used the Ren13 WT cells to perform this assay because we did not want to knockdown CD44, instead only reduce the interaction with its principal ligand by removing it.

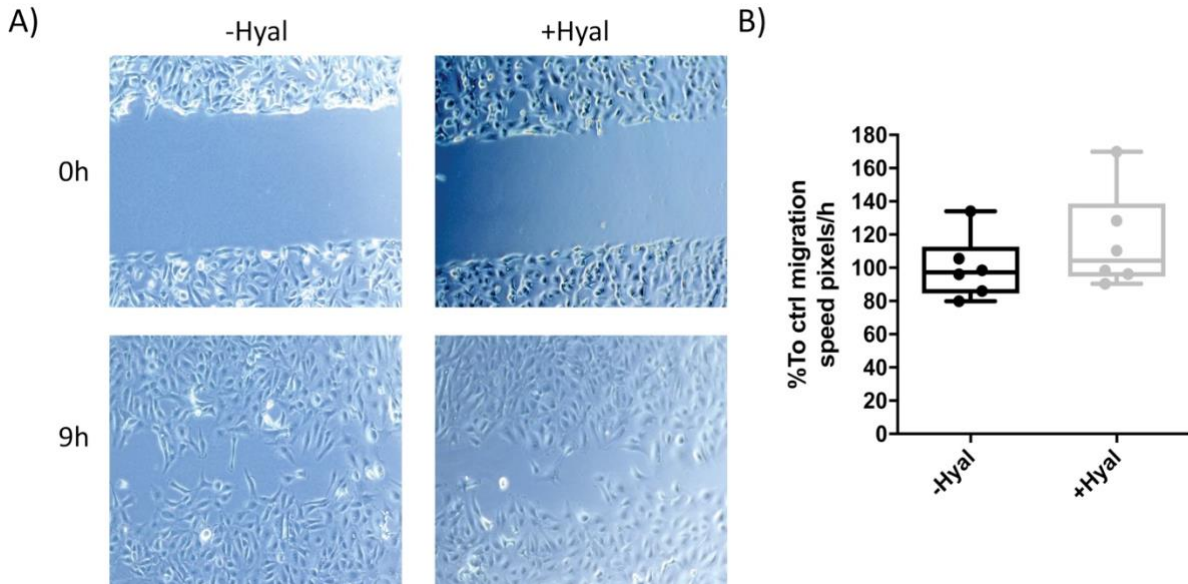


Figure 50. Hyaluronidase did not affect the migration capacity of cells. Wound Healing assay of Ren13 WT cells treated and non-treated with Hyaluronidase. 15000 cells were seeded in each well of the insert. Three images of each well were taken at 10X every 3h. Hyaluronidase was used at 20U/mL and administered at time 0. A) Images of the wounds of Ren13 cells at time 0 and after 9h of the experiment. B) Quantification of migration velocity of cells to determine the effect of the treatment. No differences could be observed between the groups.

Results of the Wound Healing assay using Hyaluronidase are represented in Figure 50. As can be observed in the images and through the quantification, removing Hyaluronic Acid of the cells did not have any consequence in their migration capacity.

However, we wanted to test if the ligand degradation and the expression reduction of the receptor (CD44) together would produce any alteration in the migration process. To do so, we used Ren13 shCD44-1 cells either induced or not with doxycycline and treated them with Hyaluronidase. Results of the Wound Healing assay are represented in Figure 51.

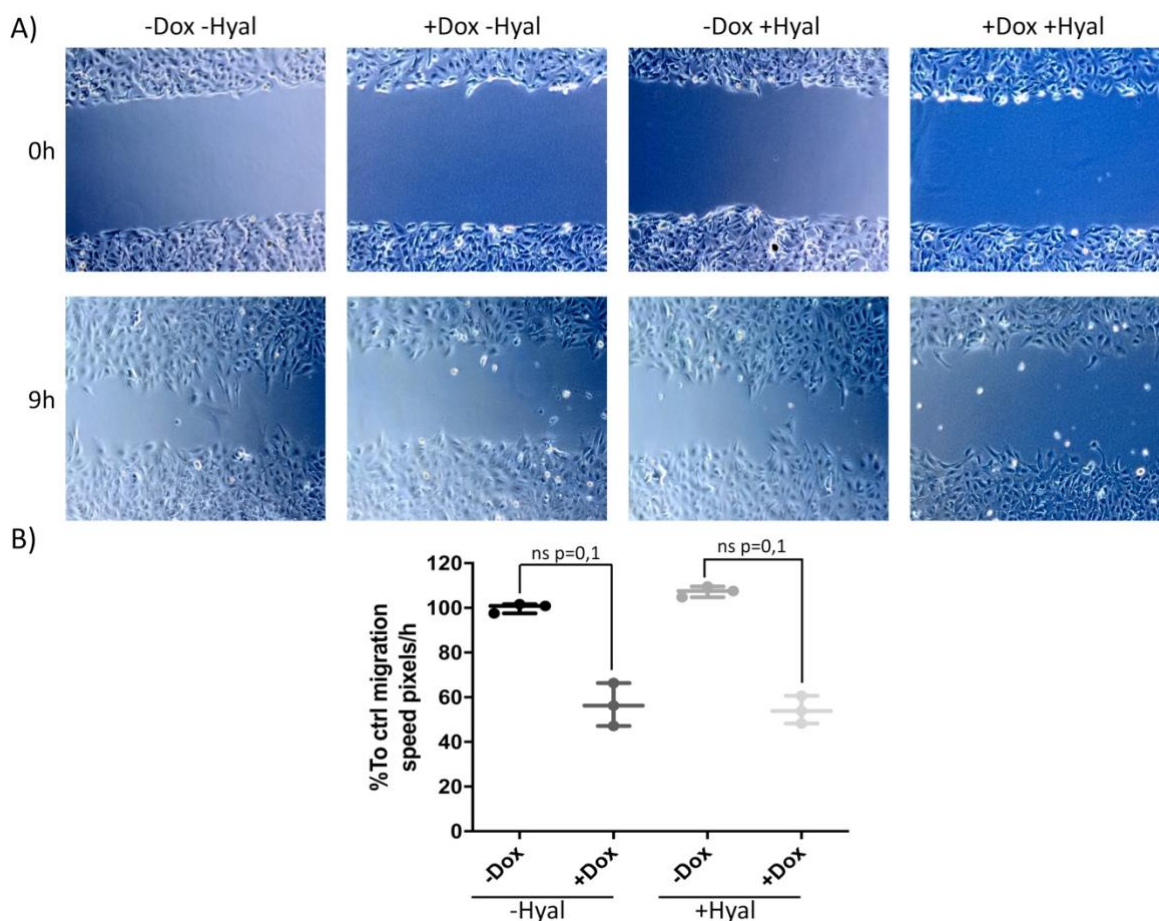


Figure 51. Hyaluronidase in combination with doxycycline did not affect the migration capacity of cells. Wound Healing assay of Ren13 shCD44-1 cells treated or non-treated with doxycycline and/or Hyaluronidase. 15000 cells were seeded in each well of the insert. Cells were treated with 2,5 μ M of doxycycline during 48h and/or 20U/mL of Hyaluronidase at time 0h. Three images of each well were taken at 10X every 3h. A) Images of the wounds of Ren13 shCD44-1 cells treated and non-treated with doxycycline and/or Hyaluronidase at time 0 and after 9h of the experiment. B) Quantification of migration velocity of cells.

Both images and quantification show a decrease in cell migration when they were treated with doxycycline, and consequently when CD44 is downregulated. However, due to the small number of experimental samples, this difference was not statistically significant. Treatment with Hyaluronidase, as previously observed, did not produce any changes in cell migration.

3.1.4 Migration Consequences of Blocking CD44 Through HA Binding Site

Another approach to determining if HA-CD44 interaction was responsible for migration and invasion processes was to block their binding. We used a CD44 blocking antibody able to attach to the hyaluronan binding site, thus avoiding the activity produced by the ligand-receptor interaction. We treated cells with a blocking antibody (IM-7 Invitrogen #14-0441-82) of CD44 and checked the effects produced in the migration ability of cells.

Given it was not necessary to downregulate CD44 expression, Ren13WT cells were used for the experiment. Two different doses of the blocking antibody were tested: 5 μ M and 10 μ M. Results of the Wound Healing assay are represented in Figure 52.

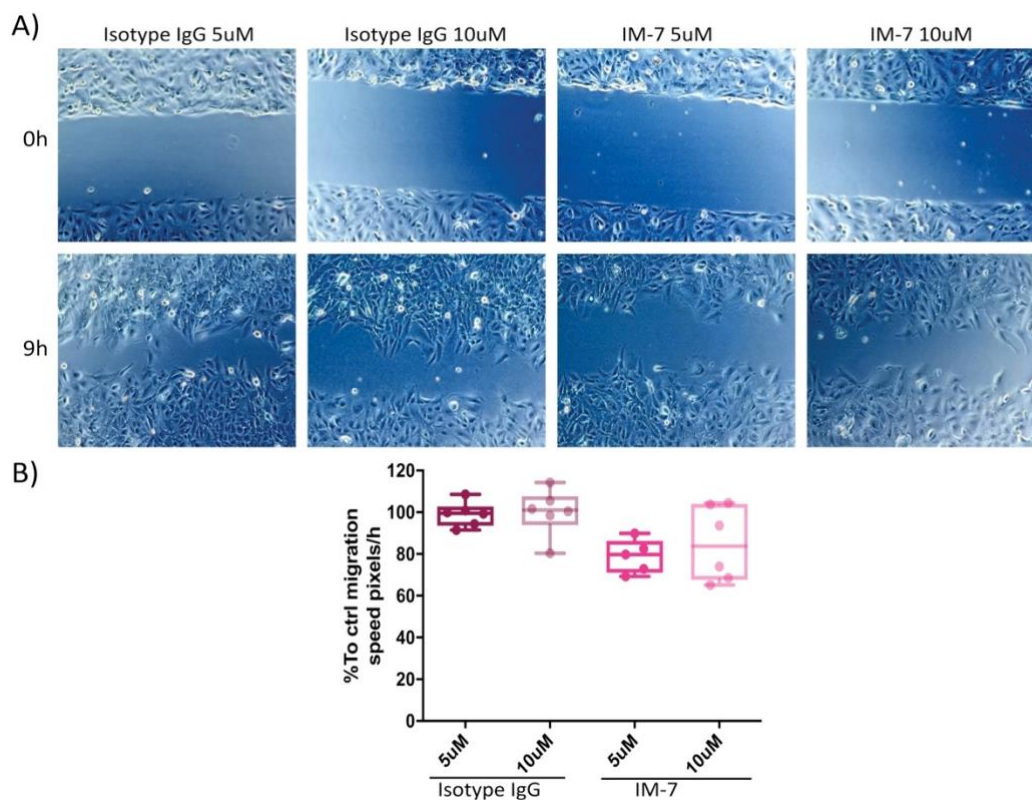


Figure 52. The CD44 blocking antibody IM-7 did not affect the migration capacity of cells. Wound Healing assay of Ren13 WT cells treated and non-treated with the blocking antibody. 15000 cells were seeded in each well of the insert. Cells were treated with 5 μ M or 10 μ M of IM7-antibody (Invitrogen #14-0441-82) or Isotype IgG (R&D Systems #MAG003), used as a control, 30min before the time 0h. Three images of each well were taken at 10X every 3h. A) Images of the wounds of Ren13 WT cells at time 0 and after 9h of the experiment. B) Quantification of migration velocity of cells. No differences could be observed between any of the groups.

Quantification of the assay, as well as the images, did not show any alteration of the cell migration. These results, together with the previous ones, provide enough evidence to discard HA as an inducer or trigger of CD44.

3.1.5 Changes in CD44 Activity Using Different Fragments of HA

Before giving up the hypothesis based on Hyaluronic Acid, we decided to perform one final test. As has been described, different fragments of Hyaluronan can also interact with CD44 and produce the induction or inhibition of the receptor. Using this, we decided to test the effect of some of them in our cell cultures. We used units between 4-18 disaccharides, considered as LMWHA.

Following the same dynamic as previously, a Wound Healing assay was developed using Ren13 cells treated with the different Hyaluronan fragments. Figure 53 shows the results obtained.

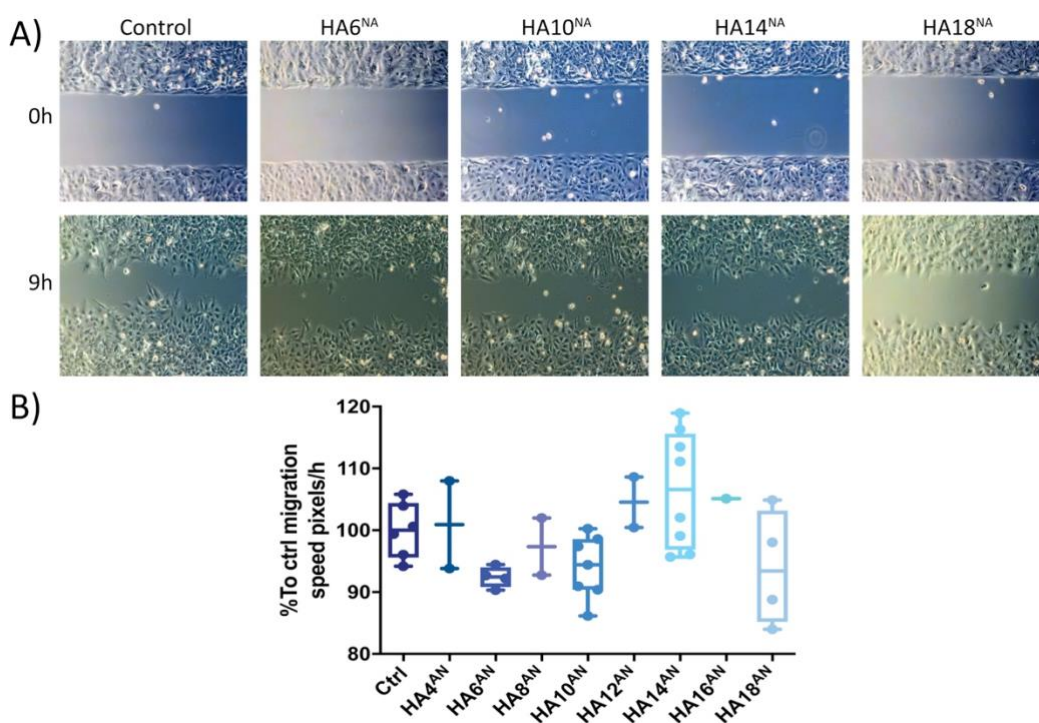


Figure 53. Hyaluronan fragment did not produce changes in the migration capacity of cells. Wound Healing assay of Ren13 WT cells treated with different fragments of Hyaluronan. 15000 cells were seeded in each well of the insert. Three images of each well were taken at 10X every 3h. Hyaluronan fragments were used at 10 μ M and administered at time 0. A) Images of the wounds of Ren13 WT cells at time 0 and after 9h of the experiment. B) Quantification of migration velocity of cells to determine the effect of the treatment. No differences could be observed between the groups.

Despite quite a variability in the results, none of the different HA units produced significant changes in the activity of cells. Neither induction nor inhibition of the migration process could be observed.

Concurrently, we developed a Western Blot analysis of different proteins involved in the signaling pathways that related to migration and invasion processes. This was in order to determine if Hyaluronic Acid fragments produced changes in its expression and compare them with the effects produced when CD44 is knocked-down. Figure 54 gathers the results.

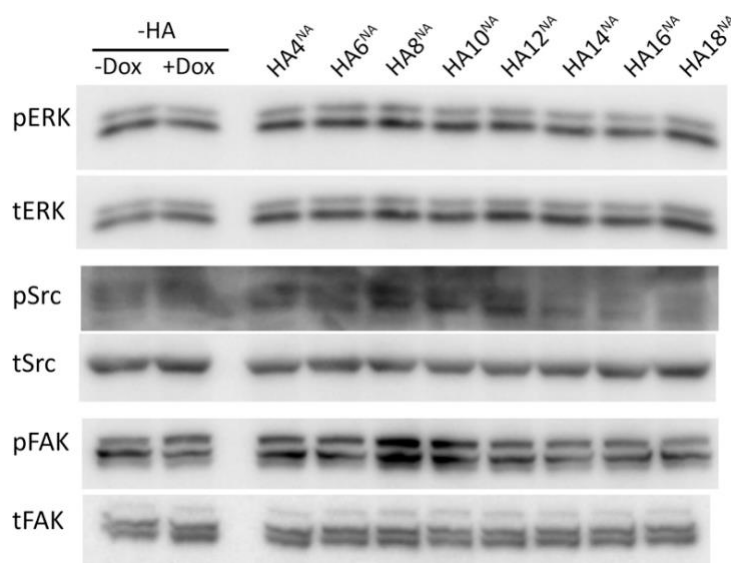


Figure 54. Hyaluronic Acid fragments did not produce any changes in the protein expression. Western Blot of Ren13 cells treated with different Hyaluronan fragments (10 μ M) compared with cells treated or not with doxycycline (2,5 μ M). Proteins determined in the experiment were pERK, tERK, pSrc, tSrc, pFAK, and tFAK. All of them are involved in migration and invasion processes.

Treating cells with Hyaluronic Acid fragments of different molecular weight did not produce any change in the expression of proteins involved in the migration process of cells. In summary, the lack of HA did not produce any effect at either a functional and protein level on our cells, but neither did its addition.

Even though HA is the main ligand of CD44, its signaling is not responsible for the induction and activation of the protein.

3.2 OTHERS CO-MODULATORS OF CD44

Once Hyaluronic Acid was discarded as the principal co-modulator of CD44, we considered looking for other candidates that could be interacting and/or modulating CD44.

We took advantage of the data obtained from the RNA sequencing performed at the beginning of the project. In this experiment, the differential expression of a set of genes was contrasted between antiangiogenic-treated (DC101) tumor samples and non-treated tumor samples of Ren13 tumors. From this set of genes, we selected those whose expression correlated with CD44 expression, obtaining a list of 127 genes.

To get closer to the clinics, we decided to verify the expression of these selected genes in patients. We used RNA data from renal cancer patients obtained from the TCGA database (data from 528 patients). From the 127 genes selected with the RNA sequencing, 81 were highly expressed in these patients. Finally, we correlated the patient's expression of CD44 with the *in silico* selected genes (81 genes). Only three candidates of the initial list showed to be expressed in patients and to correlate with CD44. These candidates were CD82, CCL5, and Serglycin (SRGN). Figure 55 summarizes the followed process.

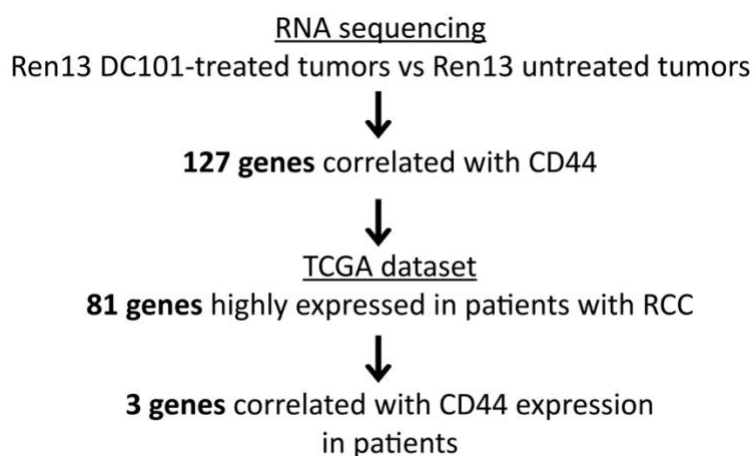


Figure 55. Diagram of the process followed to find some other candidates able to bind or interact with CD44. Data from the RNA sequencing performed at the beginning of the project and data from patients of the TCGA dataset were used to find possible CD44 modulators.

In Figure 56 is represented the correlation between the three candidate genes and CD44 expression in patients.

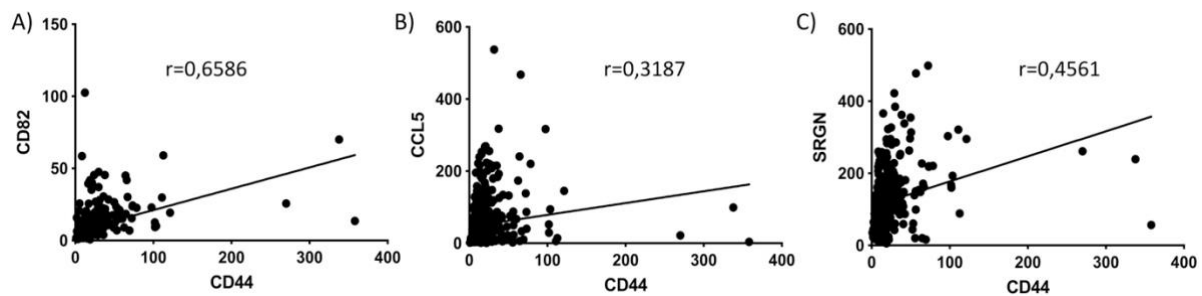


Figure 56. Correlation between CD44 and the candidate genes. CD44 expression in patients correlated with CD82 (A), CCL5 (B), and Serglycin (C). Data were obtained from the TCGA dataset. (Spearman correlation test $p < 0,0001$ ****).

3.2.1 CD82

CD82 also known as KAI-1 or HER-2 is a protein member of the tetraspanins family, concretely of the TM4SF (transmembrane 4 superfamily) responsible for mediating adhesion function between cells and between cells and the extracellular matrix (Wei et al., 2014; Sun & Zhou, 2016).

Initially, CD82 was identified as a metastasis suppressor gene in prostate cancer (Wu et al., 2015; Zhu et al., 2017). Its expression or overexpression inhibits the adhesion of cancer cells to the extracellular matrix, and its silencing produces the opposite effect (Sun & Zhou, 2016).

It has been described that CD82 plays an important role in cell fusion, adhesion, migration, signaling, fertilization, differentiation, and invasion. Also, it was demonstrated that CD82 expression limits the progression and metastasis of some types of tumors. Moreover, it takes part in the regulation of tumor angiogenesis and reduces the migration of endothelial cells by enhancing CD44 endocytosis (Wei et al., 2014).

Nevertheless, a direct interaction between CD82 and CD44 has not been demonstrated, but a negative modulation. When CD44 is overexpressed, the expression of CD82 is decreased, and vice versa (Wei et al., 2014).

3.2.2 CCL5

C-C chemokine ligand five or CCL5 is also known as Regulated upon Activation, Normal T-cell Expressed, and Secreted (RANTES). This chemokine is responsible for the recruitment of leukocytes, macrophages, eosinophils, and basophils in inflammatory sites (Aldinucci & Colombatti, 2014).

Their main receptors are CCR1, CCR3 and CCR5, but recently it come to light that CD44 can function as an auxiliary receptor for CCL5 by binding through its glycosaminoglycan (GAG) chains (Roscic-Mrkic et al., 2003).

CCL5 principal role is to induce an appropriate immune response against tumors, but in some types of cancer, it appears that this chemokine is associated with tumor progression and metastasis (Aldinucci & Colombatti, 2014). Moreover, in some cases, as in glioblastoma, CCL5 can regulate CD44 to increase and/or help the survival of tumor cells (Pan, Smithson, Ma, Hambardzumyan, & Gutmann, 2017).

3.2.3 Serglycin (SRGN)

Serglycin is a glycoprotein that was originally identified as a secretory granule proteoglycan with the function of promoting secretory granule storage in mast cells. Later, its expression was found in other cell types such as hematopoietic and endothelial cells among others (Zhang et al., 2017; Guo, Chiu, Wang, Li, & Chen, 2020).

Serglycin was described as a novel ligand for CD44 in different tumor types. It has been observed that Serglycin can bind to CD44 near the extracellular hyaluronan binding domain through its chondroitin sulfate motifs (Jing You Guo et al., 2020).

The glycoprotein is mainly distributed in the cell and the cell membrane, but it can also be secreted. That secreted Serglycin can still interact with CD44 if it conserves the chondroitin sulfate motifs (Guo et al., 2020; Zhang et al., 2017).

It has been described that interaction between CD44 and SRGN can promote the migration and invasion processes in a set of cancer cells (J. Y. Guo et al., 2016).

Some research groups have suggested different possible mechanisms of interaction and regulation of the CD44-SRGN signaling. Some examples are represented in Figure 57.

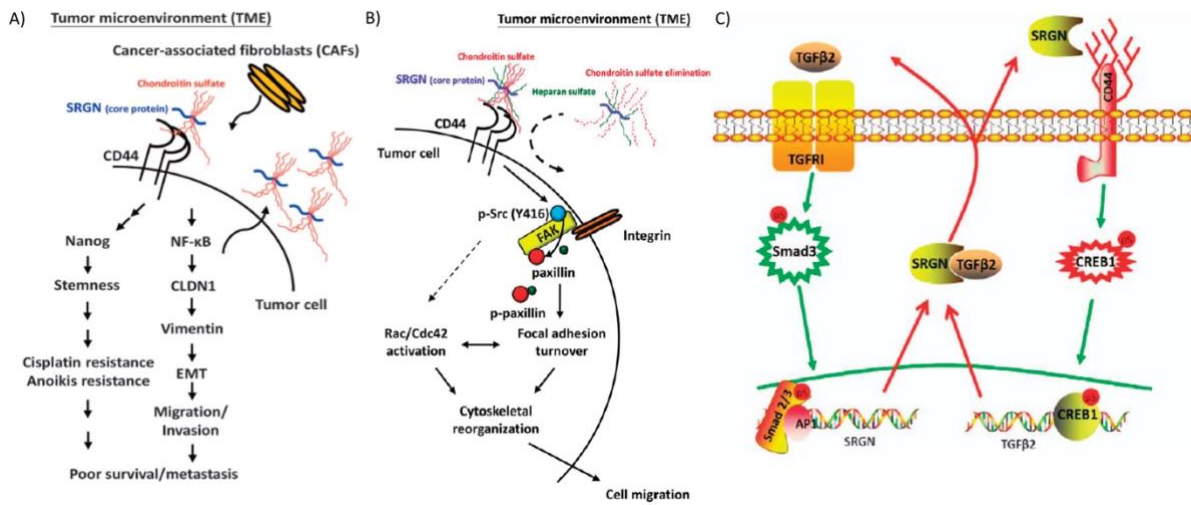


Figure 57. CD44-SRGN interaction and signaling. A, B, and C show three different mechanisms proposed for different research groups where they describe the interaction between CD44 and SRGN, the signaling pathways after their interaction, and how it is regulated. Image (A) adapted from Jing You Guo, Chiu, Wang, Li, & Chen, 2020; image (B) adapted from J. Y. Guo et al., 2016, and image (C) adapted from Zhang et al., 2017.

From the three suggested candidates, Serglycin showed the highest expression levels in patients. The differential expression between antiangiogenic-treated and non-treated tumors obtained from the RNA sequencing data, performed at the beginning of the project, was also higher than in the other candidates. Moreover, a physical interaction between both proteins was previously described. Thus, bearing these points in mind, we decided to study Serglycin as a co-modulator of CD44.

3.2.3.1 Serglycin Expression in Cells

Initially, we examined Serglycin expression in our cell cultures through Western Blot assay.

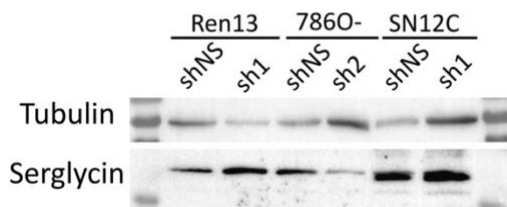


Figure 58. Expression of Serglycin in different cell models. Western Blot of Ren13, 786O-, and SN12C cells (shNS and shCD44) to evaluate the expression of Serglycin. Tubulin was determined as housekeeping.

As observed in Figure 58, our three cell models expressed Serglycin. SN12C cells were the ones that expressed more protein, and Ren13 cells the ones that had less Serglycin expression.

Furthermore, we also wanted to evaluate if CD44 could modulate the expression of Serglycin. For that, we performed another Western Blot to compare the Serglycin expression of the non-induced cells with the doxycycline-induced cells, where CD44 expression was decreased.

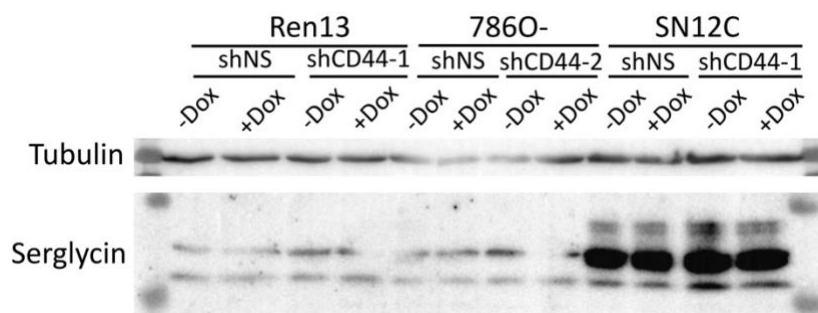


Figure 59. Expression of Serglycin in different cell models where CD44 is downregulated. Western Blot of Ren13, 786O-, and SN12C cells (shNS and shCD44) induced or not with doxycycline to determine the expression of Serglycin. Cells were treated with 2,5 μ M of doxycycline during 48h. Tubulin was used as housekeeping.

In Figure 59, it can be observed that CD44 silencing by itself did not produce any modification of Serglycin expression. In some cases, there seemed to exist different intensities between the bands, but this variability was due to the Western Blot technical difficulties and the antibody used to detect the protein. One interesting observation was that SN12C cells showed to have high levels of protein compared with the rest of the cells. Moreover, SN12C shCD44-1 cells expressed higher levels of Serglycin than the control ones (shNS).

Apart from the Serglycin expression at the protein level, we also wanted to evaluate the RNA levels present in cells when they were treated and non-treated with doxycycline. The results of the Taqman assay performed with the different cell lines are represented in Figure 60.

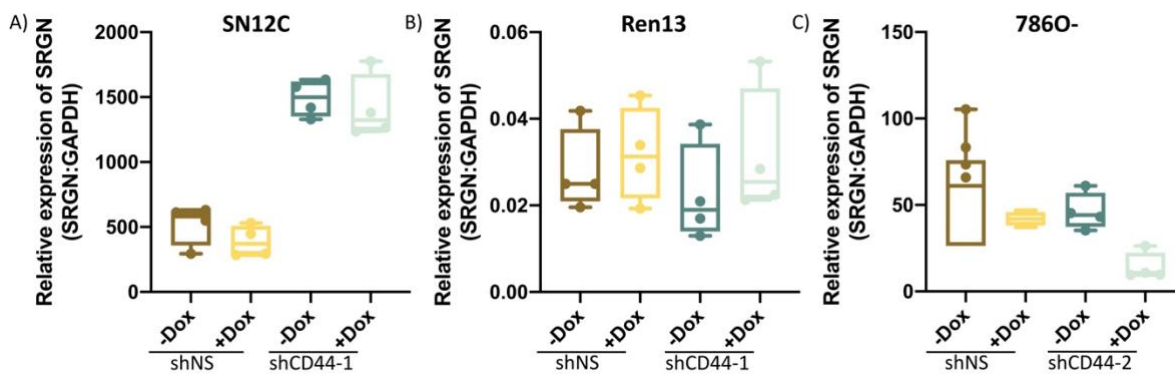


Figure 60. RNA levels of human SRGN in different cells. TaqMan assay was developed to check the Serglycin (SRGN) expression in three different cell lines: SN12C (A), Ren13 (B), and 786O- (C), treated (+Dox) and not (-Dox) with doxycycline. shNS cells were used as controls. GAPDH expression was determined as housekeeping. Cells were treated with 2,5 μ M of doxycycline during 48h.

This assay confirmed the results previously observed with the Western Blot. The cells that expressed more Serglycin were the SN12C cells, while Ren13 cells were the ones with the lowest RNA levels. Curiously, SN12C shCD44-1 cells had higher levels of Serglycin RNA than the control ones (shNS), without regarding the induction with doxycycline. Conversely, in the other two cell models, RNA levels of Serglycin were quite similar comparing the shNS and the shCD44 cells.

It could also be observed that doxycycline treatment seemed only to affect the 786O-shCD44-2 cells, as Serglycin RNA levels were lower than the non-induced cells (shCD44-2 -Dox) and the control cells (shNS).

3.2.3.2 Serglycin Expression in Tumors

Once we had demonstrated that our cell cultures expressed Serglycin, we wanted to check if tumors generated from these cells still expressed the protein. We performed Immunohistochemistry to stain the Serglycin present in the tumor tissues (Figure 61).

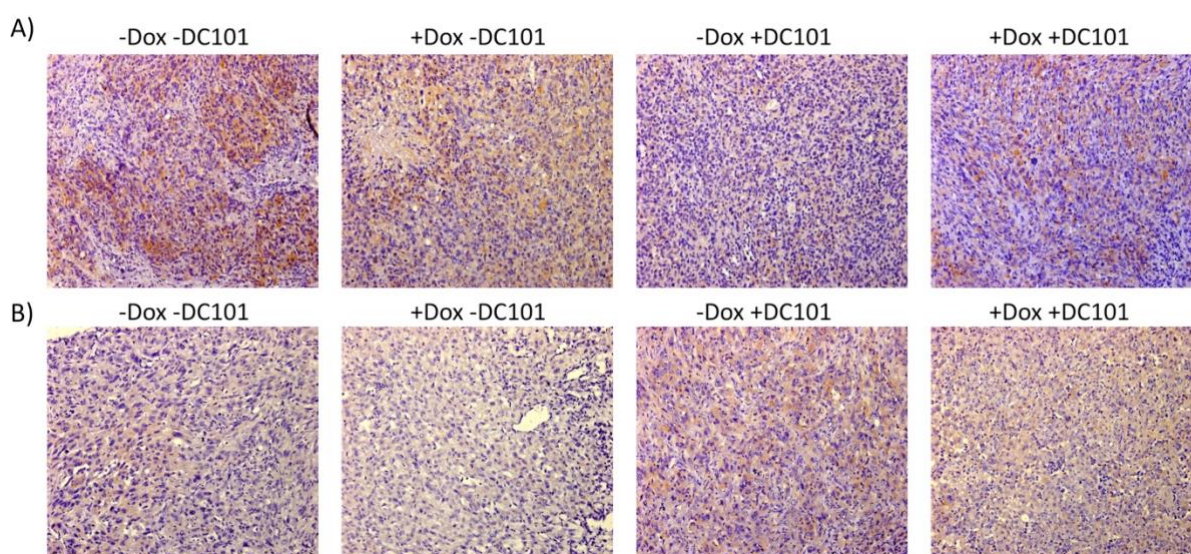


Figure 61. Serglycin was expressed in tissue tumor samples. Immunohistochemistry of Serglycin developed in SN12C shCD44-1 tumor tissues (A) and 786O- shCD44-2 tumor tissues (B).

Observing the images, we could determine that tumors generated from SN12C shCD44-1 cells and also the ones generated from 786O- shCD44-2 cells displayed Serglycin staining. However, there existed variability in Serglycin expression between the different tumors. No pattern could be determined depending on the treatment administered to the animals. The antiangiogenic drug DC101 and the doxycycline treatment did not appear to modulate the protein expression.

3.2.3.3 Determination of Serglycin Localization

Once the presence of Serglycin in our cell models and in the tumor tissues became evident, we wanted to determine its localization and if both proteins co-localized, allowing its interaction and signaling.

We performed an Immunocytofluorescence staining of Serglycin and CD44 at the same time. The assay was developed in two different cell models, Ren13 shCD44-1 and 786O-shCD44-2, as both cell types showed CD44 to have a role in migration and invasion, hence, they were the most important models for our project.

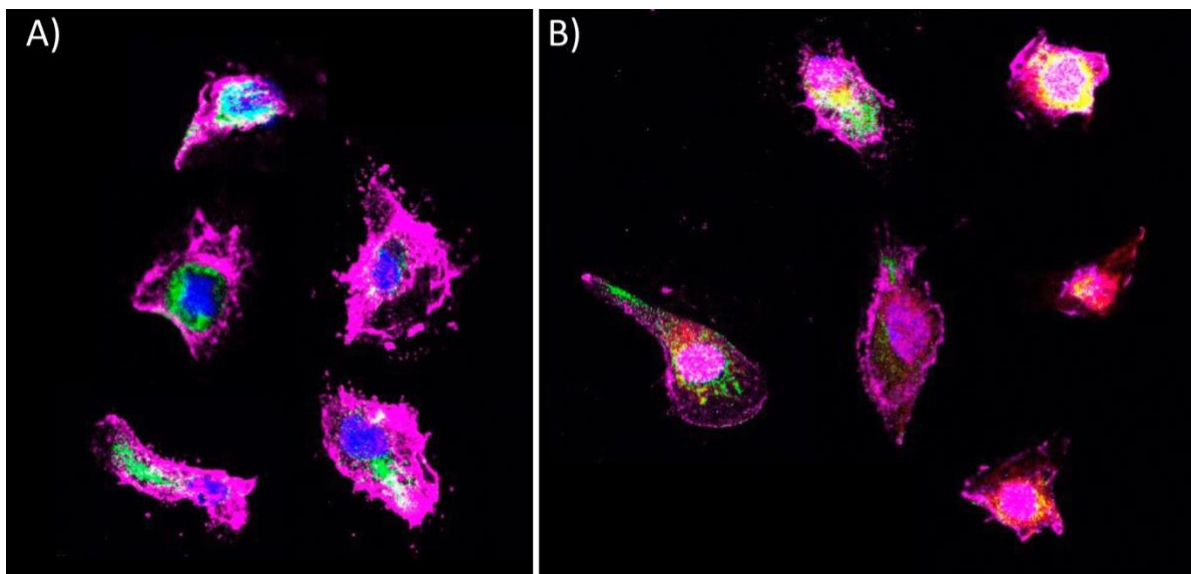


Figure 62. Serglycin expression in induced and non-induced Ren13 shCD44-1 cells. Co-Immunocytofluorescence of Serglycin and CD44 performed in Ren13 shCD44-1 cells non-treated with doxycycline (A) and after 48h of doxycycline treatment (B). 30000 cells were seeded in each well 24h before the experiment. Doxycycline was used at 2,5 μ M. Images were taken at 20X. Serglycin is represented in green and CD44 in magenta. Nucleuses of cells were stained with DAPI (blue). After doxycycline treatment cells expressed RFP, represented in red.

Figure 62 displays different images of the Immunocytofluorescence performed in non-induced Ren13 shCD44-1 cells (Figure 62 (A)) and the same cells induced with doxycycline (Figure 62 (B)). On the one hand, we could observe that doxycycline treatment produced a reduction of the CD44 expression, which is a reduction of the magenta staining. Moreover, we could validate the functioning of the shRNA system, as once treated with doxycycline, cells expressed RFP, red fluorescence that can be observed in the image.

On the other hand, if we focus on the Serglycin staining, as is represented in green fluorescence, we could observe that doxycycline treatment, and therefore the decrease of CD44 expression, also produced a reduction of Serglycin expression. This indicates that a kind of regulation may exist between both proteins.

Nevertheless, if we focus on the localization of both proteins, they were not co-localized. While CD44 protein was expressed at the cell membrane, Serglycin seemed to be in the cytoplasm of the cells forming a kind of vesicles.

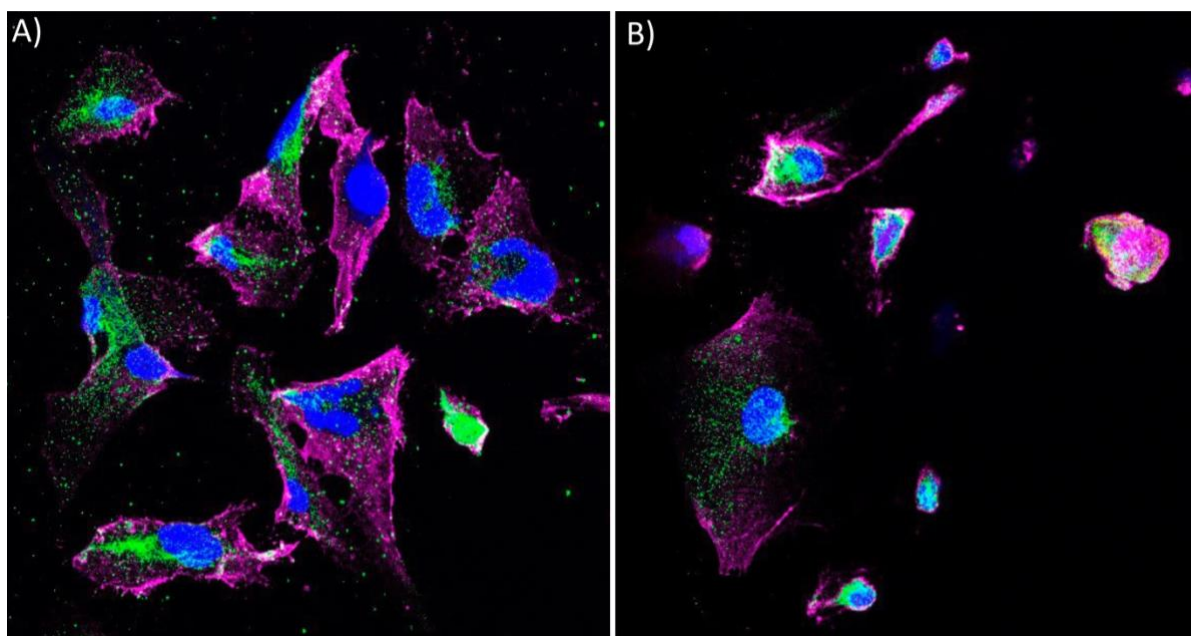


Figure 63. Serglycin expression in induced and non-induced 786O- shCD44-2 cells. Co-Immunocytofluorescence of Serglycin and CD44 performed in 786O- shCD44-2 cells non-treated with doxycycline (A) and after 48h of doxycycline treatment (B). 30000 cells were seeded in each well 24h before the experiment. Doxycycline was used at 2,5 μ M. Images were taken at 20X. Serglycin is represented in green and CD44 in magenta. Nucleuses of cells were stained with DAPI (blue). After doxycycline treatment cells expressed RFP, represented in red.

In Figure 63 some images of 786O- shCD44-2 cells treated with doxycycline (Figure 63 (B)) and non-treated (Figure 63 (A)) are represented. This time, doxycycline induction of cells did not produce much decrease in the CD44 expression (magenta staining). RFP staining was nearly undetectable, assuming a failure in the doxycycline induction. Furthermore, there were no big changes to Serglycin staining (green fluorescence) after

the CD44 silencing. This could be due to the bad efficiency of doxycycline induction and consequently the little CD44 silencing.

Focusing on the localization of both proteins, it could be confirmed that CD44 and Serglycin were not co-localized in those cells too.

Nevertheless, the interaction or signaling between both proteins needs to be deeply studied. These are only primary results that may indicate both proteins are expressed in our cell cultures, but they are not localized in the same part of the cell. Moreover, the regulation between the expression of both proteins is still not clear, and more experiments should be performed.

4. IMPORTANCE OF CD44 EXPRESSION IN PATIENTS

Finally, we wanted to clinically validate the obtained results in patients. To do so, we first determined the importance of CD44 expression in renal carcinoma patients. We obtained data of 528 kidney renal cell carcinoma (KIRC) patients at different stages of the disease from the TCGA dataset. As demonstrated in Figure 64, 418 of those patients had higher expression of CD44 protein and their survival probability was lower than the remaining 110 patients, whose CD44 expression levels were lower.

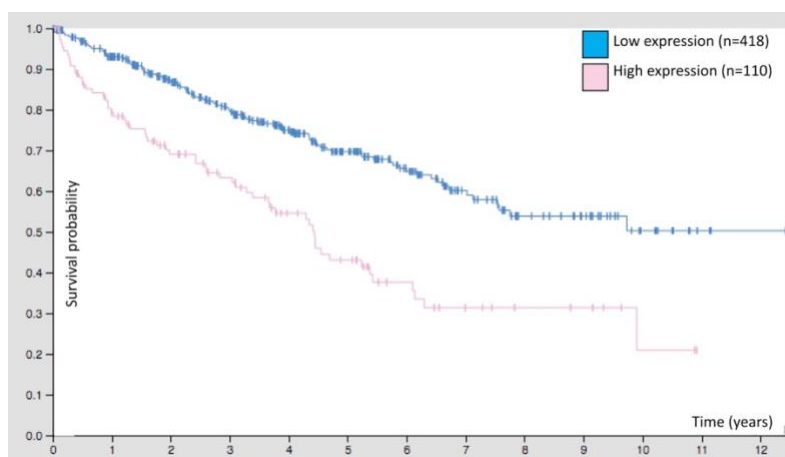


Figure 64. Survival probability of kidney renal clear cell carcinoma patients over time depending on the CD44 expression. Patients with high expression of CD44 (pink line) showed to have less survival probability over time than those patients with lower expression of the protein (blue line). Image adapted from "Protein Atlas," 2020.

Furthermore, the increase of CD44 expression after antiangiogenic treatment, which was one of the bases of our project, was validated through different Ren-PDOX mouse models. We decided to study an mRNA dataset of patients untreated and treated with Sunitinib, one of the most used antiangiogenic drugs to treat renal cancer (GSE65615). This study collects data from primary renal cancer tissue coming from a nephrectomy of 46 patients with metastatic clear cell renal cell carcinoma. From those patients, 23 were not treated and the other 23 patients were treated with Sunitinib for 18 weeks before the acquisition of the sample. Different regions of the tumor of each patient were examined, so at the end, 47 untreated tumors samples and 75 Sunitinib-treated tumors samples were obtained.

We analyzed if CD44 expression in those patients was altered due to the antiangiogenic treatment (Figure 65). Although the results were not statistically conclusive, CD44 expression tended to be increased in those patients treated with Sunitinib. Those results would be in accordance with the *in silico* results obtained at the beginning of the project using the Ren13 tumor model, and would also support the hypothesis of the CD44 involvement as a predictor of malignization response after the antiangiogenic treatment.

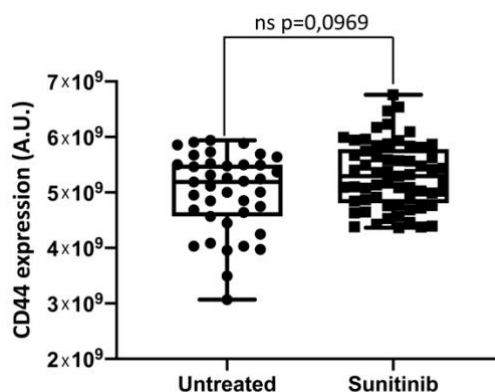


Figure 65. Expression of CD44 in untreated and Sunitinib-treated patients. Representation of the mRNA levels represented as A.U. in untreated and Sunitinib-treated patients for CD44.

Once we had analyzed the expression of CD44 in these set of patients, we decided to determine the importance of Serglycin. As observed in Figure 66, Serglycin, as well as CD44, has been described as a bad prognostic marker in patients suffering from renal

cancer. Thus, and considering it as a candidate able to interact and/or modulate CD44 activity, it was interesting to study if its expression could be altered due to the antiangiogenic treatment.

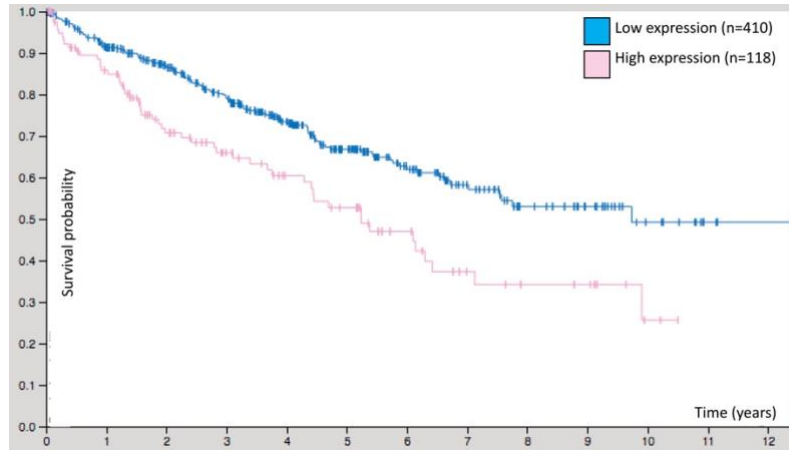


Figure 66. Survival probability of kidney renal clear cell carcinoma patients over time depending on the Serglycin expression. Patients with high expression of Serglycin (pink line) showed to have less survival probability over time than those patients with lower expression of the protein (blue line). Image adapted from “Protein Atlas,” 2020.

As previously done with CD44, Figure 67 shows the expression of Serglycin in patients treated with Sunitinib and untreated.

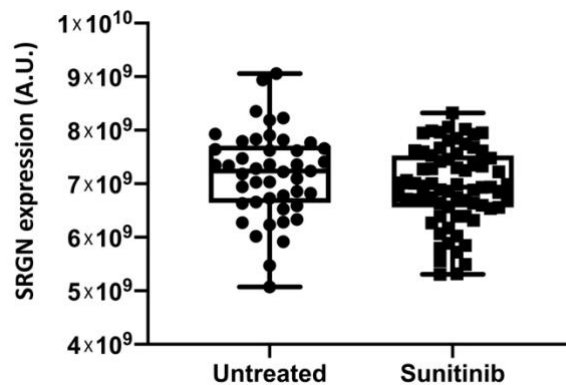


Figure 67. Expression of Serglycin in untreated and Sunitinib-treated patients. Representation of the mRNA levels represented as A.U. in untreated and Sunitinib-treated patients for Serglycin.

In this case, Sunitinib treatment did not affect the expression of Serglycin, as those patients that were treated did not show higher levels of the protein than the untreated patients.

Additionally, some researchers of our group have determined ALDH1A3 expression as a marker of tumor response to antiangiogenic treatment. It was observed that those tumors that had high levels of ALDH1A3 before the antiangiogenic treatment were the ones that after the therapy presented changes in their invasive and metastatic behavior, becoming more aggressive (Moserle, L. et al. in preparation). Subsequently, we decided to use this response predictor factor and determine the expression of Serglycin by grouping patients depending on their ALDH1A3 levels (Figure 68).

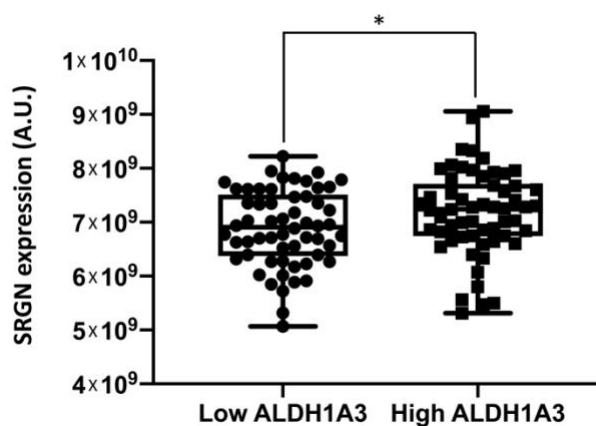


Figure 68. Expression of Serglycin depending on ALDH1A3. Representation of Serglycin mRNA levels represented as A.U. in patients with low and high expression levels of ALDH1A3. (Mann Whitney test $p < 0,05^*$)

These results may suggest that the tumors of patients that have a higher expression of ALDH1A3, and that consequently are considered as potentially aggressive after the antiangiogenic treatment, also have a high expression of Serglycin.

Thus, it could be thought that Serglycin probably is not a marker of tumor response, as no differences could be observed between treated and untreated patients. However, it could be playing a modulator factor role, as those patients with potentially aggressive tumors have higher Serglycin expression levels.

Despite these are primary results, it was suggested that CD44 expression could be important in renal cancer, as Serglycin expression. Moreover, some evidence of a link between CD44 and Serglycin was found in tumors of patients, as a correlation between them previously demonstrated. Nevertheless, it would be necessary to perform further experiments and analyze data from more patients to determine the role of CD44 and Serglycin alone and together in renal cell carcinoma patients.

DISCUSSION

1. ANTIANGIOGENIC TREATMENT AND TUMOR MALIGNIZATION

The first therapies used to treat renal cell carcinoma were based on cytokines, but only between 5-27% of tumors responded to such treatment. Moreover, in most cases, the adverse effects were extremely high due to their toxicity (Posadas, Limvorasak, & Figlin, 2017). For that, the discovery of angiogenesis and the antiangiogenic therapy represented a milestone in renal cell carcinoma treatment. These drugs improved the PFS and OS of patients suffering from this disease, apart from becoming a novelty in the cancer treatment field (Posadas et al., 2017; Barata & Rini, 2017).

Nevertheless, some studies using antiangiogenics to treat other cancer types demonstrated that, after an initial phase of drug response (characterized by a reduction of tumor progression), some tumors were able to evade the antiangiogenic effect and re-grow. Moreover, in some cases, an increase in their invasive and metastatic abilities was reported after therapy (Pàez-Ribes et al., 2009).

However, this fact was not observed in renal tumors. Therefore, some studies intended to check whether this post-treatment malignancy occurred in renal cancer. First, 786O-tumors, generated from an established renal cell carcinoma cell line, were used.

The generation of tumors from conventional cell lines is an easy, well-established method to study drugs using *in vivo* models of cancer. But they are not the best approach to mimic all the events of a patient's tumor. Cell lines adapt to grow *in vitro*, and they lose the biologic features from the original tumor, modifying some processes such as migration and invasion (Hidalgo et al., 2014).

Therefore, in order to overcome this drawback, the Ren-PDOX models were generated, using pieces of patients' tumors and implanting them orthotopically into the kidney of a mouse. Even though the difficulties the production of these models present, they are able to maintain the principal features of the donor and do not lose them through successive mouse-to-mouse passages *in vivo* (Hidalgo et al., 2014). Moreover, the orthotopic implantation also allows to mimic the metastatic ability of the original

patient, which cannot be achieved using the subcutaneous implantation of the tumors (Hoffman, 2015).

Once the best model to study tumor malignization after antiangiogenic treatment in renal cancer was determined, it could be demonstrated, as previously done in other cancer types, that short antiangiogenic periods of treatment produced a reduction in the volume and tumor progression. However, when treatment was maintained for a longer period (four weeks), tumors re-grew and became more aggressive. This discovery was an inflection point in renal cancer treatment, as the only therapy with good results in this tumor type resulted not to be as promising as it initially seemed to be.

Nevertheless, the increase in tumor malignization was not observed in all types of renal cancer. RCC is characterized to present a spatial heterogeneity that changes through time and in response to the treatment (Posadas et al., 2017). Tumors of the same type have shown to be heterogeneous between each other, and there is also heterogeneity in the same tumor, complicating their treatment (Beksac et al., 2017). Due to that, not all antiangiogenic treated Ren-PDOX responded equally. It was observed that some tumors, such as Ren50 and Ren28, did not become more aggressive after the therapy, as they preserved their characteristics; while other tumor models, such as Ren13 and Ren86, turned into a more invasive and metastatic profile (Morsele, L. et al. in preparation).

Testing the antiangiogenic drugs in different types of renal cancer allowed us to obtain different responses, reinforcing the idea of tumor heterogeneity existing between patients suffering from the same cancer.

Moreover, the divergence observed in such responses may indicate that different mechanisms are activated depending on the tumor, and that antiangiogenic treatment may produce the activation of different pathways that would, in turn, mediate the tumor response. For that, Ren13 tumors treated with antiangiogenics (DC101) and Ren13 control tumors (non-treated) were subjected to massive RNA sequencing. This study was

key to distinguish whether those genes that were altered during the treatment were upregulated or downregulated.

Another important feature of the Ren-PDOX models is that once implanted, the human tumor stroma is replaced by murine stroma. However, tumor cells are still human cells. Therefore, during the RNA sequencing, it was possible to discern the human genes from the murine ones, and consequently to identify genes codifying for stromal proteins (murine) from the ones codifying for tumor proteins (human).

From this study, some different genes appeared to be involved in the post-treatment malignization. However, it is important to keep in mind that the RNA sequencing was conducted only on one tumor type, the Ren13 tumor model. For that, the different candidates had to be evaluated through TLDA analysis in other Ren-PDOX pro-invasive models such as Ren86. Moreover, it was necessary to check that obtained results from the different analyses correlated both models, in order to select the best candidate genes.

The GEO profile platform was also useful for the study of candidate genes in different renal cancer patients. This way, the error produced by selecting one target *in silico*, using one tumor type, was reduced.

This study together with an exhaustive literature research allowed us to select CD44 as a gene candidate involved in the tumor malignization process after antiangiogenic treatment in renal carcinoma.

2. STUDYING THE ROLE OF CD44 PROTEIN: SHRNA SYSTEM

There are different methods available to determine the role of a protein. On one hand, we can opt to overexpress the protein of interest. This approach might be used when the expression levels in the cells or tumors we are working with are very low or undetectable. On the other hand, as in our case, when cells or tumors have high levels of the target protein, we can choose different methods to reduce its expression or completely remove the protein and determine the consequences.

In our study, we decided to select from a cell set the ones that had higher levels of CD44 and which, once implanted into the kidney of a mouse, could still express the protein.

Then, we decided to use the inducible shRNA system to modify the tumor cells. Through this technique, we can reduce the expression of a protein when cells are cultured in the presence of doxycycline in the medium.

The generation of a transfected cell line through shRNA is a laborious process, but it has proved to be advantageous in comparison with other methods that are not inducible (Moore, Guthrie, Huand, & Taxman, 2010).

When a stable knockdown of a protein is produced, meaning that the protein expression is reduced or removed permanently, some different compensatory mechanisms can be activated and the role of the protein of interest can be modified or masked. In our setting, as the system is inducible, the reduction of the protein expression is temporary, avoiding these compensatory mechanisms and allowing a better study of the protein's role (Czuderna et al., 2003; Tilesi, Fradiani, Socci, Willems, & Ascenzioni, 2009; Rao, Vorhies, Senzer, & Nemunaitis, 2009).

Moreover, using the inducible system, the same cells act as their own control when they are not induced, reducing the experimental variability due to the usage of different cells (Matsushita, Matsushita, Hirakawa, & Higashiyama, 2013). Nevertheless, sometimes the reduction of the protein expression obtained using the shRNA method is less than the one obtained through a constitutive silencing system. Furthermore, the inductor agent, e.g. doxycycline in our setting, can influence the silencing efficiency (Tilesi et al., 2009).

We could always observe the downregulation of CD44 expression after doxycycline treatment. However, despite using always the same dose and treatment time, the efficiency of the silencing was not always identical. Over time and cell passages, a reduction of the silencing strength could be observed. This variability could be due to experimental conditions that cannot always be under control, and also due to the cell conditions in the moment of the doxycycline treatment.

It also has to be considered that doxycycline is an antibiotic derivative from the tetracycline family that can affect cells (Matsushita et al., 2013). Therefore, it was necessary to use control cells called shNS or non-silencing, which were transfected with the same shRNA, but in this case, the short hairpin had no target. Then, when cells were treated with doxycycline, no gene was downregulated. These controls are necessary to guarantee that doxycycline only activated the shRNA and that it did not produce any secondary effect on the cells.

In some cases, doxycycline can have effects by itself, regardless of the shRNA. For example, Merentie et al., 2018 described the modulating effect of doxycycline on VEGF-A expression in murine models and cell cultures of cardiomyocytes and endothelial cells. It has also been described that doxycycline can have an antiapoptotic effect, induce inflammatory responses, and inhibit the metalloproteinases responsible for the degradation of the extracellular matrix (Koponen et al., 2003; Cerisano et al., 2014; Xie, Nair, & Hermiston, 2008).

During the development of the different experiments shown in this thesis, no effects on the migration and invasion processes of the cells, neither the expression of the studied proteins, could be observed due to the doxycycline treatment.

In some cases, the response variations between the control cells (shNS) treated and non-treated with doxycycline were due to the experimental variability. Moreover, these differences were minimal, and they did not cause any statistically relevant changes.

However, in order to reduce the possible secondary effects due to doxycycline treatment before studying the role of CD44 in migration and invasion, we performed a dose-response study over time. Thus, we were able to determine that 2,5 μ M was a highly enough dose to induce the shRNA. Although it was a little bit higher than the recommended dose (1-2 μ M) (Xie et al., 2008), induction time (48h) was sufficient to produce a silencing effect without damaging the cells.

3. ROLE OF CD44 IN TUMOR MIGRATION AND INVASION

The principal hypothesis of the project pointed to CD44 as one of the genes involved in the invasion increase observed in renal carcinoma tumor cells after the antiangiogenic treatment. CD44 appeared from a set of analyses using tumor samples treated and non-treated with antiangiogenic drugs, and also from data of patients suffering from renal carcinoma. Apart from the developed study, the amount of information existing about the role of CD44 in other tumor types, made us opt to choose CD44 for further insight, out of the other candidates.

It has been described that CD44 plays an important role in migration, adhesion, signaling and cell division, regulating different biologic processes. Moreover, its implication in cancer, inflammatory and autoimmune diseases has also been described (Basakran, 2015).

High levels of CD44 came out as a marker of metastasis and tumor malignization. It is also used as an unfavorable prognosis marker in different cancer types such as ovarian, breast, colon, gastric, prostate, and melanoma (Bourguignon, Zhu, Shao, & Chen, 2001; So et al., 2013; Misra, Hascall, Markwald, & Ghatak, 2015).

Regarding renal cancer, CD44 expression and its correlation with invasion and tumor malignization have been described in some lines of renal carcinoma. Although it has not been demonstrated yet, CD44 is believed to play a pathogenic role in clear cell renal cell carcinoma progression (Gilcrease et al., 1999; Gilcrease, Truong, & Brown, 1996).

A study using tissue samples of clear cell renal cell carcinoma patients demonstrated that CD44 expression positively correlated with the pathologic state of the tumor, metastasis, and histological grade. Moreover, it was confirmed that patients with high levels of CD44 presented a worse prognosis, in comparison with those with lower expression levels. It was also proved that the metastases of patients treated with Sunitinib (an antiangiogenic drug) and also the primary tumor showed high levels of CD44 (Mikami et al., 2015).

Other studies using ovarian cancer models demonstrated that reducing CD44 expression *in vivo* (through an shRNA system) produced a notable impairment in tumor growth (Zou et al., 2014).

All these data sustained our hypothesis of the CD44 involvement in the tumor malignization process after antiangiogenic treatment in renal cell carcinoma.

CD44 is a quite complex target. Due to alternative RNA splicing processes, more than 20 different isoforms of the protein, called variants (CD44v), can be synthesized. Those variants are characterized to show insertions of variable length exons at the proximal plasma membrane external region (Karousou et al., 2017; Misra et al., 2011). The smallest and simplest isoform, and also the most abundant, is the standard one, known as CD44s or CD44H (hematopoietic) (Basakran, 2015).

Many studies confer the tumor malignization role to the different CD44 isoforms and not to the standard one, as not all the isoforms can be found in all tumor types or stages of the disease (Basakran, 2015; Karousou et al., 2017).

Some different isoforms of CD44 have been detected in clear cell renal cell carcinomas. The main and most studied ones are CD44v5, v7, and v8 (Lučin, Matušan, Dordević, & Stipić, 2004).

During our research, we could verify that the isoform present in our Ren13 tumor samples was the standard one (CD44s), as it was the only CD44 transcript detected in the results of the RNA sequencing. Although the most common isoforms were not detected, some research groups have described that in renal cancer, CD44s expression correlates with the pathologic tumor stage as well as with the cell proliferation (Lučin et al., 2004; Gilcrease et al., 1999) supporting our results.

The role of CD44 in migration and invasion processes has been described in other cancer types such as ovarian, breast, and colon (Bourguignon et al., 2001; Gilcrease et al., 1999; So et al., 2013). In metastatic renal cancer, CD44 is used as a marker of bad prognosis, as a negative correlation has been demonstrated to exist between its expression and

tumor progression (Rioux-Leclercq et al., 2001; Lim, Young, Paner, & Amin, 2008). Nevertheless, not much is known about the involvement of CD44 in the migration and invasion processes of renal cancer (Terpe et al., 1996). This was another reason why CD44 seemed to be an interesting candidate to study.

As shown in the exposed results of this thesis, CD44 silencing through the shRNA system produced changes in the migration and invasion processes of two cell models tested, the Ren13 and the 786O-, but no changes could be observed in the SN12C cell model. These results could be validated *in vivo*, except for the Ren13 model, that we were not able to generate tumors from those cells.

The main difference between 786O- and SN12C models lied in their aggressiveness. Tumors generated from the SN12C cells showed to be aggressive from the beginning, even before starting the antiangiogenic treatment. When we studied their invasiveness, tumors had completely destroyed the normal renal parenchyma, and it was impossible to determine the presence of tumor cells' infiltration into the kidney. Moreover, in most cases, the percentage of necrotized tissue was too high. When we observed these results, we decided to reduce the treatment period of the tumors generated from the 786O- cells from three weeks to two weeks, in order to reduce the difficulties in the subsequent analysis.

However, SN12C did not show to reduce their invasiveness when CD44 expression was silenced, an effect that could indeed be demonstrated with the 786O- tumors. This result, which was also checked *in vitro*, could suggest that CD44 is not involved in the migration and invasion processes of the SN12C cells and tumors, as no functional changes were observed after the decrease of the protein's expression. Possibly, in this tumor model, some other mechanisms are responsible for these events. Otherwise, 786O- tumors were affected by the downregulation of CD44, as changes in migration and invasion could be observed. Furthermore, some other studies using 786O- cells that were resistant to Sunitinib, also demonstrated the involvement of CD44 in tumor invasion (Mikami et al., 2015).

Despite studying the role of CD44 in two different tumor models, it was not possible to determine its role in Ren13 tumors, and this has been the main limitation of the project. Ren13 cells were the ones used during the RNA sequencing where CD44 showed to be upregulated after the antiangiogenic treatment. Hence, determining the role of CD44 in the invasive process of those tumors would be highly informative, and some light has still to be shed on this matter.

However, analyzing the tumor samples of the *in vivo* experiment, we found an unexpected result. Animals that were treated with doxycycline, i.e. to induce the shRNA, showed a reduction in the number of blood vessels. This fact was only observed in tumors generated from 786O- cells and not in the ones generated from the SN12C cells, which proved to be another piece of evidence that both tumor models are regulated by different mechanisms.

Some articles describe CD44 to be involved in the vascularization and angiogenesis processes by inducing endothelial cell tubule formation (Tilesi et al., 2009). Moreover, changes during angiogenesis have been noticed when CD44 expression levels are partially or completely reduced in endothelial cells. For that, CD44 has been suggested to be a target to modulate angiogenesis in some cancer types (Pink, Skolnaja, Paell, & Valkna, 2016; Zou et al., 2014).

In light of the above, CD44 could be hypothesized to have a role in angiogenesis in some renal carcinoma types. However, more experiments would have to be performed and more evidence on the issue be provided before drawing any conclusions yet. In the case that CD44 had an angiogenic role, it would be target worth considering in renal cancer. Through CD44 downregulation we would be reducing the blood vessels and consequently the oxygen and nutrient contribution to the tumor, and, at the same time, we would be decreasing the invasive and migratory ability of cells, limiting the tumor dissemination.

4. CD44 DOWNSTREAM SIGNALING

One valuable item we aimed to comprehend about the CD44 biology was which downstream signaling pathways could be involved in the migration and invasion processes observed in our tumor models. Therefore, to find some evidence, we performed an exhaustive bibliographic research.

CD44 is a deeply studied protein in different processes, which is able to bind to some components of the extracellular matrix just as to other ligands. For that, CD44 has been showed to be involved in some signaling routes.

In breast cancer, the contribution of CD44 in some pathways has been observed to lead to tumor growth induction, the survival of cancer cells, and the increase of cell migration and invasion. Bourguignon, Singleton, Zhu, & Diedrich, 2003 described that the interaction between RhoGEF and CD44 produced the activation of AKT/PI3K, responsible for tumor malignization. CD44 signaling together with PI3K has also been described by Abdraboh et al., 2011 as an inducer of the breast cancer cells invasiveness. However, other authors studying the same cancer type reported the role of CD44 together with Src as the main responsible for the modulation of migration and cell proliferation (Nam, Oh, Lee, Yoo, & Shin, 2015). In ovarian cancer, Bourguignon et al., 2001 also described the interaction between CD44 and Src related to cancer cell migration.

Park, Huh, Lee, & Kim, 2012 and Cho et al., 2012 identified CD44 as the leading controller of the Wnt/AKT pathway in colon cancer, responsible for inducing cellular apoptosis. Lee et al., 2017 put the downregulation of GSK-3 β produced by CD44 forward as the cause of the changes observed in cell proliferation and survival. Another important issue determined in colon cancer was the interaction between CD44 and Stat3. This binding unchained the JAK/Stat signaling and promoted the tumor malignization. This fact was also detected in some breast cancer types by So et al., 2013.

From all the possible pathways that were identified to be involved downstream of CD44, AKT, Src, and JAK/Stat were the most frequently described in different cancer types, so we decided to focus on those three.

The role of AKT/PI3K pathway had previously been described in renal cancer. Some studies demonstrated that inhibition of its signaling produced a reduction of cell proliferation, apoptosis, and invasion in cell cultures and mice models of renal carcinoma (Fang et al., 2013; Hung et al., 2017).

In order to study the role of this signaling pathway in our cell cultures, we decided to use Perifosine, an AKT inhibitor. As previously shown in the results of this thesis, on one hand, the usage of low doses of the inhibitor did not produce any effect on cell migration. On the other hand, when higher doses were tested, the reduction of the cell migration observed was due to its toxicity. Thus, we decided set this study line aside and focus on the other two candidates.

JAK/Stat signaling pathway was also described in renal cell carcinoma as a responsible for promoting cell proliferation, metastasis, angiogenesis, and cell invasion and migration *in vivo* and *in vitro* (Fang et al., 2013; Li et al., 2013; Wu, Miao, & Khan, 2007). Moreover, the overexpression of some proteins involved in this signaling route has been observed in renal cancer patients, as well as its correlation with a bad prognostic of the disease (Lue et al., 2015; Tao et al., 2018). These proofs suggested that JAK/Stat could be important in our tumor models.

Ruxolitinib was used as an inhibitor of the signaling produced by JAK/Stat to determine the effect of its blockade on the migration process of our cell cultures. It is a small molecule that serves as a JAK1/2 inhibitor and has been approved by the FDA to treat myelofibrosis and polycythemia vera. It is also in phase II of clinical trials for the treatment of other malignancies such as chronic lymphocytic leukemia (Ding, Kloss, Tuncali, Tran, & Loftus, 2020; Abikhair Burgo et al., 2018).

It has been reported that Ruxolitinib can reduce the migration and invasion processes of different cancer cells, such as breast, glioblastoma, and hepatocellular (Wilson et al., 2013; Kim, Gautam, Kim, Kim, & Kang, 2019; Ding et al., 2020).

Contrarily to what was described, results of the Wound Healing experiments performed using renal cancer cells did not show Ruxolitinib to have any effects on the migration ability of cells.

Despite the lack of functional effect, we could demonstrate through Western Blot that Ruxolitinib was indeed inhibiting the JAK/Stat pathway, as phosphorylation of Stat3 protein was reduced in treated cells. This event has also been described by other authors as evidence of Ruxolitinib activity (Komar et al., 2017; Lue et al., 2015).

Therefore, JAK/Stat signaling pathway was also discarded to be involved as downstream of CD44 and to affect the migration and invasion processes of our cell models.

The third candidate pathway to take part in these events was Src. It has been described to have a role in cell morphology, adhesion, migration, invasion, proliferation, differentiation, survival, growth, angiogenesis, and apoptosis in biologic and pathologic processes of mammalian cells (Sen & Johnson, 2011; Bai et al., 2012). Src has also been reported to be involved in malignant cell transformation, disease progression, and metastatic spread of some solid tumors, such as prostate and breast cancer (Rusconi, Piazza, Vagge, & Gambacorti-Passerini, 2014; Rabbani, Valentino, Arakelian, Ali, & Boschelli, 2010). Moreover, the study of tumor samples of patients suffering from renal carcinoma showed a correlation between high levels of Src protein expression and a reduction of patients' survival (Suwaki et al., 2012).

Furthermore, Bourguignon et al., 2001 described that in ovarian cancer there is a direct interaction of the CD44 cytoplasmic tail with a specific region of Src, which is responsible for the regulation of the tumorigenic process.

To study Src signaling, we used Bosutinib, a dual inhibitor of Src and BCR-Abl approved for the treatment of chronic myeloid leukemia Ph⁺ and acute lymphoblastic leukemia

(Rusconi et al., 2014; Isfort & Brümmendorf, 2018; Roskoski, 2015). It is also in clinical trials for breast cancer and glioblastoma treatment (Rabbani et al., 2010; Roskoski, 2015).

Some studies described an inhibition of the proliferation, invasion, and migration of breast and prostate cancer cells when they were treated with Bosutinib. The reduction of the primary tumor growth and metastasis formation in the lungs, liver, and spleen were also observed with Bosutinib treatment (Rabbani et al., 2010).

When we administered Bosutinib to our cell cultures, their migratory ability was notably reduced, demonstrating the role of Src signaling in our cell models. Then, we decided to verify if this pathway was associated with CD44. Thus, we performed an assay to determine the migration effect on cells after treating them with Bosutinib together with doxycycline, used to downregulate the CD44 expression.

The results of the assay did not show greater inhibition of the cells' migration when we treated them with both drugs, in comparison with when they were only treated with one drug. It might indicate that CD44 and Src are involved in the same signaling pathway, as the inhibition of two different nodes of the same pathway did not increase the effect.

Src downstream presence of CD44 has been described by some authors in breast cancer, where separated inhibition of CD44 and Src produced changes in the cell migration. Moreover, CD44 silencing through the shRNA system was described to bring about changes in Src expression among other proteins that were involved in the pathway (Nam et al., 2015; Ouhtit, Rizeq, Saleh, Rahman, & Zayed, 2018; Chen, Zhao, Karnad, & Freeman, 2018).

As previously done with Ruxolitinib, we decided to verify that the migration effect observed with Bosutinib treatment was due to the inhibition of Src and not because of other side effects. Through Western Blot, we were able to check the reduction of the Src phosphorylation after Bosutinib administration to the cells.

One intriguing aspect of the assay was that despite using the same dose and timing of the Wound Healing assay, no changes in the phosphorylation of Src were observed. During migration assays, we used a Bosutinib dose that allowed us to observe changes in the migration capacity of cells without completely inhibiting the process. As 1 μ M of the drug produced a dramatic reduction of cell migration, we decided to treat cells with 0,1 μ M, a dose high enough to impair the process. However, when we checked the phosphorylation of Src produced using the latter dose, the reduction of the phosphorylation was imperceptible, and not many changes could be observed. For that, we decided to use higher doses (1 μ M and 5 μ M) to verify that Bosutinib was truly inhibiting the pathway.

1 μ M of Bosutinib has been described in breast, colon, prostate cancer to be enough to reduce cell migration and invasion, and also to cause an observable reduction of the Src phosphorylation, while maintaining total protein expression (Rabbani et al., 2010; Vultur et al., 2008). However, Segrelles et al., 2018 described the need to use higher doses of Bosutinib in order to obtain some effects in different types of head and neck squamous cell carcinoma. Moreover, they also reported changes in the phosphorylation and total expression levels of Src due to the treatment.

Regarding the modulating role that CD44 can exert over Src, in our cell cultures no changes in Src phosphorylation could be detected in our cell cultures when CD44 expression was downregulated.

These results showed that not all cancer cells respond equally to Bosutinib treatment and support the results obtained during our assays.

Furthermore, some authors have described the existence of a modulating effect between Src and FAK, another protein involved in the signaling pathway (Rabbani et al., 2010; Guarino, 2010).

Due to FAK dependence on Src, the reduction of Src phosphorylation after Bosutinib treatment can alter FAK signaling too (Brunton et al., 2005). For example, in thyroid

cancer, the decrease of both proteins phosphorylation was described to happen after treating cells with Bosutinib (Kim et al., 2019). However, in other tumors such as breast cancer, the inhibition of Src due to Bosutinib treatment does not affect FAK phosphorylation (Vultur et al., 2008).

Therefore, we aimed to check, in our cell cultures, if Bosutinib treatment affected FAK and/or its phosphorylation, but no changes in the protein expression were observed.

Thus, bearing the results obtained through migration assays and Western Blot in mind, and considering the observations done by other authors in different cancers, we hypothesized that it might be possible that the Src signaling pathway is involved downstream of CD44, and consequently, it is responsible for effect on the migration and invasion processes that take place in our experimental setting. Nevertheless, further experiments need to be performed so as to validate and confirm our hypothesis.

5. CD44 UPSTREAM SIGNALING

Apart from the signaling pathways downstream of CD44, we also wanted to study its upstream events. The main candidate described to regulate CD44 and also the most studied one is Hyaluronic Acid (HA). Despite it has been described that CD44 can be independent of this polysaccharide, in most cases its performance is developed through HA interaction (Misra et al., 2015).

It is widely studied that Hyaluronic Acid is the main ligand of CD44, although it can also interact with other ligands (Bourguignon et al., 2001). Interaction between CD44-HA has been observed to produce conformational and post-transcriptional changes to the receptor that can modify some pathways that regulate inflammation, wound-healing, tumor growth, and metastasis (Karousou et al., 2017). Moreover, most studies demonstrate that CD44 implication in the tumor invasion is due to its interaction with HA (Basakran, 2015).

Hyaluronic Acid consists of repetitions of disaccharides, so its length and molecular weight will depend on the number of bounded units of disaccharides. Thus, different

fragments or units of Hyaluronan are classified into two groups: Low Molecular Weight Hyaluronic Acid (LMWHA) and High Molecular Weight Hyaluronic Acid (HMWHA) (Misra et al., 2015).

The effects produced by the CD44-HA signaling have been describe to depend on the molecular weight of the polysaccharide (Sugahara et al., 2003). For example, in breast cancer, an increase in the tumor cell invasion and metastasis have been observed , which are due to the signaling produced for the interaction of CD44 and high molecular weight units of Hyaluronan (Basakran, 2015). However, other authors have reported that, also in breast tumors, high molecular weight fragments of HA have an inhibitory effect over the metastatic capacity of cells through CD44 signaling (Zhao et al., 2017). Thus, there is no consensus about the effect of the different Hyaluronan fragments.

In our research, we studied the effect of the Low Molecular Weight Hyaluronan fragments binding to CD44, but neither a reduction nor an increase in the migration of cells was observed.

We did not test the effect of the High Molecular Weight fragments. Instead, we tried two different approaches that would allow us to determine if HA played an important role in our setting. These approaches, previously described by some authors, were the usage of Hyaluronidase and the inhibition of the HA-CD44 binding through a blocking antibody (Mikami et al., 2015).

When we demonstrated the presence of Hyaluronic Acid in our cell cultures, we thought that maybe different fragments of this HA were bound to CD44, and for that, no changes in the migration were observed when we added more Hyaluronan, as the binding sites were already occupied. Then, we decided to eliminate the HA using Hyaluronidase and determine if cell migration was altered due to the lack of Hyaluronan. No response could be observed after treating cells with Hyaluronidase.

The other option was to inhibit the interaction between CD44 and HA through a blocking antibody that was able to bind to the same binding pocket than Hyaluronan. However, no migration changes were observed either due to the binding inhibition.

These results together made us conclude that probably Hyaluronic Acid is not the main inducer of CD44 activity in our setting. Intriguingly, although we know that HA is indeed expressed in tumors and cells that were used to develop our research, it might not be the main responsible for the migration processes of our tumor models.

Similarly to CD44 silencing, which has not the same effects on all tumors, maybe Hyaluronic Acid has not either. For that, it would be interesting to check if HA plays a relevant role in other renal carcinoma models, different from the Ren13 model, which was the one we used during our research.

Once Hyaluronic Acid was discarded as the main inducer of CD44 activity, we decided to look for other candidates. As previously explained in section 3.2 of the results chapter, a set of correlation analyses using data from the RNAseq of the beginning of the project were performed, and data from patients with renal cell carcinoma obtained from the TCGA database were also taken into consideration for such analyses. Thus, we could move closer to the clinical reality of patients.

From the analysis, three candidates came out as possible interactors and inducers of CD44: CD82, CCL5, and Serglycin. Among them, Serglycin showed higher expression levels in the tumors used during the RNAseq than the other candidates. Moreover, its expression correlated with CD44 in the *in silico* study, and also in the samples of patients obtained from the TCGA. For that and due to the information about the CD44-SRGN interaction in cancer, we decided to study this candidate first.

The binding between Serglycin and CD44 had previously been described by Toyama-Sorimachi et al., 1995 in endothelial cells. Later, the presence of Serglycin and its interaction with CD44 were found in different cancer cells, such as non-small cell lung

cancer and triple-negative breast cancer (Guo, Chiu, Wang, Li, & Chen, 2020; Zhang et al., 2017; Korpetinou et al., 2013).

Despite Serglycin expression and its role together with CD44 have not been described in renal carcinoma cells, high levels of the protein have been related to a bad prognostic in patients suffering from renal carcinoma (“Protein Atlas,” 2020).

Different authors have reported that Serglycin can be secreted by some components of the tumor microenvironment, such as CAFs (J. Y. Guo et al., 2016). Nevertheless, it can also be secreted by the tumor cells (Karousou et al., 2017; Jing You Guo et al., 2020).

During the experiments to detect the expression of the protein in our cell cultures, we tried to determine the presence of Serglycin in the cells’ supernatants, to check if, in our experimental setting, the protein was secreted to the medium by cancer cells. After some attempts, we could not detect Serglycin in the supernatant of the cells, which may be indicative of two things: on one hand, the protein could have not been secreted to the medium, and on the other hand, the levels of secreted protein could be so low that it was impossible to detect them. For that, and to be sure of the presence of Serglycin in the medium of cells, it would be appropriate to find other methods sensitive enough to detect low levels of the protein, as by Western Blot we were not able to detect them. Another option would be to more efficiently concentrate proteins present on the supernatant of cells, and hence try to identify Serglycin.

Initially, Serglycin was described as a proteoglycan that was able to interact with different inflammatory mediators, and consequently, to participate in the inflammatory response. Later, it was described that it could also have a role in tumor progression and metastasis, and that it could even be involved in the regulation of angiogenesis (Karousou et al., 2017).

Some authors described that the role of Serglycin in tumor malignization was due to its interaction with CD44 enabled through the GAG moieties, specifically through the chondroitin sulfate residues. It was demonstrated that, in the absence of CD44 and/or

the chondroitin sulfate residues, Serglycin was not able to induce any tumor malignization processes (Jing You Guo et al., 2020; 2016).

In our study, the Serglycin regulation after CD44 silencing was difficult to observe by Western Blot. However, the results of the Taqman assay showed that in the case of 786O- shCD44-2 cells, CD44 silencing produced a reduction of the SRGN RNA levels. When 786O- shNS cells were analyzed, no changes in the SRGN expression were observed after doxycycline treatment, demonstrating that this event was due to CD44 downregulation.

The other cells, Ren13 and SN12C, did not show any decrease in SRGN expression due to CD44 silencing.

Through Immunocytofluorescence we could observe signs of Serglycin downregulation due to CD44 silencing. This event was better observed in the assay developed in Ren13 cells than in 786O-, as doxycycline induction did not work properly when the experiment was developed in this last cell line.

Nevertheless, and although this technique is not the best to determine the expression dependency between two proteins, it provided information about the localization of CD44 and Serglycin in our cell models.

Our hypothesis was based on a direct interaction between SRGN and CD44, for that, we expected to observe the co-localization of both proteins in the cell membrane. However, the staining performed combining the antibodies to detect both proteins at the same time showed that they were localized in two different areas of cells. While CD44 was expressed specifically on the cell membrane, Serglycin was found in the cytoplasm of cells, in some occasions packaged in some kind of vesicles. The observation of these vesicles had been previously described in tumor samples of lung adenocarcinoma patients (Jing You Guo et al., 2020b) and in breast tumor cells (Korpetinou et al., 2013). However, these results challenged our hypothesis about the direct interaction between SRGN and CD44.

An interesting experiment to be sure about the SRGN role in our models would be a functional assay where Serglycin was inhibited. Then, we could determine the effects of the protein in the migration and invasion processes of cells. Unfortunately, this approach has not been developed yet.

6. RELEVANCE OF CD44 AND SERGLYCIN IN THE CLINICS

The alteration of CD44 expression has been described in tumor tissues of colorectal, breast, gastric cancer, squamous carcinoma, non-small lung cancer, and malignant melanoma compared with their respective healthy tissues (Gilcrease et al., 1999; Gilcrease et al., 1996; X. P. Li, Zhang, Zheng, & Guo, 2015).

Moreover, a correlation between CD44 expression and a reduction of disease-free survival and distant metastasis was discovered in breast cancer, giving a prognostic role to CD44 (Bartakova et al., 2018; McFarlane et al., 2015). Furthermore, an association between CD44 presence and poor overall survival was also established in pancreatic cancer. It was observed that those patients with high CD44 expression showed a significant reduction of the survival probability, compared to the ones with low or absence CD44 levels (X. P. Li et al., 2015).

In different types of renal carcinoma, including clear cell carcinoma and chromophobe carcinoma, the presence of CD44 and some of its isoforms was described. However, this was not observed in papillary renal cancer, neither in the healthy renal tissue (Terpe et al., 1996; Gilcrease et al., 1999). It was also reported that CD44 expression was higher in those tumors of patients that developed metastasis than the ones that did not metastasize. Moreover, the metastases of those patients expressed higher levels of CD44 than the primary tumor (Lim et al., 2008; Semeniuk-Wojtaś, Stec, & Szczylik, 2016). These observations are in accordance with the results obtained during the RNA sequencing at the beginning of the project, where among different studied genes, CD44 was overexpressed in those tumors that, after the antiangiogenic treatment, became more malignant.

Our hypothesis about the CD44 involvement in the tumor invasion has been supported by the observation of high protein expression in those tumors that showed renal capsular invasion and/or metastasis, in comparison with the ones that were confined to the kidney (Rioux-Leclercq et al., 2001).

Different authors have established a correlation between CD44 expression and Furhman grade, tumor recurrence, and microvascular invasion, associating the role of an adverse prognostic factor to CD44 in renal cell carcinoma (X. Li et al., 2015; Bamias et al., 2003).

In this thesis, we aimed to determine the importance of CD44 expression in tumors of patients with renal cancer that were subjected to antiangiogenic treatment. We were interested in demonstrating our hypothesis based on the observation of an increased tumor invasion and aggressiveness after antiangiogenic treatment, where CD44 was put forward as responsible for tumor malignization. These affirmations were demonstrated by use of the 786O- *in vivo* model. We also wanted to validate them in tumor samples of patients with renal cancer. However, as it was not possible for us to have access to them, we used databases where the expression of some genes from different patients treated or not with Sunitinib (antiangiogenic drug) was available.

Analyzing this data, we observed that antiangiogenic treated patients showed a tendency to have higher levels of CD44 than untreated patients. Nonetheless, the results were not statistically conclusive.

However, it is worth pointing out that data from treated and untreated tumors did not belong to the same patient before and after the treatment.

As exposed at the beginning of the thesis and according to the rational basis of the project, not all tumors responded equally to the antiangiogenic treatment. Some tumors became more invasive after the therapy but some others did not. In the same way, some tumors showed an increase in CD44 expression among other genes, and some others did not change their genetic profile. Consequently, we speculate that the same could be happening in tumor samples of patients. While not all the analyzed Sunitinib treated-

tumors were necessarily expected to show an increase in CD44 expression, some untreated tumors could have high basal levels of the protein.

Moreover, we ascribed the increase of the CD44 expression to the antiangiogenic treatment. That way, the best analysis to validate our hypothesis would be the determination of CD44 expression in the same tumor patient before and after the treatment, so as to demonstrate that the upregulation of the protein was due to Sunitinib treatment.

Despite the lack of documentation about Serglycin expression in renal cancer patients, as with CD44, we determined its expression in those tumor samples depending on the antiangiogenic treatment. No differences were observed between untreated and Sunitinib-treated patients. As has been commented on before, the ideal analysis would be the determination of the protein in the same tumor samples before and after patients received the Sunitinib treatment, but this information was unfortunately not in our possession.

However, when patients were grouped depending on ALDH1A3 expression levels, we could observe differences in Serglycin expression. As explained, ALDH1A3 was discovered as a marker of tumor response, so that those tumors that showed high levels of ALDH1A3 before the antiangiogenic treatment were the ones that, once treated, became more aggressive and invasive. Then, the separation of patients in two groups according to high or low ALDH1A3 levels allowed us to distinguish between patients with potentially aggressive tumors and non-aggressive tumors after treatment.

Patients with high expression of ALDH1A3 in their tumors also presented high levels of Serglycin, which linked Serglycin to tumor malignization. These results do not confirm that Serglycin would be a marker of tumor response, but they do suggest Serglycin could have a role as a modulator in those potentially aggressive tumors.

Finally, we were able to demonstrate the existence of a correlation between CD44 and Serglycin expression in patients with renal cell carcinoma. This correlation, together with

the ones exposed in this section, may suggest a possible modulation between Serglycin and CD44. A direct interaction between both proteins was discarded due to the lack of its co-localization. However, the expression of the proteins *in vitro*, *in vivo*, and in clinical tumor samples, provides the basis for further research focused on the study of the intricate signaling and relation between CD44 and Serglycin.

CONCLUSIONS

1. *In vitro*, CD44 protein is involved in the migration and invasion processes of the kidney cancer primary tumor cells Ren13 and cell line 786O-, but not in the highly aggressive SN12C tumor cell line.
2. The role of CD44 in tumor invasion has been demonstrated *in vivo* in tumors generated from 786O- cells. Meanwhile, in tumors generated from metastatic SN12C cells, CD44 does not have a role in the invasion process.
3. Ruxolitinib treatment inhibits the JAK/Stat signaling pathway by reducing the phosphorylation of Stat3, but it does not affect the migration ability of Ren13 cells. Thus, JAK/Stat signaling does not seem to be involved in the migration and invasion processes downstream of CD44.
4. CD44 downstream signaling implicates Src because a specific inhibitor of this pathway, Bosutinib, produces a reduction of the migration and invasion capacities of Ren13 cells.
5. Concomitant knockdown of CD44 together with Src does not increase the effects observed in the migration and invasion processes, further confirming the involvement of Src signaling pathway downstream of CD44.
6. Hyaluronic Acid, the main ligand of CD44, is present in our cell cultures and tumor tissues, but it is not associated to CD44-mediated migration.
7. Expression of Serglycin, a novel CD44 modulator recently described, correlates with CD44 in patient kidney cancer samples, but does not seem to be associated with antiangiogenic response.
8. In the clinical setting, the expression of CD44 and Serglycin are independently associated with bad prognosis in renal cancer patients.
9. Tumors of Sunitinib-treated patients tend to express higher levels of CD44 than tumors of untreated patients, while no changes in the Serglycin expression is observed between both groups.
10. Clinically, Serglycin is upregulated in a subgroup of kidney cancer patients with highly aggressive tumors, suggesting a possible role as a bad prognosis biomarker in renal cancer.

REFERENCES

- Abdraboh, M. E., Gaur, R. L., Hollenbach, A. D., Sandquist, D., Raj, M. H. G., & Ouhtit, A. (2011). Survivin is a novel target of CD44-promoted breast tumor invasion. *The American Journal of Pathology*, *179*(2), 555–563.
- Abikhair Burgo, M., Roudiani, N., Chen, J., Santana, A. L., Doudican, N., Proby, C., Felsen, D., Carucci, J. A. (2018). Ruxolitinib inhibits cyclosporine-induced proliferation of cutaneous squamous cell carcinoma. *JCI Insight*, *3*(17), 1–18.
- Al-Husein, B., Abdalla, M., Trepte, M., DeRemer, D. L., & Somanath, P. R. (2012). Antiangiogenic therapy for cancer: An update. *Pharmacotherapy*, *32*(12), 1095–1111.
- Aldinucci, D., & Colombatti, A. (2014). The inflammatory chemokine CCL5 and cancer progression. *Mediators of Inflammation*, *2014*, 1–12.
- American Cancer Society. (2020) Retrieved April 2, 2020, Available from <https://www.cancer.org/cancer/kidney-cancer/detection-diagnosis-staging/staging.html>
- Arjumand, W., & Sultana, S. (2012). Role of VHL gene mutation in human renal cell carcinoma. *Tumor Biology*, *33*(1), 9–16.
- Baeriswyl, V., & Christofori, G. (2009). The angiogenic switch in carcinogenesis. *Seminars in Cancer Biology*, *19*(5), 329–337.
- Bai, L., Yang, J. C., Ok, J. H., MacK, P. C., Kung, H. J., & Evans, C. P. (2012). Simultaneous targeting of Src kinase and receptor tyrosine kinase results in synergistic inhibition of renal cell carcinoma proliferation and migration. *International Journal of Cancer*, *130*(11), 2693–2702.
- Bamias, A., Chorti, M., Deliveliotis, C., Trakas, N., Skolarikos, A., Protogerou, B., Legaki, S., Tsakalou, G., Tamvakis, N., Dimopoulos, M. A. (2003). Prognostic significance of CA 125, CD44, and epithelial membrane antigen in renal cell carcinoma. *Urology*, *62*(2), 368–373.
- Barata, P. C., & Rini, B. I. (2017). Treatment of renal cell carcinoma: Current status and future directions. *CA: A Cancer Journal for Clinicians*, *67*(6), 507–524.
- Bartakova, A., Michalova, K., Presl, J., Vlasak, P., Kostun, J., & Bouda, J. (2018). CD44 as a cancer stem cell marker and its prognostic value in patients with ovarian carcinoma. *Journal of*

Obstetrics and Gynaecology, 38(1), 110–114.

Basakran, N. S. (2015). CD44 as a potential diagnostic tumor marker. *Saudi Medical Journal*, 36(3), 273–279.

Beksac, A. T., Paulucci, D. J., Blum, K. A., Yadav, S. S., Sfakianos, J. P., & Badani, K. K. (2017). Heterogeneity in renal cell carcinoma. *Urologic Oncology: Seminars and Original Investigations*, 35(8), 507–515.

Bergers, G., & Benjamin, L. E. (2003). Tumorigenesis and the angiogenic switch. *Nature Reviews Cancer*, 3(6), 401–410.

Bergers, G., & Hanahan, D. (2008). Modes of resistance to anti-angiogenic therapy. *Nature Reviews Cancer*, 8(8), 592–603.

Bielecka, Z. F., Czarnecka, A. M., Solarek, W., Kornakiewicz, A., & Szczylik, C. (2013). Mechanisms of Acquired Resistance to Tyrosine Kinase Inhibitors in Clear - Cell Renal Cell Carcinoma (ccRCC). *Current Signal Transduction Therapy*, 8(3), 219–228.

Boschelli, F., Arndt, K., & Gambacorti-Passerini, C. (2010). Bosutinib: A review of preclinical studies in chronic myelogenous leukaemia. *European Journal of Cancer*, 46(10), 1781–1789.

Bourguignon, L. Y. W., Singleton, P. A., Zhu, H., & Diedrich, F. (2003). Hyaluronan-mediated CD44 interaction with RhoGEF and Rho kinase promotes Grb2-associated binder-1 phosphorylation and phosphatidylinositol 3-kinase signaling leading to cytokine (macrophage-colony stimulating factor) production and breast tumor progressio. *The Journal of Biological Chemistry*, 278(32), 29420–29434.

Bourguignon, L. Y. W., Zhu, H., Shao, L., & Chen, Y.-W. (2001). CD44 Interaction with c-Src Kinase Promotes Cortactin-mediated Cytoskeleton Function and Hyaluronic Acid-dependent Ovarian Tumor Cell Migration. *The Journal of Biological Chemistry*, 276(10), 7327–7336.

Brabletz, T. (2012). EMT and MET in Metastasis: Where Are the Cancer Stem Cells? *Cancer Cell*, 22(6), 699–701.

Brabletz, T., Kalluri, R., Nieto, M. A., & Weinberg, R. A. (2018). EMT in cancer. *Nature Reviews*

- Cancer*, 18(2), 128–134.
- Brunton, V. G., Avizienyte, E., Fincham, V. J., Serrels, B., Metcalf, C. A., Sawyer, T. K., & Frame, M. C. (2005). Identification of Src-specific phosphorylation site on focal adhesion kinase: Dissection of the role of Src SH2 and catalytic functions and their consequences for tumor cell behavior. *Cancer Research*, 65(4), 1335–1342.
- Capitano, U., & Montorsi, F. (2016). Renal cancer. *The Lancet*, 387(10021), 894–906.
- Carmeliet, P. (2000). Mechanisms of angiogenesis and arteriogenesis. *Nature Medicine*, 6(4), 389–395.
- Casanovas, O., Hicklin, D. J., Bergers, G., & Hanahan, D. (2005). Drug resistance by evasion of antiangiogenic targeting of VEGF signaling in late-stage pancreatic islet tumors. *Cancer Cell*, 8(4), 299–309.
- Cerisano, G., Buonamici, P., Valenti, R., Sciagrà, R., Raspanti, S., Santini, A., Carrabba, N., Dovellini, E.V., Romito, R., Pupi, A., Colonna, P., Antoniucci, D. (2014). Early short-term doxycycline therapy in patients with acute myocardial infarction and left ventricular dysfunction to prevent the ominous progression to adverse remodelling: The TIPTOP trial. *European Heart Journal*, 35(3), 184–191.
- Chen, C., Zhao, S., Karnad, A., & Freeman, J. W. (2018). The biology and role of CD44 in cancer progression: Therapeutic implications. *Journal of Hematology and Oncology*, 11(1), 1–23.
- Cho, S. H., Park, Y. S., Kim, H. J., Kim, C. H., Lim, S. W., Huh, J. W., Lee, J.H., Kim, H. R. (2012). CD44 enhances the epithelial-mesenchymal transition in association with colon cancer invasion. *International Journal of Oncology*, 41(1), 211–218.
- Cohen, H. T., & McGovern, F. J. (2005). Renal-Cell Carcinoma. *The New England Journal of Medicine*, 353, 2477–2490.
- Czauderna, F., Santel, A., Hinz, M., Fechtner, M., Durieux, B., Fisch, G., Leenders, F., Arnold, W., Giese, K., Klippel, A., Kaufmann, J. (2003). Inducible shRNA expression for application in a prostate cancer mouse model. *Nucleic Acids Research*, 31(21), 1–7.
- De Falco, S. (2014). Antiangiogenesis therapy: An update after the first decade. *Korean Journal*

- of Internal Medicine*, 29(1), 1–11.
- Deryugina, E. I., & Quigley, J. P. (2006). Matrix metalloproteinases and tumor metastasis. *Cancer and Metastasis Reviews*, 25(1), 9–34.
- Ding, Z., Kloss, J. M., Tuncali, S., Tran, N. L., & Loftus, J. C. (2020). TROY signals through JAK1-STAT3 to promote glioblastoma cell migration and resistance. *Neoplasia*, 22(9), 352–364.
- Draffin, J. E., McFarlane, S., Hill, A., Johnston, P. G., & Waugh, D. J. J. (2004). CD44 potentiates the adherence of metastatic prostate and breast cancer cells to bone marrow endothelial cells. *Cancer Research*, 64(16), 5702–5711.
- Ellis, L. M., & Hicklin, D. J. (2008). VEGF-targeted therapy: Mechanisms of anti-tumour activity. *Nature Reviews Cancer*, 8(8), 579–591.
- Fang, Z., Tang, Y., Fang, J., Zhou, Z., Xing, Z., Guo, Z., Guo, X., Wang, W., Jiao, W., Xu, Z., Liu, Z. (2013). Simvastatin Inhibits Renal Cancer Cell Growth and Metastasis via AKT/mTOR, ERK and JAK2/STAT3 Pathway. *PLoS ONE*, 8(5), 1–13.
- Ferrara, N., Gerber, H. P., & LeCouter, J. (2003). The biology of VEGF and its receptors. *Nature Medicine*, 9(6), 669–676.
- Fidler, I. J. (2003). The pathogenesis of cancer metastasis: the “seed and soil” hypothesis revisited. *Nature Reviews Cancer*, 3(1), 1–6.
- Fujisaki, T., Tanaka, Y., Fujii, K., Mine, S., Saito, K., Yamada, S., Yamashita, U., Irimura, T., Eto, S. (1999). CD44 stimulation induces integrin-mediated adhesion of colon cancer cell lines to endothelial cells by up-regulation of integrins and c-Met and activation of integrins. *Cancer Research*, 59(17), 4427–4434.
- Garg, H. G., Quinn, D. A., Mascarenhas, M. M., & Hales, C. A. (2004). *Chapter 12 Hyaluronan in Ventilator-Induced Lung Injury. Chemistry and Biology of Hyaluronan*. Elsevier Ltd.
- Gilcrease, M. Z., Guzman-Paz, M., Niehans, G., Cherwitz, D., McCarthy, J. B., & Albores-Saavedra, J. (1999). Correlation of CD44S expression in renal clear cell carcinomas with subsequent tumor progression or recurrence. *Cancer*, 86(11), 2320–2326.

- Gilcrease, M. Z., Truong, L., & Brown, R. W. (1996). Correlation of very late activation integrin and CD44 expression with extrarenal invasion and metastasis of renal cell carcinomas. *Human Pathology*, *27*(12), 1355–1360.
- Grimm, M. O., Wolff, I., Zastrow, S., Fröhner, M., & Wirth, M. (2010). Advances in renal cell carcinoma treatment. *Therapeutic Advances in Urology*, *2*(1), 11–17.
- Guarino, M. (2010). Src signaling in cancer invasion. *Journal of Cellular Physiology*, *223*(1), 14–26.
- Guo, J. Y., Chiu, C. H., Wang, M. J., Li, F. A., & Chen, J. Y. (2020). Proteoglycan serglycin promotes non-small cell lung cancer cell migration through the interaction of its glycosaminoglycans with CD44. *Journal of Biomedical Science*, *27*(2), 1–18.
- Guo, J. Y., Hsu, H. S., Tyan, S. W., Li, F. Y., Shew, J. Y., Lee, W. H., & Chen, J. Y. (2016). Serglycin in tumor microenvironment promotes non-small cell lung cancer aggressiveness in a CD44-dependent manner. *Oncogene*, *36*(17), 2457–2471.
- Gupta, G. P., & Massagué, J. (2006). Cancer Metastasis: Building a Framework. *Cell*, *127*(4), 679–695.
- Harshman, L. C., & Srinivas, S. (2010). The bevacizumab experience in advanced renal cell carcinoma. *OncoTargets and Therapy*, *3*, 179–189.
- Hertweck, M. K., Erdfelder, F., & Kreuzer, K. A. (2011). CD44 in hematological neoplasias. *Annals of Hematology*, *90*(5), 493–508.
- Hidalgo, M., Amant, F., Biankin, A. V., Budinská, E., Byrne, A. T., Caldas, C., ... Villanueva, A. (2014). Patient-derived Xenograft models: An emerging platform for translational cancer research. *Cancer Discovery*, *4*(9), 998–1013.
- Hoffman, R. M. (2015). Patient-derived orthotopic xenografts: Better mimic of metastasis than subcutaneous xenografts. *Nature Reviews Cancer*, *15*(8), 451–452.
- Hsieh, J. J., Le, V., Cao, D., Cheng, E. H., & Creighton, C. J. (2018). Genomic classifications of renal cell carcinoma: a critical step towards the future application of personalized kidney cancer care with pan-omics precision. *Journal of Pathology*, *244*(5), 525–537.

- Hsieh, J. J., Purdue, M. P., Signoretti, S., Swanton, C., Albiges, L., Schmidinger, M., Heng, D.Y., Larkin, J., Ficarra, V. (2017). Renal cell carcinoma. *Nature Reviews Disease Primers*, 3, 1–19.
- Hung, T.-W., Chen, P.-N., Wu, H.-C., Wu, S.-W., Tsai, P.-Y., Hsieh, Y.-S., & Chang, H.-R. (2017). Kaempferol inhibits the invasion and migration of renal cancer cells through the downregulation of AKT and FAK pathways. *International Journal of Medical Sciences*, 14(10), 984–993.
- Instituto Nacional del Cancer. (2020). Retrieved March 24, 2020, Available from <https://www.cancer.gov/espanol/cancer/naturaleza/que-es>
- Isfort, S., & Brümmendorf, T. H. (2018). Bosutinib in chronic myeloid leukemia: Patient selection and perspectives. *Journal of Blood Medicine*, 9, 43–50.
- Iyer, N. V., Kotch, L. E., Agani, F., Leung, S. W., Laughner, E., Wenger, R. H., Gassmann, M., Gearhart, J.D., Lawler, A.M., Yu, A.Y., Semenza, G. L. (1998). Cellular and developmental control of O₂ homeostasis by hypoxia-inducible factor 1 α . *Genes and Development*, 12(2), 149–162.
- Jiménez Valerio, G., & Casanovas, O. (2013). Anti-angiogenic therapy for cancer and the mechanisms of tumor resistance. *Contributions to Science*, 9(1), 67–73.
- Jordan, A. R., Racine, R. R., Hennig, M. J. P., & Lokeshwar, V. B. (2015). The role of CD44 in disease pathophysiology and targeted treatment. *Frontiers in Immunology*, 6(182), 1–14.
- Kang, Y., & Massagué, J. (2004). Epithelial-mesenchymal transitions: Twist in development and metastasis. *Cell*, 118(3), 277–279.
- Karousou, E., Misra, S., Ghatak, S., Dobra, K., Götte, M., Vigetti, D., Passi, A., Karamanos, N.K., Skandalis, S. S. (2017). Roles and targeting of the HAS/hyaluronan/CD44 molecular system in cancer. *Matrix Biology*, 59, 3–22.
- Kim, J. W., Gautam, J., Kim, J. E., Kim, J. A., & Kang, K. W. (2019). Inhibition of tumor growth and angiogenesis of tamoxifen-resistant breast cancer cells by ruxolitinib, a selective JAK2 inhibitor. *Oncology Letters*, 17(4), 3981–3989.
- Kodani, M., Yang, G., Conklin, L. M., Travis, T. C., Whitney, C. G., Anderson, L. J., Schrag, S.J.,

- Taylor, T.H., Beall, B.W., Breiman, R.F., Feikin, D.R., Njenga, M.K., Oberste, M.S., Tondella, M.L.C., Winchell, J.M., Lindstrom, S.L., Erdman, D.D., Fields, B. S. (2011). Application of TaqMan low-density arrays for simultaneous detection of multiple respiratory pathogens. *Journal of Clinical Microbiology*, 49(6), 2175–2182.
- Komar, H. M., Serpa, G., Kerscher, C., Schwoegl, E., Mace, T. A., Jin, M., Yang, M.C., Chen, C.S., Bloomston, M., Ostrowski, M.C., Hart, P.A., Conwell, D.L., Lesinski, G. B. (2017). Inhibition of Jak/STAT signaling reduces the activation of pancreatic stellate cells in vitro and limits caerulein-induced chronic pancreatitis in vivo. *Scientific Reports*, 7(1), 1–10.
- Koponen, J. K., Kankkonen, H., Kannasto, J., Wirth, T., Hillen, W., Bujard, H., & Ylä-Herttuala, S. (2003). Doxycycline-regulated lentiviral vector system with a novel reverse transactivator rtTA2S-M2 shows a tight control of gene expression in vitro and in vivo. *Gene Therapy*, 10(6), 459–466.
- Korpetinou, A., Skandalis, S. S., Moustakas, A., Happonen, K. E., Tveit, H., Prydz, K., Labropoulou, V.T., Giannopoulou, E., Kalofonos, H.P., Blom, A.M., Karamanos, N.K., Theocharis, A. D. (2013). Serglycin is implicated in the promotion of aggressive phenotype of breast cancer cells. *PloS One*, 8(10).
- Larkin, J. M. G., & Eisen, T. (2006). Renal cell carcinoma and the use of sorafenib. *Therapeutics and Clinical Risk Management*, 2(1), 87–98.
- Lee, S. Y., Kim, K. A., Kim, C. H., Kim, Y. J., Lee, J. H., & Kim, H. R. (2017). CD44-shRNA recombinant adenovirus inhibits cell proliferation, invasion, and migration, and promotes apoptosis in HCT116 colon cancer cells. *International Journal of Oncology*, 50(1), 329–336.
- Li, S., Priceman, S. J., Xin, H., Zhang, W., Deng, J., Liu, Y., Huang, J., Zhu, W., Chen, M., Hu, W., Deng, X., Zhang, J., Yu, H., He, G. (2013). Icaritin inhibits JAK/STAT3 signaling and growth of renal cell carcinoma. *PLoS ONE*, 8(12), 1–8.
- Li, X., Ma, X., Chen, L., Gu, L., Zhang, Y., Zhang, F., Ouyang, Y., Gao, Y., Huang, Q., Zhang, X. (2015). Prognostic value of CD44 expression in renal cell carcinoma: A systematic review and meta-analysis. *Scientific Reports*, 5(13157), 1–8.
- Li, X. P., Zhang, X. W., Zheng, L. Z., & Guo, W. J. (2015). Expression of CD44 in pancreatic cancer

- and its significance. *International Journal of Clinical and Experimental Pathology*, 8(6), 6724–6731.
- Lim, S. D., Young, A. N., Paner, G. P., & Amin, M. B. (2008). Prognostic role of CD44 cell adhesion molecule expression in primary and metastatic renal cell carcinoma: A clinicopathologic study of 125 cases. *Virchows Archiv*, 452(1), 49–55.
- Linehan, W. M., & Zbar, B. (2004). Focus on kidney cancer. *Cancer Cell*, 6(3), 223–228.
- Ljungberg, B., Hanbury, D. C., Kuczyk, M. A., Merseburger, A. S., Mulders, P. F. A., Patard, J. J., & Sinescu, I. C. (2007). Renal Cell Carcinoma Guideline. *European Urology*, 51(6), 1502–1510.
- Lu, P., Weaver, V. M., & Werb, Z. (2012). The extracellular matrix: A dynamic niche in cancer progression. *The Journal of Cell Biology*, 196(4), 395–406.
- Lučin, K., Matušan, K., Dordević, G., & Stipičić, D. (2004). Prognostic significance of CD44 molecule in renal cell carcinoma. *Croatian Medical Journal*, 45(6), 703–708.
- Lue, H., Cole, B., Rao, S. A. M., Podolak, J., Gaest, A. Van, King, C., Eide, C.A., Wilmot, B., Xue, C., Spellman, P.T., Heiser, L.M., Tyner, J.W., Thomas, G. V. (2015). Src and STAT3 inhibitors synergize to promote tumor inhibition in renal cell carcinoma. *Oncotarget*, 6(42), 44675–44687.
- Matsushita, N., Matsushita, S., Hirakawa, S., & Higashiyama, S. (2013). Doxycycline-dependent inducible and reversible RNA interference mediated by a single lentivirus vector. *Bioscience, Biotechnology and Biochemistry*, 77(4), 776–781.
- McFarlane, S., Coulter, J. A., Tibbits, P., O’Grady, A., McFarlane, C., Montgomery, N., Hill, A., McCarthy, H.O., Young, L.S., Kay, E.W., Isacke, C.M., Waugh, D. J. J. (2015). CD44 increases the efficiency of distant metastasis of breast cancer. *Oncotarget*, 6(13), 11465–11476.
- Merentie, M., Rissanen, R., Lottonen-Raikaslehto, L., Huusko, J., Gurzeler, E., Turunen, M. P., Holappa, L., Mäkinen, P., Ylä-Herttuala, S. (2018). Doxycycline modulates VEGF-A expression: Failure of doxycycline-inducible lentivirus shRNA vector to knockdown VEGF-A expression in transgenic mice. *PLoS ONE*, 13(1), 1–15.
- Mikami, S., Mizuno, R., Kosaka, T., Saya, H., Oya, M., & Okada, Y. (2015). Expression of TNF- α and

- CD44 is implicated in poor prognosis, cancer cell invasion, metastasis and resistance to the sunitinib treatment in clear cell renal cell carcinomas. *International Journal of Cancer*, 136(7), 1504–1514.
- Misra, S., Hascall, V. C., Markwald, R. R., & Ghatak, S. (2015). Interactions between hyaluronan and its receptors (CD44, RHAMM) regulate the activities of inflammation and cancer. *Frontiers in Immunology*, 6(201), 1–31.
- Misra, S., Heldin, P., Hascall, V. C., Karamanos, N. K., Skandalis, S. S., Markwald, R. R., & Ghatak, S. (2011). Hyaluronan-CD44 interactions as potential targets for cancer therapy. *FEBS Journal*, 278(9), 1429–1443.
- Moch, H., Cubilla, A. L., Humphrey, P. A., Reuter, V. E., & Ulbright, T. M. (2016). The 2016 WHO Classification of Tumours of the Urinary System and Male Genital Organs—Part A: Renal, Penile, and Testicular Tumours. *European Urology*, 70(1), 93–105.
- Moore, M., Guthrie, E. H., Huand, M. T.-H., & Taxman, D. J. (2010). Short Hairpin RNA (shRNA): Design, Delivery, and Assessment of Gene Knockdown. *Methods in Molecular Biology (Clifton, N.J.)*, 629(2), 141–158.
- Moserle, L., Jiménez-Valerio, G., & Casanovas, O. (2014). Antiangiogenic therapies: Going beyond Their Limits. *Cancer Discovery*, 4(1), 31–41.
- Motzer, R. J., Hutson, T. E., Tomczak, P., Michaelson, M. D., Bukowski, R. M., Oudard, S., Negrier, S., Szczylik, C., Pili, R., Bjarnason, G.A., Garcia-del-Muro, X., Sosman, J.A., Solska, E., Wilding, G., Thomposon, J.A., Kim, S.T., Chen, I., Huang, X., Figlin, R. A. (2009). Overall survival and updated results for sunitinib compared with interferon alfa in patients with metastatic renal cell carcinoma. *Journal of Clinical Oncology*, 27(22), 3584–3590.
- Motzer, R. J., Rini, B. I., McDermott, D. F., Arén Frontera, O., Hammers, H. J., Carducci, M. A., Salaman, P., Excudier, B., Beuselinck, B., Amin, A., Porta, C., George, S., Neiman, V., Bracarda, S., Tykodi, S.S., Barthélémy, P., Leibowitz-Amit, R., Plimack, E.R., Oosting, S.F., Redman, B., Melichar, B., Powles, T., Nathan, P., Oudard, S., Pook, D., Choueiri, T.K., Donskow, F., Grimm, M.O., Gurney, H., Heng, D.Y.C., Kollmannsberger, C.K., Harrison, M.R., Tomita, Y., Duran, I., Grünwald, V., McHenry, M.B., Mekan, S., Tannir, N. M. (2019). Nivolumab plus ipilimumab versus sunitinib in first-line treatment for advanced renal cell carcinoma:

- extended follow-up of efficacy and safety results from a randomised, controlled, phase 3 trial. *The Lancet Oncology*, 20(10), 1370–1385.
- Nam, K., Oh, S., Lee, K., Yoo, S., & Shin, I. (2015). CD44 regulates cell proliferation, migration, and invasion via modulation of c-Src transcription in human breast cancer cells. *Cellular Signalling*, 27(9), 1882–1894.
- Naor, D., Nedvetzki, S., Golan, I., Melnik, L., & Faitelson, Y. (2002). CD44 in cancer. *Critical Reviews in Clinical Laboratory Sciences*, 39(6), 527–579.
- National Cancer Institute. (2020). Retrieved March 24, 2020, Available from <https://seer.cancer.gov/statfacts/html/kidrp.html%0D>
- Negi, L. M., Talegaonkar, S., Jaggi, M., Ahmad, F. J., Iqbal, Z., & Khar, R. K. (2012). Role of CD44 in tumour progression and strategies for targeting. *Journal of Drug Targeting*, 20(7), 561–573.
- New Health Advisor. (2020). Retrieved April 08, 2020, Available from <https://www.newhealthadvisor.org/Renal-Cell-Carcinoma-Staging.htm>
- Orian-Rousseau, V. (2010). CD44, a therapeutic target for metastasising tumours. *European Journal of Cancer*, 46(7), 1271–1277.
- Ouhtit, A., Rizeq, B., Saleh, H. A., Rahman, M. D. M., & Zayed, H. (2018). Novel CD44-downstream signaling pathways mediating breast tumor invasion. *International Journal of Biological Sciences*, 14(13), 1782–1790.
- Pàez-Ribes, M., Allen, E., Hudock, J., Takeda, T., Okuyama, H., Viñals, F., Inoue, M., Bergers, G., Hanahan, D. (2009). Antiangiogenic Therapy Elicits Malignant Progression of Tumors to Increased Local Invasion and Distant Metastasis. *Cancer Cell*, 15(3), 220–231.
- Pan, Y., Smithson, L. J., Ma, Y., Hambardzumyan, D., & Gutmann, D. H. (2017). Ccl5 establishes an autocrine high-grade glioma growth regulatory circuit critical for mesenchymal glioblastoma survival. *Oncotarget*, 8(20), 32977–32989.
- Park, Y. S., Huh, J. W., Lee, J. H., & Kim, H. R. (2012). shRNA against CD44 inhibits cell proliferation, invasion and migration, and promotes apoptosis of colon carcinoma cells.

- Oncology Reports*, 27(2), 339–346.
- Pearson, P., & Van Der Luitj, R. (1998). The genetic analysis of cancer. *Journal of Internal Medicine*, 243, 413–417.
- Pink, A., Skolnaja, M., Paell, T., & Valkna, A. (2016). CD44 Controls Endothelial Proliferation and Functions as Endogenous Inhibitor of Angiogenesis. *bioRxiv*, 1–23.
- Plosker, G. L. (2015). Ruxolitinib: A review of its use in patients with myelofibrosis. *Drugs*, 75(3), 297–308.
- Posadas, E. M., Limvorasak, S., & Figlin, R. A. (2017). Targeted therapies for renal cell carcinoma. *Nature Reviews Nephrology*, 13(8), 496–511.
- Protein Atlas. (2020). Retrieved August 24, 2020, Available from <https://www.proteinatlas.org/ENSG00000122862-SRGN/pathology/renal+cancer>
- Protein Atlas. (2020). Retrieved September 8, 2020, Available from <https://www.proteinatlas.org/ENSG00000122862-SRGN/pathology/renal+cancer/KIRC>
- Protein Atlas. (2020). Retrieved April 24, 2020, Available from <https://www.proteinatlas.org/ENSG00000026508-CD44/pathology/renal+cancer/KIRC>
- Psaila, B., & Lyden, D. (2009). The metastatic niche: Adapting the foreign soil. *Nature Reviews Cancer*, 9(4), 285–293.
- Rabbani, S. A., Valentino, M.-L., Arakelian, A., Ali, S., & Boschelli, F. (2010). SKI-606 (Bosutinib) Blocks Prostate Cancer Invasion , Growth , and Metastasis In vitro and In vivo through Regulation of Genes Involved in Cancer Growth and Skeletal Metastasis. *Molecular Cancer Therapeutics*, 530(18), 1147–1158.
- Rao, D. D., Vorhies, J. S., Senzer, N., & Nemunaitis, J. (2009). siRNA vs. shRNA: Similarities and differences. *Advanced Drug Delivery Reviews*, 61(9), 746–759.
- Reymond, N., D'Água, B. B., & Ridley, A. J. (2013). Crossing the endothelial barrier during metastasis. *Nature Reviews Cancer*, 13(12), 858–870.
- Richardson, P. G., Eng, C., Kolesar, J., Hideshima, T., & Anderson, K. C. (2012). Perifosine, an oral,

- anti-cancer agent and inhibitor of the Akt pathway: mechanistic actions, pharmacodynamics, pharmacokinetics, and clinical activity. *Expert Opinion on Drug Metabolism & Toxicology*, 8(5), 623–633.
- Rini, B. I., Campbell, S. C., & Escudier, B. (2009). Renal cell carcinoma. *The Lancet*, 373(9669), 1119–1132.
- Rini, B. I., Halabi, S., Rosenberg, J. E., Stadler, W. M., Vaena, D. A., Ou, S. S., Archer, L., Atkins, J.N., Picus, J., Czaykowski, P., Dutcher, J., Small, E. J. (2008). Bevacizumab plus interferon alfa compared with interferon alfa monotherapy in patients with metastatic renal cell carcinoma: CALGB 90206. *Journal of Clinical Oncology*, 26(33), 5422–5428.
- Rioux-Leclercq, N., Epstein, J. I., Bansard, J. Y., Turlin, B., Patard, J. J., Manunta, A., Chan, T., Ramee, M.P., Lobel, B., Moulinoux, J. P. (2001). Clinical significance of cell proliferation, microvessel density, and CD44 adhesion molecule expression in renal cell carcinoma. *Human Pathology*, 32(11), 1209–1215.
- Rizzo, M., & Porta, C. (2017). Sunitinib in the treatment of renal cell carcinoma: an update on recent evidence. *Therapeutic Advances in Urology*, 9(8), 195–207.
- Roscic-Mrkic, B., Fischer, M., Leemann, C., Manrique, A., Gordon, C. J., Moore, J. P., Proudfoot, A.E.I., Trkola, A. (2003). RANTES (CCL5) uses the proteoglycan CD44 as an auxiliary receptor to mediate cellular activation signals and HIV-1 enhancement. *Blood*, 102(4), 1169–1177.
- Roskoski, R. (2015). Src protein-tyrosine kinase structure, mechanism, and small molecule inhibitors. *Pharmacological Research*, 94, 9–25.
- Rusconi, F., Piazza, R., Vagge, E., & Gambacorti-Passerini, C. (2014). Bosutinib: A review of preclinical and clinical studies in chronic myelogenous leukemia. *Expert Opinion on Pharmacotherapy*, 15(5), 701–710.
- Segrelles, C., Contreras, D., Navarro, E. M., Gutiérrez-Muñoz, C., García-Escudero, R., Paramio, J. M., & Lorz, C. (2018). Bosutinib inhibits EGFR activation in head and neck cancer. *International Journal of Molecular Sciences*, 19(7), 1–14.
- Semeniuk-Wojtaś, A., Stec, R., & Szczylik, C. (2016). Are primary renal cell carcinoma and

- metastases of renal cell carcinoma the same cancer? *Urologic Oncology: Seminars and Original Investigations*, 34(5), 215–220.
- Semenza, G. L. (2007). Hypoxia-Inducible Factor 1 (HIF-1) Pathway. *Science STKE*, 1, 24–27.
- Sen, B., & Johnson, F. M. (2011). Regulation of Src Family Kinases in Human Cancers. *Journal of Signal Transduction*, 2011, 1–14.
- So, J. Y., Smolarek, A. K., Salerno, D. M., Maehr, H., Uskokovic, M., Liu, F., & Suh, N. (2013). Targeting CD44-STAT3 Signaling by Gemini Vitamin D Analog Leads to Inhibition of Invasion in Basal-Like Breast Cancer. *PLoS ONE*, 8(1), 1–10.
- Stewart, G. D., O'Mahony, F. C., Laird, A., Eory, L., Lubbock, A. L. R., Mackay, A., Nanda, J., O'Donnell, M., Mullen, P., McNeill, S.A., Riddick, A.C.P., Berney, D., Bex, A., Aitchison, M., Overton, I.M., Harrison, D.J., Powles, T. (2015). Sunitinib treatment exacerbates intratumoral heterogeneity in metastatic renal cancer. *Clinical Cancer Research*, 21(18), 4212–4223.
- Sugahara, K. N., Murai, T., Nishinakamura, H., Kawashima, H., Saya, H., & Miyasaka, M. (2003). Hyaluronan oligosaccharides induce CD44 cleavage and promote cell migration in CD44-expressing tumor cells. *Journal of Biological Chemistry*, 278(34), 32259–32265.
- Sun, J. S., & Zhou, M. Q. (2016). Expression of KAI1/CD82 and CD44v6 in laryngeal squamous cell carcinoma and its significance. *International Journal of Clinical and Experimental Pathology*, 9(9), 9113–9125.
- Suwaki, N., Vanhecke, E., Atkins, K. M., Graf, M., Swabey, K., Huang, P., Schraml, P., Moch, H., Cassidy, A., Brewer, D., Al-lazikani, B., Workman, P., De-bono, J., Kaye, S.B., Larkin, J., Gore, M.E., Sawyers, C.L., Nelson, P., Beer, T.M., Geng, H., Gao, L., Qian, D.Z., Alumkal, J.J., Thomas, G., Thomas, G. V. (2012). A HIF-regulated VHL-PTP1B-Src signaling axis identifies a therapeutic target in Renal Cell Carcinoma. *Science Translational Medicine*, 3(85), 1–21.
- Tao, J., Mariani, L., Eddy, S., Maecker, H., Kambham, N., Mehta, K., Hartman, J., Wang, W., Kretzler, M., Lafayette, R. A. (2018). JAK-STAT signaling is activated in the kidney and peripheral blood cells of patients with focal segmental glomerulosclerosis. *Kidney International*, 94(4), 795–808.

- Terpe, H.-J., Störkel, S., Zimmer, U., Anquez, V., Fischer, C., Pantel, K., & Günthert, U. (1996). Expression of CD44 isoforms in renal cell tumors: Positive correlation to tumor differentiation. *American Journal of Pathology*, *148*(2), 453–463.
- Tilesi, F., Fradiani, P., Socci, V., Willems, D., & Ascenzioni, F. (2009). Design and validation of siRNAs and shRNAs. *Current Opinion in Molecular Therapeutics*, *11*(2), 156–164.
- Toyama-Sorimachi, N., Sorimachi, H., Tobita, Y., Kitamura, F., Yagita, H., Suzuki, K., & Miyasaka, M. (1995). A Novel Ligand for CD44 Is Serglycin, a Hematopoietic Cell Lineage-specific Proteoglycan. *The Journal of Biological Chemistry*, *270*(13), 7437–7444.
- Tun, H. W., Marlow, L. A., von Roemeling, C. A., Cooper, S. J., Kreinest, P., Wu, K., Luxon, B.A., Sinha, M., Anastasiadis, P.Z., Copland, J. A. (2010). Pathway signature and cellular differentiation in Clear Cell Renal Cell Carcinoma. *PLoS ONE*, *5*(5), 1–14.
- Valastyan, S., & Weinberg, R. A. (2011). Tumor metastasis: Molecular insights and evolving paradigms. *Cell*, *147*(2), 275–292.
- Vultur, A., Buettner, R., Kowolik, C., Liang, W., Smith, D., Boschelli, F., & Jove, R. (2008). SKI-606 (bosutinib), a novel Src kinase inhibitor, suppresses migration and invasion of human breast cancer cells. *Molecular Cancer Therapeutics*, *7*(5), 1185–1194.
- Wang, H. S., Hung, Y., Su, C. H., Peng, S. T., Guo, Y. J., Lai, M. C., Liu, C.Y., Hsu, J. W. (2005). CD44 Cross-linking induces integrin-mediated adhesion and transendothelial migration in breast cancer cell line by up-regulation of LFA-1 ($\alpha\text{L}\beta\text{2}$) and VLA-4 ($\alpha\text{4}\beta\text{1}$). *Experimental Cell Research*, *304*(1), 116–126.
- Wang, S. J., & Bourguignon, L. Y. W. (2011). Role of hyaluronan-mediated CD44 signaling in head and neck squamous cell carcinoma progression and chemoresistance. *The American Journal of Pathology*, *178*(3), 956–963.
- Wei, Q., Zhang, F., Richardson, M. M., Roy, N. H., Rodgers, W., Liu, Y., Zhao, W., Fu, C., Ding, Y., Huang, C., Chen, Y., Sun, Y., Ding, L., Hu, Y., Ma, J.X., Boulton, M.E., Pasula, S., Wren, J.D., Tanaka, S., Huang, S., Thali, M., Hämmerling, G.J., Zhang, X. A. (2014). CD82 restrains pathological Angiogenesis by altering lipid raft clustering and CD44 trafficking in endothelial cells. *Circulation*, *130*(17), 1493–1504.

- Wilson, G. S., Tian, A., Hebbard, L., Duan, W., George, J., Li, X., & Qiao, L. (2013). Tumoricidal effects of the JAK inhibitor Ruxolitinib (INC424) on hepatocellular carcinoma in vitro. *Cancer Letters*, *341*(2), 224–230.
- World Health Organization. (2020). Retrieved March 24, 2020, Available from <http://www.euro.who.int/en/health-topics/noncommunicable-diseases/cancer/data-and-statistics>
- Wu, K. L., Miao, H., & Khan, S. (2007). JAK kinases promote invasiveness in VHL-mediated renal cell carcinoma by a suppressor of cytokine signaling-regulated, HIF-independent mechanism. *American Journal of Physiology - Renal Physiology*, *293*(6), 1836–1846.
- Wu, Q., Yang, Y., Wu, S., Li, W., Zhang, N., Dong, X., & Ou, Y. (2015). Evaluation of the correlation of KAI1/CD82, CD44, MMP7 and β -catenin in the prediction of prognosis and metastasis in colorectal carcinoma. *Diagnostic Pathology*, *10*(1), 1–9.
- Xie, J., Nair, A., & Hermiston, T. W. (2008). A comparative study examining the cytotoxicity of inducible gene expression system ligands in different cell types. *Toxicology in Vitro*, *22*(1), 261–266.
- Zhang, Z., Deng, Y., Zheng, G., Jia, X., Xiong, Y., Luo, K., Qiu, Q., Qiu, N., Yin, J., Lu, M., Liu, H., Gu, Y., He, Z. (2017). SRGN-TGF β 2 regulatory loop confers invasion and metastasis in triple-negative breast cancer. *Oncogenesis*, *6*(7), 1–12.
- Zhao, Y., Qiao, S., Shi, S., Yao, L., Hou, X., Li, C., Lin, F-H., Guo, K., Acharya, A., Chen, X., Nie, Y., Tian, W. (2017). Modulating Three-Dimensional Microenvironment with Hyaluronan of Different Molecular Weights Alters Breast Cancer Cell Invasion Behavior. *ACS Applied Materials and Interfaces*, *9*(11), 9327–9338.
- Zhu, J., Liang, C., Hua, Y., Miao, C., Zhang, J., Xu, A., Ahao, K., Liu, S., Tian, Y., Dong, H., Zhang, C., Li, P., Su, S., Wang, Z. (2017). The metastasis suppressor CD82/KAI1 regulates cell migration and invasion via inhibiting TGF- β 1/Smad signaling in renal cell carcinoma. *Oncotarget*, *8*(31), 51559–51568.
- Zou, L., Song, X., Yi, T., Li, S., Deng, H., Chen, X., Li, Z., Bai, Y., Zhong, Q., Wei, Y., Zhao, X. (2013). Administration of PLGA nanoparticles carrying shRNA against focal adhesion kinase and

CD44 results in enhanced antitumor effects against ovarian cancer. *Cancer Gene Therapy*, 20(4), 242–250.

Zou, L., Yi, T., Song, S., Wei, Y., & Zhao, X. (2014). Efficient inhibition of intraperitoneal human ovarian cancer growth by short hairpin RNA targeting CD44. *Neoplasma*, 61(3), 274–282.